

DOKUZ EYLÜL UNIVERSITY
GRADUATE SCHOOL OF NATURAL AND APPLIED
SCIENCES

CORE MATERIAL EFFECT ON IMPACT
BEHAVIOR OF GLASS FIBER SANDWICH
COMPOSITES

by
Okan ÖZDEMİR

August, 2012
İZMİR

**CORE MATERIAL EFFECT ON IMPACT
BEHAVIOR OF GLASS FIBER SANDWICH
COMPOSITES**

**A Thesis Submitted to the
Graduate School of Natural and Applied Sciences of Dokuz Eylül University
In Partial Fulfillment of the Requirements for the Degree of Master of Science
in Mechanical Engineering, Mechanics Program**

**by
Okan ÖZDEMİR**

**August, 2012
İZMİR**

M.Sc THESIS EXAMINATION RESULT FORM

We have read the thesis entitled “**CORE MATERIAL EFFECT ON IMPACT BEHAVIOR OF GLASS FIBER SANDWICH COMPOSITES**” completed by **OKAN ÖZDEMİR** under supervision of **PROF. DR. RAMAZAN KARAKUZU** and we certify that in our opinion it is fully adequate, in scope and in quality, as a thesis for the degree of Master of Science.



Prof. Dr. Ramazan KARAKUZU

Supervisor




Assoc. Prof. Dr. Bülent Murat İÇTEN

(Jury Member)



Assist. Prof. Dr. Bahadır UYULGAN

(Jury Member)



Prof. Dr. Mustafa SABUNCU
Director

Graduate School of Natural and Applied Sciences

ACKNOWLEDGMENTS

I would like to take this opportunity to express my sincere thanks to all the people who have been instrumental to my success throughout my master's study here at Dokuz Eylül University.

First and foremost, I feel like expressing my sincere gratitude and respect to my supervisor, Prof. Dr. Ramazan KARAKUZU, for his help, excellent guidance and continuous encouragement throughout my student life at Dokuz Eylül University.

I also would like to thank Assoc. Prof. Dr. Bülent Murat İÇTEN, research assistants, Dr. Mustafa ÖZEN, Eray SABANCI, Akar DOĞAN, Volkan ARIKAN and Mechanical Engineer Umut POTOĞLU (M.Sc), Aidel Kadum Jassim AL-SHAMARY for their endless patience, help and support during experimental stages of the study.

Finally, I would like to thank my family for their great support. Especially, I would like to thank to my mother who taught me how to be, think and act.

Okan ÖZDEMİR

CORE MATERIAL EFFECT ON IMPACT BEHAVIOR OF GLASS FIBER SANDWICH COMPOSITES

ABSTRACT

The objective of this thesis is to investigate the effects of core material and its thickness on impact behavior of sandwich composite plates subjected to low velocity impact, experimentally. Two PVC foams and PET foam were selected as the core material, having approximate density of 60 kg/m³ and thicknesses of 5, 10 and 15 mm. The stacking sequence of the sandwich composites are [+45/-45/0/90/core/90/0/-45/+45].

Impact tests were carried out by using Fractovis Plus Impact testing machine under room temperature. Various impact energies were selected from 10J to 70J to analyze the impact energy level. The dimensions of the specimens are 100 mm x 100 mm. After the impact tests, absorbed energy, maximum contact time, maximum deflection and maximum contact force versus impact energy, contact force versus deflection and contact force versus time curves were obtained for mentioned impact energies for sandwich composites with PVC and PET foams, and [+45/-45/0/90] laminated composites.

As a result, it is seen that the core material and its thickness have notable effects on the impact behavior of sandwich composite plates. Sandwich composites have also higher absorbed energy, penetration and perforation threshold.

Keywords: Sandwich composite, PVC foam, PET foam, Core thickness, Low velocity impact

CAM FİBER SANDVİÇ KOMPOZİTLERİN DARBE DAVRANIŞINA ÇEKİRDEK MALZEMESİ ETKİSİ

ÖZ

Bu tez çalışmasının amacı, düşük hızlı darbeye maruz sandviç kompozit plakaların darbe davranışı üzerine çekirdek malzemesinin ve kalınlığının etkilerini deneysel olarak incelemektir. Yaklaşık olarak 60 kg/m³ yoğunluğa ve 5, 10 ve 15 mm kalınlığa sahip PVC ve PET köpükler çekirdek malzemesi olarak seçilmiştir. Sandviç kompozitlerin oryantasyonu [+45/-45/0/90/çekirdek/90/0/-45/+45] şeklindedir.

Darbe deneyleri, Fractovis Plus darbe test cihazı kullanılarak oda sıcaklığında gerçekleştirilmiştir. Darbe enerjisi seviyesini incelemek için 10J'den 70J'e kadar çeşitli darbe enerjileri seçilmiştir. Numunelerin ölçüleri 100 mm x 100 mm'dir. Darbe deneylerinden sonra, absorbe edilen enerji, maksimum temas süresi, maksimum çökme ve maksimum temas kuvveti-darbe enerjisi, temas kuvveti-çökme ve temas kuvveti-zaman eğrileri bahsedilen darbe enerjileri için, PVC ve PET köpüklerden oluşan sandviç kompozitler ve [+45/-45/0/90] oryantasyonuna sahip tabakalı kompozitler için elde edilmiştir.

Sonuç olarak, çekirdek malzemesinin ve kalınlığının sandviç kompozitlerin darbe davranışı üzerinde önemli etkilerinin olduğu görülmüştür. Sandviç kompozitler ayrıca yüksek absorbe edilen enerjiye, nüfuziyet ve delinme eşiklerine sahiptir.

Anahtar sözcükler: Sandviç kompozit, PVC köpük, PET köpük, Çekirdek kalınlığı, Düşük hızlı darbe

CONTENTS

	Page
THESIS EXAMINATION RESULT FORM	ii
ACKNOWLEDGEMENTS	iii
ABSTRACT	iv
ÖZ	v
CHAPTER ONE – INTRODUCTION	1
1.1 Overview	1
CHAPTER TWO – ESSENTIAL BACKGROUND AND IMPACT CHARACTERIZATION OF SANDWICH COMPOSITES	7
2.1 Introduction	7
2.2 Sandwich Composites	7
2.2.1 Face Sheet Materials	8
2.2.2 Core Materials	9
2.3 Vacuum Assisted Resin Infusion Molding Process (VARIM)	10
2.4 Impact Properties of Sandwich Composites	11
2.5 Impact Test Equipment of Low Velocity Impact (LVI)	12
2.5.1 Charpy and Izod Test Systems	13
2.5.2 Drop Weight Impact Test Systems	13
2.6 Failure Modes in Low Velocity Impact	14
2.6.1 Matrix Cracking	14
2.6.2 Delamination	15
2.6.3 Fiber Failure	16
2.6.4 Penetration	16
2.7 Low Velocity Impact of Sandwich Composites	16

CHAPTER THREE – EXPERIMENTAL STUDY	18
3.1 Introduction	18
3.2 Manufacturing of Sandwich Composite Plates and Material Preparation	18
3.3 Impact Tests	24
CHAPTER FOUR – RESULTS AND DISCUSSION	26
4.1 Impact Tests	26
4.1.1 Effect of Core Thicknesses on Impact Behavior of Sandwich Composites	30
4.1.2 Effect of Core Materials on Impact Behavior of Sandwich Composites	46
4.1.3 Damages of Specimens	61
CHAPTER FIVE – CONCLUSIONS AND RECOMMENDATIONS	73
REFERENCES	75
APPENDICES	80

CHAPTER ONE

INTRODUCTION

1.1 Overview

Sandwich composite structures have been widely used in numerous application fields such as aerospace, marine, automotive, windmill, sports industries etc, and have specific advantages like high bending stiffness, low weight, excellent thermal insulation, acoustic damping, ease of repairs when compared to other conventional laminated composites. In spite of having these advantages, sandwich composite structures are sensitive to impact loading and may be subjected to various impacts such as tool drops, bird strikes, runway debris and hail storms during the service life. These impacts cause reduction in the strength of the structures.

To ensure the reliability and safety of sandwich composite structures, impact behavior of sandwich composite structures are intensively studied by many researchers for a long time. Impact behavior of sandwich structures is mainly affected by core and face sheet materials and their thickness. Some of the relevant previous studies are presented in the below.

(Anderson & Madenci, 2000) investigated the low velocity impact response of sandwich composites, experimentally. They used a variety of sandwich configurations with graphite/epoxy face sheets and foam or honeycomb cores. The impact damage was utilized in the foam and honeycomb cores by using destructive and non-destructive test methods. Impact response of sandwich composite panels with PVC foam core and balsa wood core was studied by (Atas & Sevim, 2010). They performed a number of tests under various impact energies. To analyze the damage process of the sandwich composites, they obtained load-deflection curves and energy profile diagrams. They observed damage modes including fiber fractures at upper and lower skins, delaminations between glass-epoxy layers, core shear fractures and face/core debonding.

(Dear, Lee, & Brown, 2005) studied the impact toughness of different lightweight sandwich panels and composite sheet materials. They prepared the specimens from sheet moulding compound (SMC), glass mat thermoplastic (GMT) and honeycomb sandwich panels employing different skin and core materials. (Hazizan & Cantwell, 2002) studied the low velocity impact response of 11 sandwich structures based on low density polymeric foams. They obtained different failure modes and observed that the dynamic response of sandwich structures depends on elastic properties of the foam core material. Xiong et al. (2012) performed quasi-static uniform compression tests and concentrated on low velocity impact tests to reveal the failure mechanisms and energy absorption capacity of two-layer carbon fiber composite sandwich panels with pyramidal truss cores. They fabricated three different volume-fraction cores having different relative densities. They obtained the failure modes and deformation mechanisms of carbon fiber sandwich composite and compared with glass fiber woven textile truss cores.

Impact, compression after impact, and tensile stiffness properties of carbon fiber and Kevlar combination sandwich composites were investigated by (Gustin, Joneson, Mahinfalah, & Stone, 2005). The impact-side face sheets consisted of different combinations of carbon fiber/Kevlar and carbon fiber/hybrid while the bottom face sheets remained entirely carbon fiber. They have obtained information about absorbed energy and maximum impact force. Park et al. (2008) investigated the damage resistance of sandwich structure. The Nomex[®] honeycomb core was selected as a core material, having thicknesses of 10 mm and 20 mm and two kinds of face sheets (carbon/epoxy and glass/epoxy laminates) were used and samples were exposed to low velocity impact. Results show that their impact response was greatly influenced by core thickness and the effect of core thickness varied with the face sheet materials. Mohan et al. (2011) investigated the impact responses of aluminum foams with various tailored face sheets and foam thicknesses. They carried out the experiment by using hemispherical indenters on blocks of aluminum foam with and without the face sheet. Their results show that increase in thickness of foam and the use of face sheet enhance the impact energy absorption capacity. (Sawal & Akil, 2011) performed low velocity impact tests on sandwich panels composed of

aluminum face sheets and thermoplastic honeycomb cores to characterize the impact performance as a function of core thickness and drop heights. They evaluated and compared impact parameters such as maximum impact force, impact energy and impact damage area. They found that panels with thicker core exhibited higher impact force than thinner core counterparts. (Herup & Palazotto, 1997) performed low velocity impact and static indentation tests on sandwich plates composed of 4 to 48 ply graphite/epoxy cross-ply laminate face sheets and Nomex honeycomb cores to characterize damage initiation as a function of face sheet thickness and loading rate.

The effect of integrated sandwich structure with an orthogrid stiffened syntactic foam core on impact characterization was investigated by (Li & Muthyala, 2008). To evaluate the impact response, they performed the low velocity impact tests and compression after impact (CAI) tests. C-scan and SEM observation were implemented to investigate the impact damage. They have observed that the integrated core enhanced the impact energy transfer and energy absorption. Impact response of integrated sandwich core composites was carried out by (Vaidya, Hosur, Earl, & Jeelani, 2000). They considered three thicknesses of integrated and functionality-embedded E-glass/epoxy sandwich core, including 6, 9 and 17 mm. They have observed that the functionality-embedded cores provided enhanced low velocity impact resistance due to additional energy absorption mechanisms. (Hosur, Abdullah, & Jeelani, 2005) investigated the foam filled 3-D integrated core sandwich composite laminates with and without additional face sheets. For additional facing, they used plain weave S2-glass and twill weave carbon fabrics on top and bottom sides of the panels in four different monolithic combinations. They evaluated and compared the peak load, deflection and absorbed energy for different types of laminates and studied the failure modes by sectioning the samples and observing under optical microscope.

(Avila, Carvalho, Dias, & Cruz, 2009) studied the influence of nano-structures on sandwich composites under impact loadings. They prepared a set of sandwich plates made of fiberglass/nano-modified epoxy face sheets and polystyrene foams. The fiber volume fraction used was around 65%, while the nanoclay content varied from

0 wt.% to 10 wt.%. The results show that the addition of 5 wt.% of nanoclay leads to more efficient energy absorption. (Bhuiyan, Hosur, & Jeelani, 2009) evaluated the low velocity impact behavior of sandwich panels which consist of different types of core (neat and nanophased) and biaxial braided carbon fiber/epoxy face sheets. They have observed that nanophased foams have smaller damage area than neat counterparts. Also, nanophased foams have higher peak loads compared with the neat foam sandwich.

(Apetre, Sankar, & Ambur, 2006) investigated the effects of functionally graded core properties such as core and face sheet thickness. The two-dimensional elasticity equations for the plane sandwich structure were solved using a combination of Fourier series and Galerkin method. Results indicate that the contact stiffness of the beam with graded core increases causing the contact stresses and other stress components in the vicinity of contact to increase. A genetic algorithm was implemented for optimization of sandwich panel with laminated composite face sheets by Kalanteri et al. (2010). They investigated the effect of ply angles of the face sheets to maximize the strength of panel. The results show that the stacking sequence of face sheets plays an important role in the strength of the composite sandwich panels.

Two-layer panels with polymer matrix composite laminated face sheets and a thin internal sheet subjected to low velocity impact were studied by (Jiang & Shu, 2005). The commercial LS-DYNA3D software was used to model and analyze the dynamic problem. They have observed that the local displacement of the core along the direction of the impact has been decreased significantly by introducing the internal sheet into a traditional single sandwich structure. Two types of sandwich panels with carbon epoxy skins and aluminum honeycomb core were investigated using finite element methods by Davies et al. (2004). They prepared the samples from thin skin-thick core and thick skin-thin core and performed low velocity impact and compression after impact tests. They obtained that panels which consist of thin skin-thick core have the worst CAI strength. Three-dimensional finite element simulations were conducted for analyzing low velocity impact behavior of sandwich beams with

a functionally graded core by (Etemadi, Khatibi, & Takaffoli, 2009). Using analytical data, the effects of projectile initial velocity and kinetic energy, as well as the beam's dimensions on the impact behavior and indentation and displacement history were studied. Results show that for sandwich beams having functionally graded cores, the maximum contact force increases and the maximum strain decreases compared to sandwich beams with homogenous core.

Salehi-Khojin et al. (2007) presented the impact response of sandwich composites with Kevlar/hybrid and carbon face sheets subjected to different temperatures. Specimens were tested at temperature range of -50°C to 120°C and were subjected to low velocity impact energies of 15J, 25J and 45J. It is seen that impact performance of these sandwich composites changes over the range of temperature, significantly. Impact properties and fatigue properties of sandwich composites subjected to low velocity impact were studied by Freeman et al. (2005). Two and four layer face sheet carbon fiber sandwich composite samples with foam filled honeycomb core having high and low densities were used in the tests. After impact, the area of damage was determined using ultrasonic techniques. The fatigue life was then determined and compared to the fatigue life of non-impacted samples in a four point bending test.

(Schubel, Luo, & Daniel, 2005) investigated the low velocity impact behavior of sandwich panels consisting of woven carbon/epoxy and a PVC foam core. Samples were impacted with a drop mass setup and the load, strain and deflection values were obtained. They characterized and quantified the damage area after the tests. Experimental results were compared with analytical and finite element model analysis and found to be in good agreement. (Besant, Davies, & Hitchings, 2001) examined dynamic analysis of the sandwich panels consisting of carbon fiber skins supported by an aluminium honeycomb core, experimentally and numerically using finite element procedure. The obtained results were compared with the experimental data and a good agreement was seen.

The primary objective of this thesis is to investigate the effects of core material and its thickness on the impact behavior of sandwich composites subjected to low velocity impact, experimentally. In this context, contact force versus time, contact force versus deflection and maximum contact force, maximum deflection, maximum contact time and absorbed energy versus impact energy graphs have been drawn for each impact energy level and comparisons between of core materials and their thicknesses have been made.

CHAPTER TWO

ESSENTIAL BACKGROUND AND IMPACT CHARACTERIZATION OF SANDWICH COMPOSITES

2.1 Introduction

Composite materials can be described as a combination of two or more materials which results in better properties than those of the individual components used alone. In contrast to other alloys, each material keeps its separate chemical, physical and mechanical properties. In a composite material, there are two constituents as a reinforcement and a matrix. The reinforcement is usually fiber or a particulate and the strength, stiffness and load carrying are provided by reinforcing phase. The continuous phase is the matrix, which is classified as a polymer, metallic and ceramic. The matrix performs several functions, including maintaining the fibers in the adequate orientation, spacing and protecting them from abrasion and the environment (Campbell, 2010).

2.2 Sandwich Composites

“A structural sandwich typically consists of two thin ‘face sheets’ made from stiff and strong relatively dense material such as metal or fiber composite bonded to a thick lightweight material called ‘core.’” (Carlsson & Kardomateas, 2011, p.1). Schematic drawing of a sandwich composite is given in Figure 2.1.

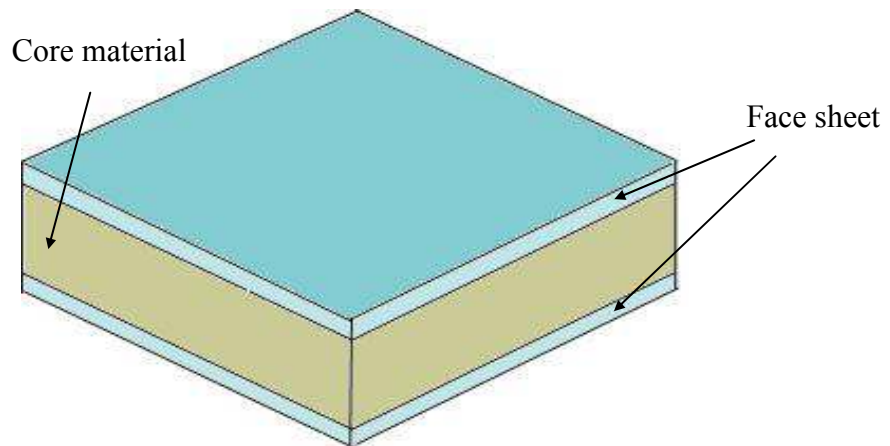
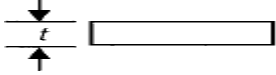
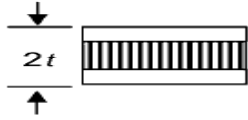
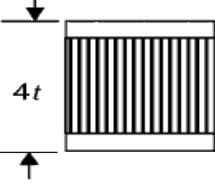


Figure 2.1 Schematic drawing of a sandwich composite

The core material carries the shear loads and provides the shear strength to the sandwich composite. Face sheets materials carry the bending loads in a sandwich composite and are glued to the core material. By choosing the appropriate core and face sheets materials, it is possible to obtain more efficient structures compared to solid panels (Table 2.1). It is seen that stiffness is increased over seven times by doubling the core thickness with three percent weight gain and is increased over thirty-seven times by quadrupling the core thickness with six percent weight gain.

Table 2.1 Efficiency of the sandwich structure (Campbell, 2010)

			
	Solid Material	Sandwich Construction	Thicker Sandwich
Stiffness	1.0	7.0	37.0
Flexural Strength	1.0	3.5	9.2
Weight	1.0	1.03	1.06

Sandwich composite materials can be classified two broad parts as the type of facing sheets and the type of core used.

2.2.1 Face Sheet Materials

Face sheet materials can be made from aluminum, glass, carbon, aramid and stainless steel. Also, resin impregnated paper, plaster board, glass reinforcement cement are used as face sheet materials. The thicknesses of face sheet materials commonly vary from 0.25 to 3 mm.

The most common face sheet materials for the polymer matrix composites are glass fibers which are divided three types as E-glass, S-glass and C-glass.

In this thesis, E-glass fiber was used as facing sheet materials of sandwich composite.

2.2.2 Core Materials

Core materials consist of honeycomb core, open and closed cell foams and corrugated core (Figure 2.2). The densities of core materials vary from 16 to 480kg/m³.

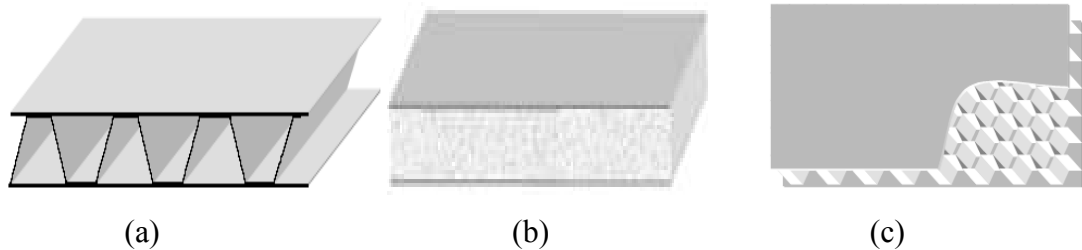


Figure 2.2 Sandwich panels with (a) corrugated (b) foam and (c) honeycomb core (Petras, 1998)

In a sandwich composite, the core is an important element. The honeycomb cores, which are commonly used in aeronautical applications, are usually manufactured from an aluminum foil. Unfortunately, these are expensive and cannot resist the high impact loads very well. The corrugated cores are used marine and packaging industry. The foam cores are used intensely commercial applications like boat building and light aircraft construction. Cost versus performance for core material is given in Figure 2.3. As seen in the figure, honeycomb cores are more expensive than foam cores. But, they can offer superior performance to the sandwich composite.

In this thesis, PVC and PET foams are used as core material.

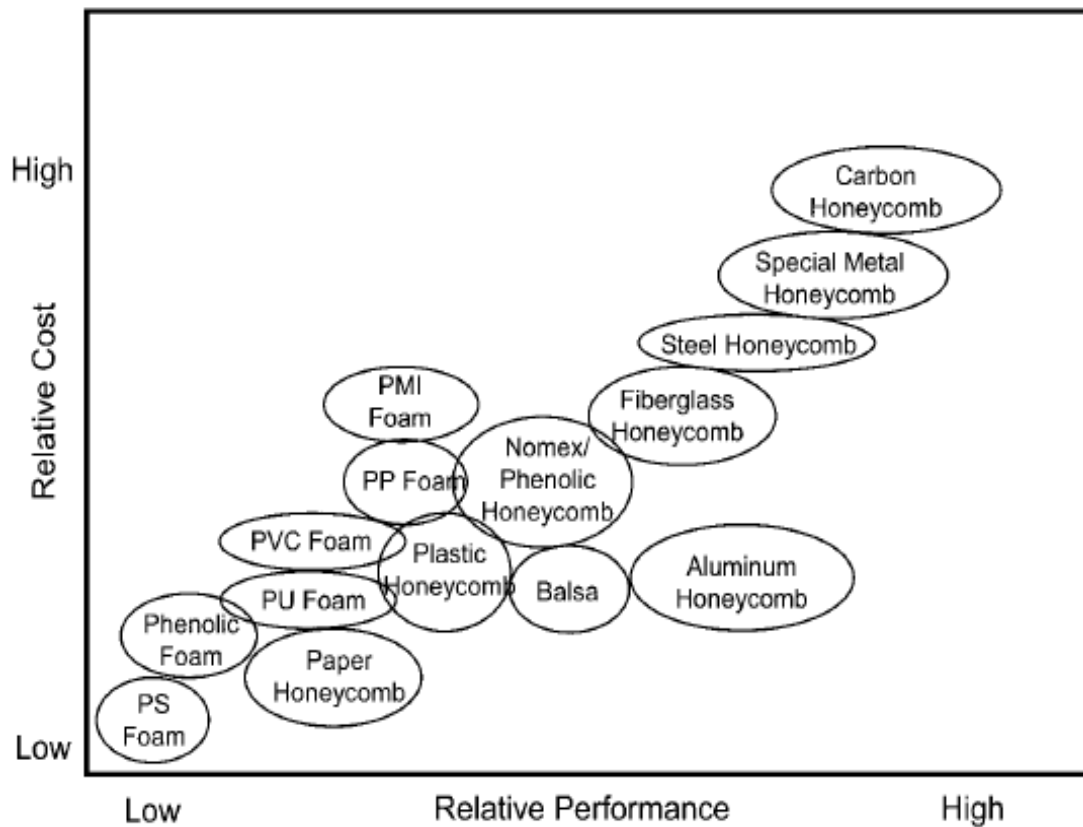


Figure 2.3 Cost versus performance for core material (Campbell, 2010)

2.3 Vacuum Assisted Resin Infusion Molding Process (VARIM)

Most composite sandwich panels are manufactured by vacuum assisted resin infusion molding process (VARIM). There are several materials, which are used in the VARIM process, as shown in Figure 2.4.

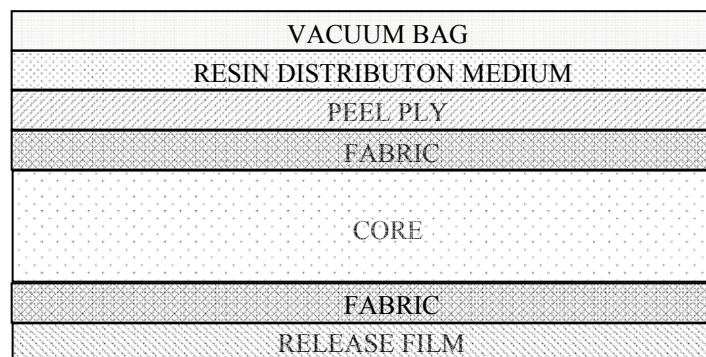


Figure 2.4 Schematic drawing of components of VARIM process

In this process, the mold surface is covered with release film in order to prevent resin to the mold surface during manufacturing. Then, the fabrics place on the release film. The core material is set between the fabrics. The peel ply and resin distribution medium place on the fabrics, respectively. The peel ply provides clean and uncontaminated surface to the composite and resin distribution medium spreads the resin equally and quickly over the fabrics. The final element is vacuum bag which seals all surface of the system. So, a closed system is occurred. By the help of the vacuum, resin is penetrated to dry fabrics. After that, the curing process is carried out all the system.

The most common sandwich composite products manufactured by the VARIM process are spacecraft structures, blades for wind-power generation, sailboats, racing cars, bridge decks etc. Also, composites materials are repaired by using this process. Some of the examples of sandwich composites are shown in Figure 2.5.



Figure 2.5 Examples of sandwich structures (Carlsson & Kardomateas, 2011)

The all specimens, which were used in this thesis, were manufactured by using VARIM process.

2.4 Impact Properties of Sandwich Composites

Impact may be defined as the rapid application of impulsive load to a specific volume of material or part of a structure. The impact response of materials generally

classified into low (large mass) velocity, intermediate velocity, high/ballistic (small mass) velocity, and hyper velocity regimes as shown in Figure 2.6. Low velocity impact (LVI) is also known large mass impact results from stemming from tool drops, which generally occur at velocities below 10m/s . Blast debris, hurricane and tornado debris, and foreign object debris on roads are the some examples of intermediate velocity regime and occur in the 10m/s to 50m/s range. Intermediate velocity regime shows both low and high velocity impact characteristics. High velocity impact is typically a result of small arms fire or explosive warhead fragments and occur in the 50m/s to 100m/s range. The last impact regime is hyper velocity impact which occurs bigger than $2 - 5\text{km/s}$ velocity range. This regime is commonly studied in the context of developing protection against micrometeorites of objects and personnel in low earth orbit (Abrate, 2011).

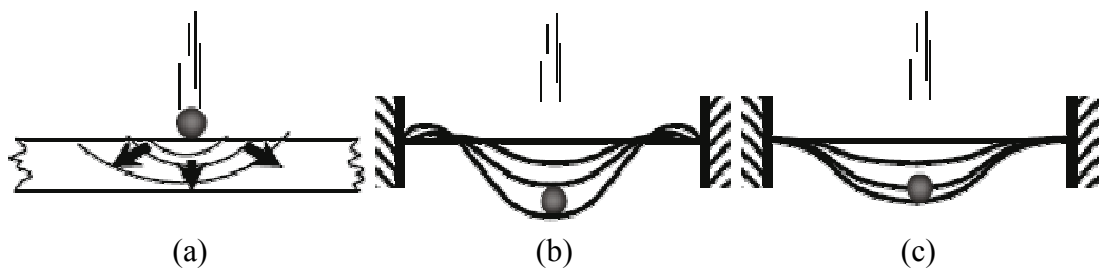


Figure 2.6 Impact Regimes; (a) ballistic impact, very short impact times with dilatational wave dominated response, (b) intermediate velocity impact, short impact times with flexural and shear wave dominated response, and (c) low velocity impact, long impact times with quasi-static response (Abrate, 2011)

In this thesis, the tests were performed at low velocity impact regime.

2.5 Impact Test Equipment of Low Velocity Impact (LVI)

There are several test equipment which was conducted the LVI testing of composites. The impact is generally explained the use of a swinging pendulum, dropping weight, a rotating flywheel or a gas-gun driven projectile. The most common test systems for LVI are Charpy and Izod test systems and Instrumented falling weight impact testing (Abrate, 2011).

2.5.1 Charpy and Izod Test Systems

These test systems were initially developed for the testing of isotropic materials, see Figure 2.7. When the kinetic energy of a striking mass is varied, energy is transferred to specimen and work is done on the specimen. In the Charpy and Izod test systems, the specimen is supported as a simple beam and a cantilever beam, respectively. Charpy specimens may be fabricated U and V notches on the tension side in the center of the specimen. As the fracture phenomenon is more complex in the polymer composites, these test systems may not be adequate to represent a realistic impact condition (Abrate, 2011).

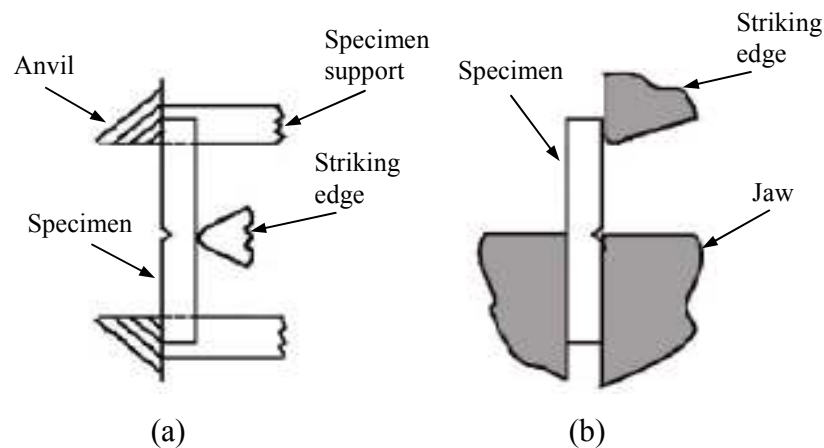


Figure 2.7 (a) Charpy and (b) Izod test systems (Abrate, 2011)

2.5.2 Drop Weight Impact Test Systems

The drop-weight test systems use the free fall of a specific weight to supply the energy to break a beam or a plate specimen. The drop-weight testing apparatus are illustrated in Figure 2.8. The specimen can be either simply supported or fixed. The kinetic energy of falling mass is adjusted by changing its drop height. The impact load on the specimen is calculated by instrumenting either the striking head or the specimen supports (Mallick, 2008).

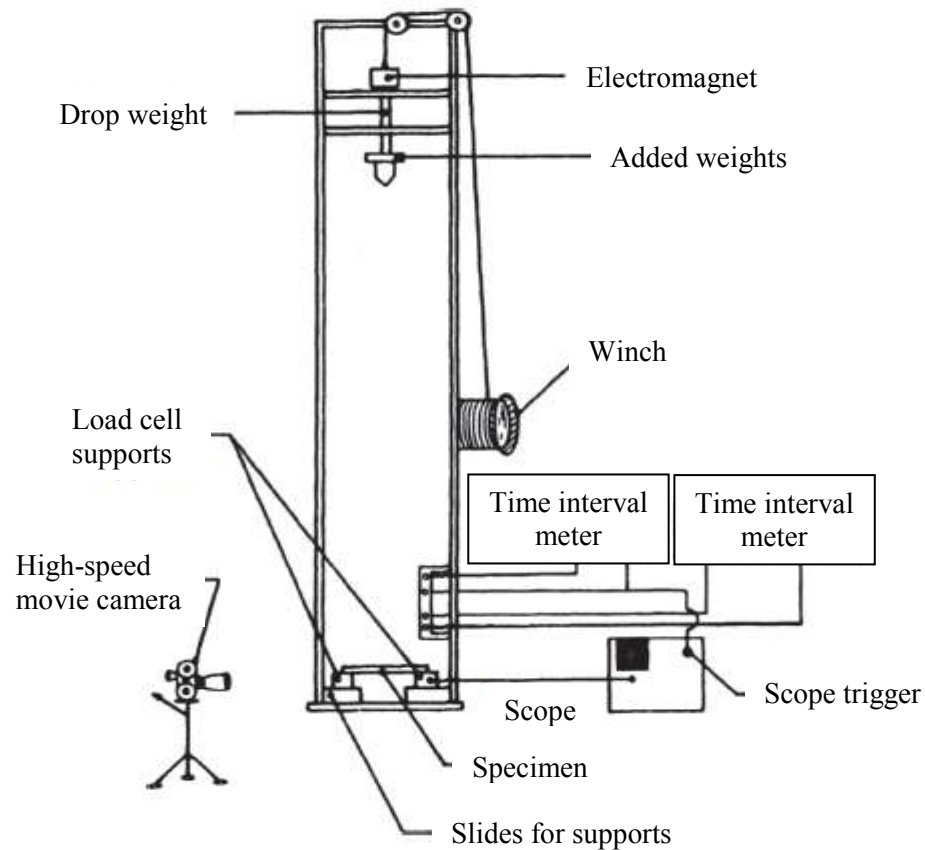


Figure 2.8 Schematic illustration of drop-weight impact test (Mallick, 2008)

2.6 Failure Modes in Low Velocity Impact

Even though many macroscopic and microscopic failure modes occur after low velocity impact, the heterogeneous and anisotropic nature of fiber reinforced plastic laminates typically give rise to four primary failure modes. These are matrix cracking, delamination, fiber failure and penetration. The interaction between these failure modes influences damage modes initiation and propagation (Abrate, 2011).

2.6.1 Matrix Cracking

Because matrix material is more breakable than fibers, matrix cracking occurs in brittle matrix like epoxy in the impact loading. When the composite structure is subjected to impact loading, cracks initially form in the matrix. There are two kinds of matrix cracks in the literature such as shear cracks and tensile cracks (Figure 2.9).

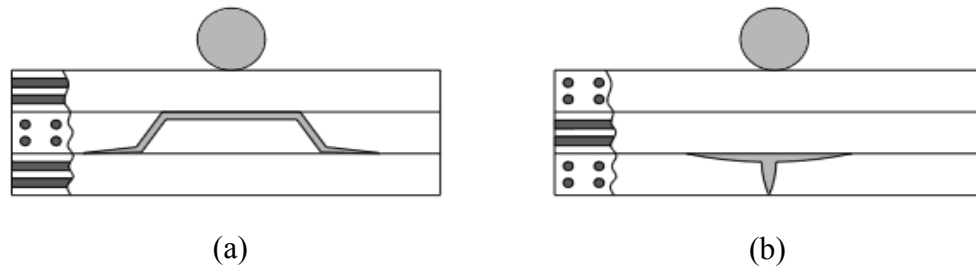


Figure 2.9 Two types of matrix cracking; (a) tensile crack, (b) shear crack (Abrate, 1998)

When in-plane normal stresses exceed the transverse tensile strength of the ply, tensile cracks occur. Shear cracks are at an angle from the mid-surface, which indicates that transverse shear stresses play a significant role in their formation. Because of the high, localized contact stresses, in thick laminates, matrix cracks occur in the first layer impacted by the impactor. Damage advances like a pine tree pattern from the top to down as shown in Figure 2.10-a. For thin laminates, matrix cracks can be introduced in the lowest layer because of the bending stresses in the back side of the laminate (Figure 2.10-b). And, damage again advances a pattern of matrix cracks and delaminations (Abrate, 1998).

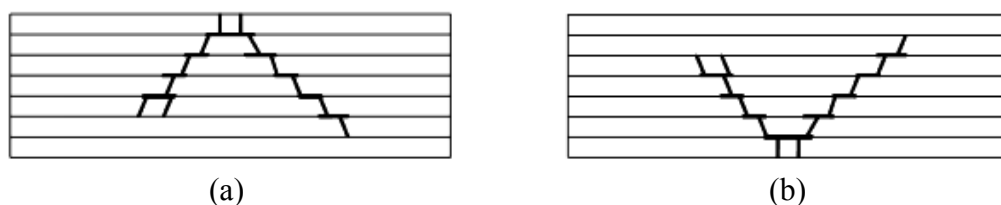


Figure 2.10 Pine tree (a) for thick laminate (b) for thin laminate (Abrate, 1998)

2.6.2 Delamination

A delamination is a separation of plies which runs in the rich resin area between adjacent laminas. If two adjacent plies have the same fiber orientations, delaminations will not be introduced at the interface between plies. This damage reduces the strength of the laminate (Abrate, 1998). For $[0/90]$ laminates, the delamination type becomes as a peanut and delamination elongation oriented in the fiber direction. These results have been commonly studied in the literature (Choi & Chang, 1992; Joshi & Sun, 1985; Wu & Springer, 1988).

2.6.3 Fiber Failure

In the impact loading, fiber failure occurs later than the matrix cracking and delaminations. Because of the locally high stresses and indentation effects, fiber failure typically occurs below the impactor. On the other hand, this damage occurs on the non impacted face due to high bending stresses. Fiber failure is a precursor to the catastrophic penetration mode which increases by increasing the areas of fiber matrix debonding (Dorey, 1988).

These are macroscopic modes of failure.

2.6.4 Penetration

Penetration, which is microscopic failure mode, occurs when the fiber failure reaches the critical extent, enabling the impactor to completely penetrate the structure. (Cantwell, Curtis, & Morton, 1989) observed that the impact energy penetration threshold rises rapidly with specimen thickness. Shear out, delamination and elastic flexure are the major forms of energy absorption during laminate penetration and shear out accounts for % 50-60 depending on the plate thickness. Fiber sizing, orientation, weave architecture, matrix type and interface have an influence on the penetration process (Abrate, 2011).

2.7 Low Velocity Impact of Sandwich Composites

In a sandwich composite, the low velocity impact damage occurs as follows;

- Face sheet of the impact side is subjected to transverse shear force. If the face sheet resists penetration, there is extensive damage limited to face sheet. Some debonding can occur between the face sheet and core material because of the strain mismatch. If the impact energy is increased, the impactor penetrates the top face sheet and progress into the core material.

- The core failure occurs in the form of cell crushing, shear failure and debonding of the face sheet to the core.
- Then, face sheet of the tensile side gets loaded by the impactor, causing tensile bending on the back face. After all, the debonding area between the core to the back face sheet is extensive. Important delamination of the back face sheet can occur before complete penetration of the impactor.

Impact damage modes in a sandwich composite depend on the panel support condition, projectile shape, geometric and material properties of face sheet and core material. If the face sheet is thin (< 10 times the core thickness), the deflections tend to be large and high in-plane tensile forces cause tensile cracking in the core. If the face sheet is thick ($< 2 - 5$ times the core thickness), the deflection is less than the face sheet thickness and transverse shear forces cause shear cracking in the core (Abrate, 2011).

CHAPTER THREE

EXPERIMENTAL STUDY

3.1 Introduction

In this chapter, the experimental overview of the thesis is presented in two subchapters. First subchapter is about the production and preparation of the sandwich and laminated composite specimens. Mechanical properties of the core materials and unidirectional glass/epoxy composite are given in this subchapter. Second subchapter is related to impact characterization of the sandwich composite plates. Also, the impact testing machine which was used in this study will be introduced in this subchapter.

3.2 Manufacturing of Sandwich Composite Plates and Material Preparation

In this study, all sandwich and laminated composite specimens, which have been impacted, were manufactured using vacuum assisted resin infusion molding process (VARIM) in the Composite Research Laboratory of Dokuz Eylül University in İzmir. E-glass fabrics ± 45 and $0/90$ having density of 300 g/m^2 were used as reinforcing material and Epoxy ARALDITE LY 1564 SP resin and ARADUR 3487 B hardener were selected as matrix material. The mixing ratio of the resin and hardener was 3/1. After the resin and hardener have been mixed by the drill with mixer apparatus, they implemented the sandwich panels via vacuum infusion process. The curing process was carried out at 80°C for 8 h. Because heat transfer coefficient of foam material was low, upper face of the sandwich panels were heated by the infrared heatings during curing process, as shown in Figure 3.1. Therefore, the homogeneous temperature distribution was obtained in the upper face of the sandwich panels. After that, the composite plates were cooled to room temperature. The orientation of the sandwich composites manufactured was $[\pm 45/0/90/\textit{core}/90/0/\mp 45]$. Also, another composite plate was manufactured without core material from stacking sequence $[\pm 45/0/90]_s$ to analyze the effect of

core material on low velocity impact behavior. All specimens were obtained in the form of 0.75 m^2 composite panels.

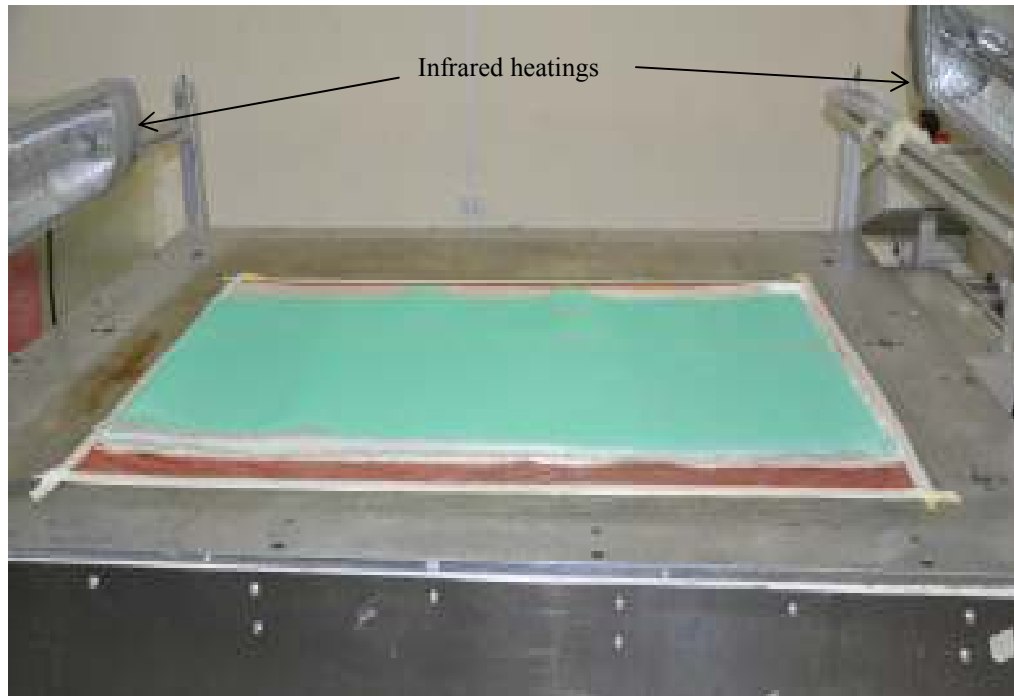


Figure 3.1 Photo of sandwich panels fabrication layout

In this study, three different core materials were used in manufacturing sandwich composites.

- PET: PET foam (AIREX T.90.60)
- PVC-1: PVC foam (AIREX C.71.55)
- PVC-2: PVC foam (AIREX R.63.50)

In the next pages of the thesis, PET, PVC-1 and PVC-2 were used instead of the trade name of the core materials.

To obtain the mechanical properties of the unidirectional glass/epoxy, $[0]_8$ oriented laminated composite plate was manufactured. Thickness of specimens is approximately 2.15 mm. Laminated composite plate is cut according to ASTM standards. All tests were performed by using SHIMADZU tension-compression test

machine having capacity of 100 kN at a ratio of 2 mm/min in the Composite Research Laboratory of Dokuz Eylül University.

To determine the tensile properties, ASTM D3039-76 test method was used. Longitudinal Young modulus E_1 , poisson ratio ν_{12} and longitudinal tensile strengths X_t are obtained by using longitudinal $[0]_8$ samples. Transverse Young modulus E_2 and transverse tensile strengths Y_t are also obtained by using transverse $[90]_8$ samples.

To determine the compressive properties, ASTM D3410-87 test method was used. Longitudinal and transverse compressive strengths (X_c and Y_c) are obtained by using longitudinal $[0]_8$ and transverse $[90]_8$ samples, respectively.

ASTM D3518/D3518M-91 test method was used to determine the shear strength and shear modulus, S_{12} and G_{12} , respectively. Specimens for this test method are cut in the $[\pm 45]_{2s}$ orientation.

Mechanical properties of unidirectional glass/epoxy composites are given in Table 3.1.

Table 3.1 Mechanical properties of the unidirectional glass/epoxy composite

Properties	Magnitude
longitudinal modulus, E_1	28.60 GPa
transverse modulus, E_2	10.76 GPa
poison's ratio, ν_{12}	0.26
longitudinal tensile strength, X_t	653 MPa
transverse tensile strength, Y_t	62 MPa
longitudinal compressive strength, X_c	301 MPa
transverse compressive strength, Y_c	100 MPa
in-plane shear modulus, G_{12}	7.39 GPa
in-plane shear strength, S_{12}	56 MPa

The thicknesses of core material were selected 5, 10 and 15 mm for every foam to investigate the effect of core thickness on low velocity impact behavior. The mechanical properties of the core material given in Table 3.2 are taken from manufacturer's data sheet. The orientation of face skins was selected identical in every type of sandwich composite panels. The core material and its thickness were only varied in this study.

Table 3.2 Mechanical properties of the core materials (Typical properties for AIREX®, <http://www.metyx.com/Turkish/Composites>)

Typical properties for core materials		Unit (metrical)	Value	T.90.60 <i>PET</i>	C.71.55 <i>PVC-1</i>	R.63.50 <i>PVC-2</i>
<i>Density</i>	ISO 845	kg/m ³	Average Typ. range	65 60-70	60 54-69	60
<i>Compressive strength</i>	ISO 844	MPa	Average Min.	0.80 0.7	0.95 0.85	0.38
<i>Compressive modulus</i>	DIN 53421	MPa	Average Min.	50 35	70 60	30
<i>Tensile strength</i>	ASTM C297	MPa	Average Min.	1.5 1.2	1.5 1.0	0.90
<i>Tensile modulus</i>	ASTM C297	MPa	Average Min.	85 70	42 30	30
<i>Shear strength</i>	ISO 1922	MPa	Average Min.	0.46 0.4	0.93 0.7	0.50
<i>Shear modulus</i>	ISO 1922	MPa	Average Min.	12 10.5	21.5 18	11

As shown in Table 3.2, the densities of core materials were selected low and nearly same each other. The mechanical properties of specimens with PVC-2 core except for shear strength are the lowest when compared to other type of core materials.

After the curing process was over, the sandwich and laminated composite panels were cut into the squares which every specimens have the edge length of 100 mm. Finished specimens for every type and thickness of core material are shown in Figure

3.2. The final thickness and weight of the composite specimens manufactured without core material are approximately 2.12 mm and 33 g, respectively. The final thicknesses of all type of the sandwich composite specimens having 5 mm, 10 mm and 15 mm core thickness are approximately 7.12 mm, 12.12 mm and 17.12 mm, respectively and the final weights of the specimens are given for every core material and thickness in Table 3.3.

Table 3.3 Final weights for every core material and thickness

Core Type	Final weight for 5 mm (g)	Final weight for 10 mm (g)	Final weight for 15 mm (g)
PET	47.1	50.6	54.4
PVC-1	40.8	45.9	49.7
PVC-2	36.6	41.8	47.2

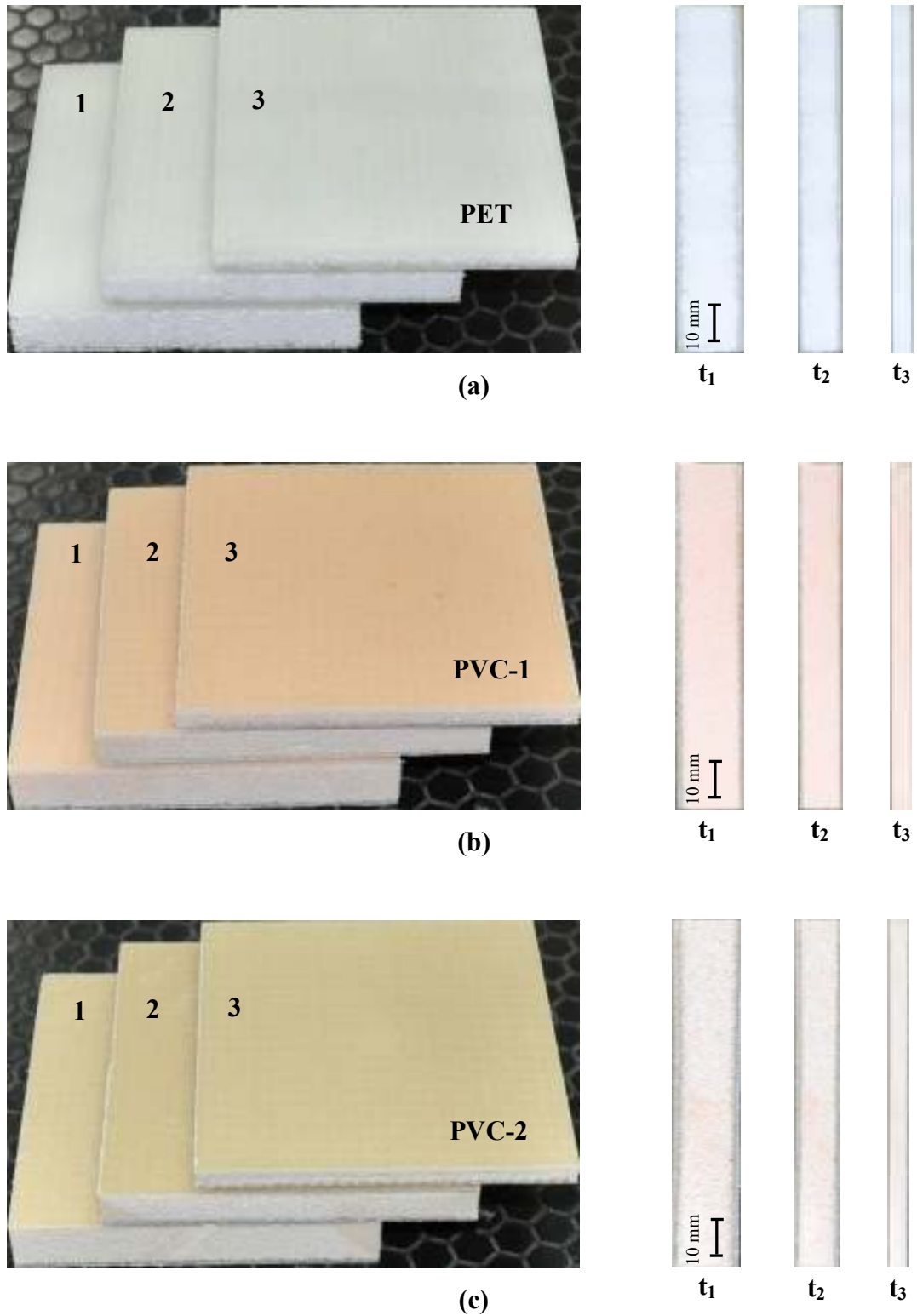


Figure 3.2 Photos of finished test specimens with (a) PET (b) PVC-1 and (c) PVC-2 cores having thicknesses of $t_1=15$ mm, $t_2=10$ mm and $t_3=5$ mm

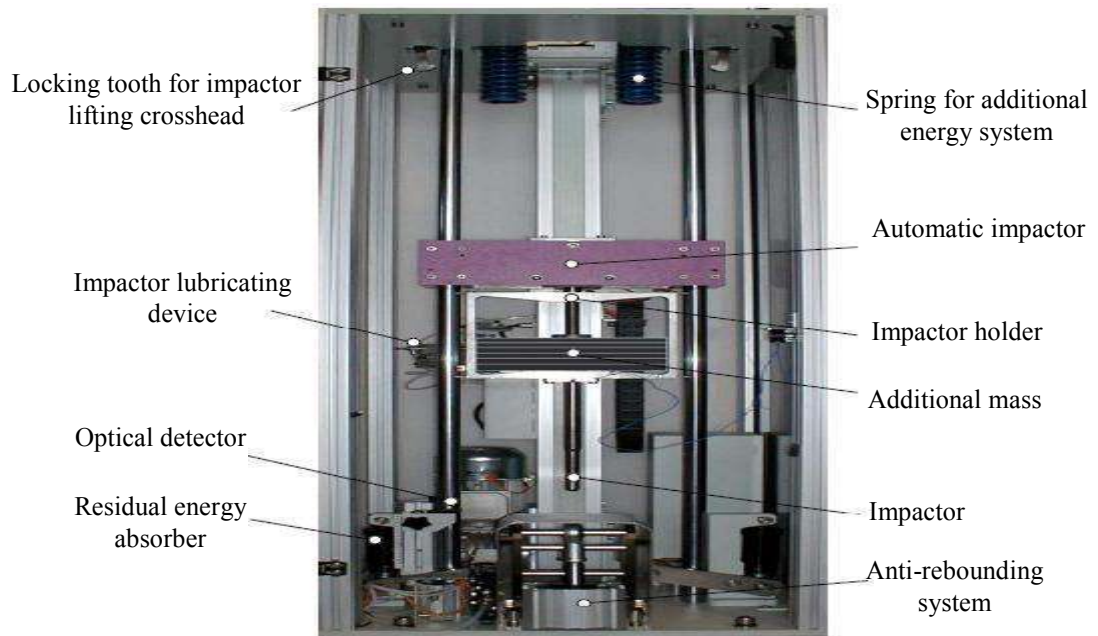
3.3 Impact Test

In this study, The Fractovis Plus impact testing machine in the Composite Research Laboratory of Dokuz Eylül University was used to conduct the low velocity impact tests, as shown in Figure 3.3. A broad range of applications requiring from low to high impact energies can be performed with this machine. The impactor, which was used to strike the specimens, is a hemispherical indenter with a 12.7 mm diameter and attach to maximum loading capacity of 22.4 kN piezoelectric force transducer. The total falling mass of the impactor is 5 kg (included impactor and crosshead mass). There is an anti-rebounding system in the testing machine to prevent the repeated impacts on the specimen. The drop-weight testing machine generates up to 1800 J maximum potential energies via the additional mass and this additional mass increases the speed of the impactor up to 24 m/s. A data acquisition system (DAS), which allows acquiring 16000 data throughout the tests, was used to perform the history of the impact event.

The impact energies for this study were selected 10J, 20J, 25J, 30J, 35J, 40J, 50J and 70J to investigate the impact energy effect on the low velocity impact behavior of sandwich composites. Each test was repeated five times and average values and standard deviations were calculated for every parameter. Impact characteristics such as contact force versus time, contact force versus deflection and absorbed energy, maximum contact force, maximum deflection and maximum contact time versus impact energy curves were obtained for some special impact energy levels such as 15J, 25J, 30J and 40J. The test results are given in the next chapter.



(a)



(b)

Figure 3.3 (a) Fractovis Plus impact test machine and its equipment and (b) upper part of test machine

CHAPTER FOUR

RESULTS AND DISCUSSION

4.1 Impact Tests

After the impact tests, three specific tests results may be occurred in a specimen including *rebounding*, *penetration* and *perforation* as shown in the Figure 4.1. In Figure 4.1, the contact force-time curve is shown for three specific cases. It is obviously seen that, the contact force increases by increasing the impact energy. The contact force reaches the zero and the curve looks like a mountain shape in the rebounding case. With increasing the impact energy, rebounding case goes to penetration and perforation cases, respectively. The contact force never becomes zero in the perforation case because of the friction which occurs between the impactor and specimen (Aktas, 2007).

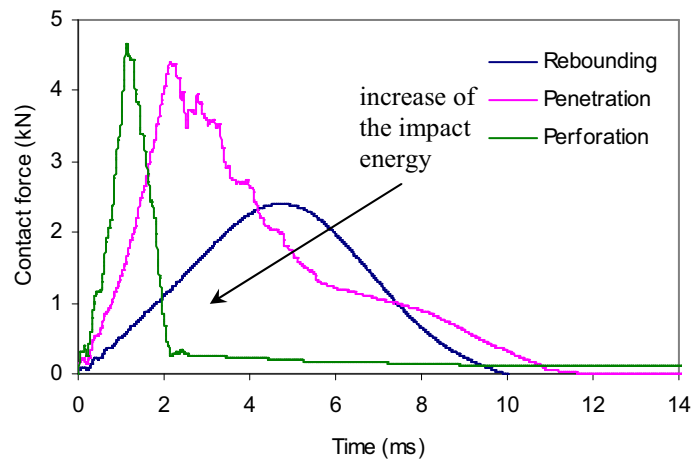


Figure 4.1 Contact force versus time curve

Absorbed energy (E_a) and impact energy (E_i) are two important parameters to evaluate the impact characterization of composite plates. The absorbed energy is energy which absorbed by the composite specimen during the impact event. The impact energy is defined as the total energy implemented to a composite specimen. The energy profile diagram shows the relationship between the impact energy and absorbed energy. And, this method gives us some impact properties such as penetration (P_n) and perforation (P_r) thresholds.

The energy profile diagram consists of three regions AB, BC and CD as shown in Figure 4.2. AB region shows the rebounding (non-penetrated) case. In this region, the curve is under the equal energy line. The excessive energy (E_e) retained in the impactor and rebound the impactor from the specimen (Liu, 1998). BC region represents the penetration case and in this region, the total impact energy is absorbed by specimen. CD region stands for perforation case. Absorbed energy remains nearly constant (Aktas, 2007).

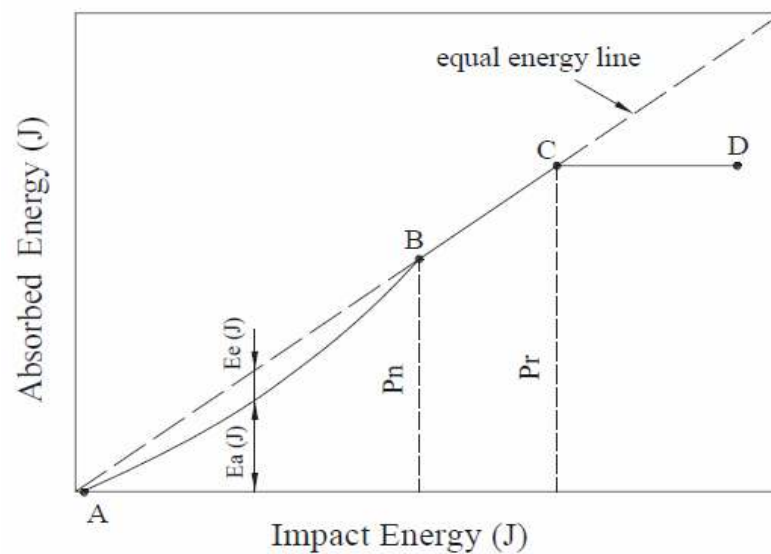
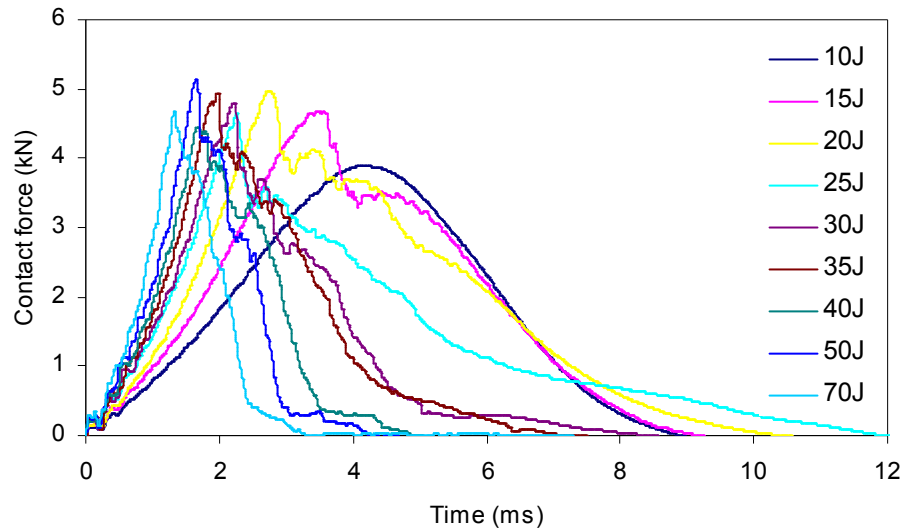


Figure 4.2 Energy profile diagram of composite structure (Aktas, 2007)

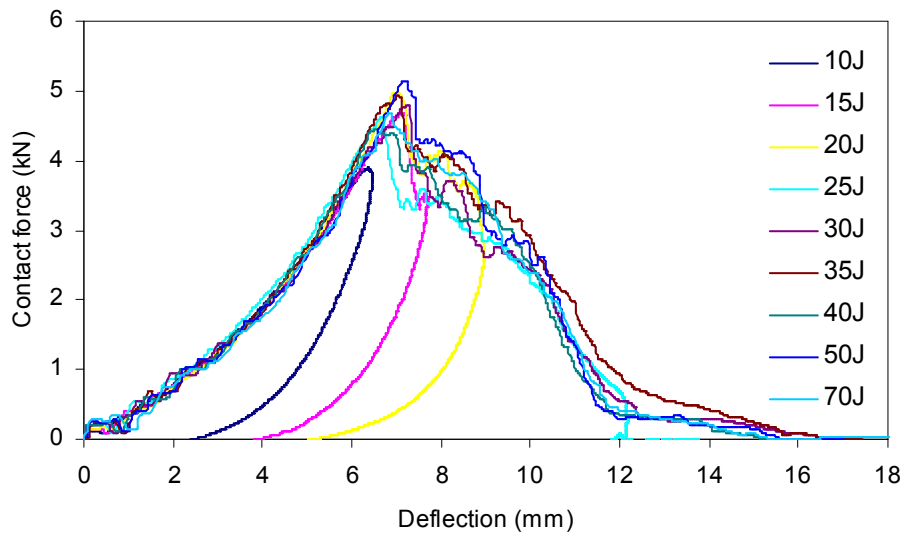
Impact tests were conducted on at least of five specimens for each experimental parameter (increased from 10J to 70J impact energies and specimens with PET, PVC-1 and PVC-2 foam cores, having 5 mm, 10 mm and 15 mm core thicknesses and also composite plate manufactured without core material).

Contact force-time and deflection histories of specimens manufactured without core material and with PET foam core, having 10 mm core thickness impacted at 10J, 15J, 20J, 25J, 30J, 35J, 40J, 50J and 70J are given for an example in Figure 4.3-4, respectively. It is seen from the Figure 4.3.a-b, contact time increases by increasing the impact energy level until 25J. Then, it decreases rapidly. Because, 25J energy level is the penetration-perforation transition energy. Also, with increasing the impact energy level, the deflection of the specimens increases. Contact forces do not change significantly with increasing the impact energy level after 20J. Unloading

portions of the contact force-deflection curves return after peak contact force in the parallel to loading portion of the curves in the rebounding cases (10J, 15J, 20J). In the penetration (25J) and perforation (30J, 35J, 40J, 50J and 70J) cases, unloading portions of the curves do not return parallel to the loading portion of the curves.



(a)

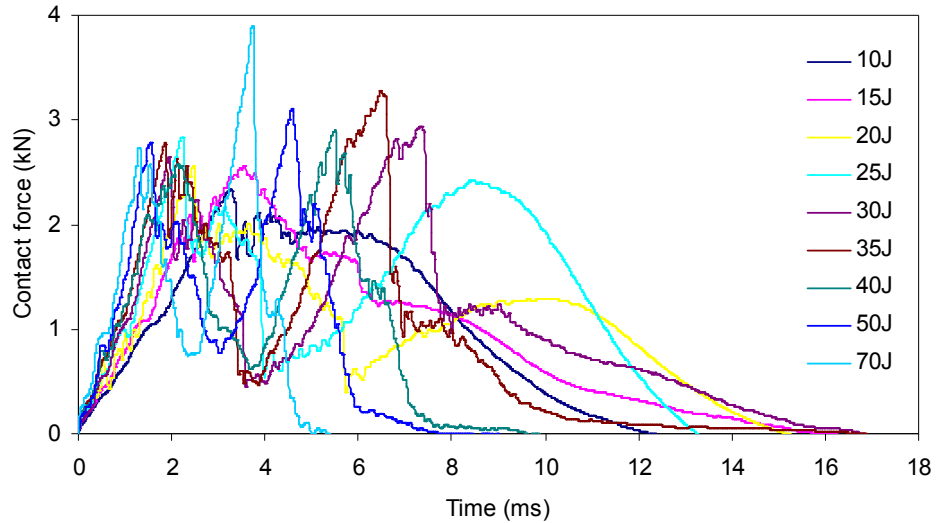


(b)

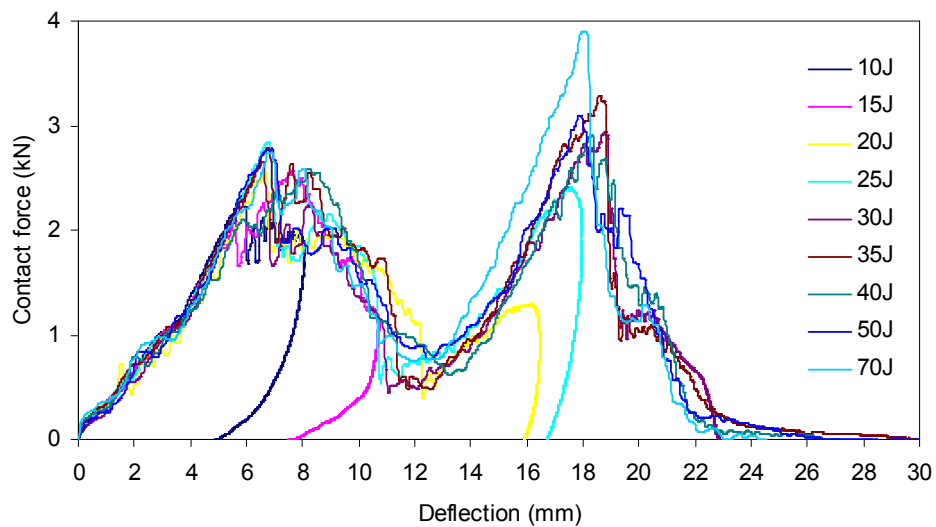
Figure 4.3 (a) The contact force-time (b) the contact force-deflection histories of specimens without core material

As can be seen from the Figure 4.4.a-b, contact time increases by increasing the impact energy level until 35J. Then, contact time decreases rapidly. Because, 35J energy level is the initial of the penetration-perforation transition energy. And, by increasing the impact energy level, deflection of the specimens increases. In the

small energy levels or rebounding cases (10J and 15J), the curves have only one peak. This situation can be explained with the damages of top face sheet. But, in the higher impact energy level or penetration (20J) and perforation (25J, 30J, 35J, 40J, 50J and 70J) cases, the curves have two peaks as the top and bottom face sheets are damaged by the impactor, respectively.



(a)



(b)

Figure 4.4 (a) The contact force-time (b) the contact force-deflection histories of specimens with PET foam core having 10 mm core thickness

The experimental test results are classified in two main titles as effect of core thicknesses at constant core material and effect of core materials at constant core thickness.

4.1.1 Effect of Core Thicknesses on Impact Behavior of Sandwich Composites

Contact force-time histories of specimens with PET foam core, impacted at 15J, 25J, 30J and 40J energies for three different core thicknesses and specimens without core materials or with 0 mm core are given in Figure 4.5. From the result of this figure, it can be seen that the contact force values decrease by increasing the core thickness in each energy level. Nevertheless, impact time values increase by increasing the core thickness in each energy level.

Specimens having 5 mm core thickness show the nearly same behavior with specimens without core material. Because the core thickness is selected small, the specimens behave as a whole. Namely, top and bottom face sheets and core material show the similar characteristic with laminated composite plate. And so, effect of core material on impact behavior of specimens is less than the other core thicknesses. The contact force-time behavior of the specimens impacted at 15J energy is also different from those of other impact energies. In the other impact energy levels, there are two peaks except for specimens having 5 mm core thickness. This situation can be explained with the damages of top and bottom face sheets, respectively. Since the 15J energy level is the rebounding case, the impactor returns from the top face sheet and the bottom face sheet in each core thickness does not damage. So, only one peak occurs in that energy level.

Contact force versus contact time diagrams of specimens with PVC-1 and PVC-2 foam cores impacted at 15J, 25J, 30J and 40J energies for three different core thickness and specimens with 0 mm core thickness are given in Figure 4.6-7, respectively. Contact force-time behaviors of these specimens are similar to specimens with PET foam core.

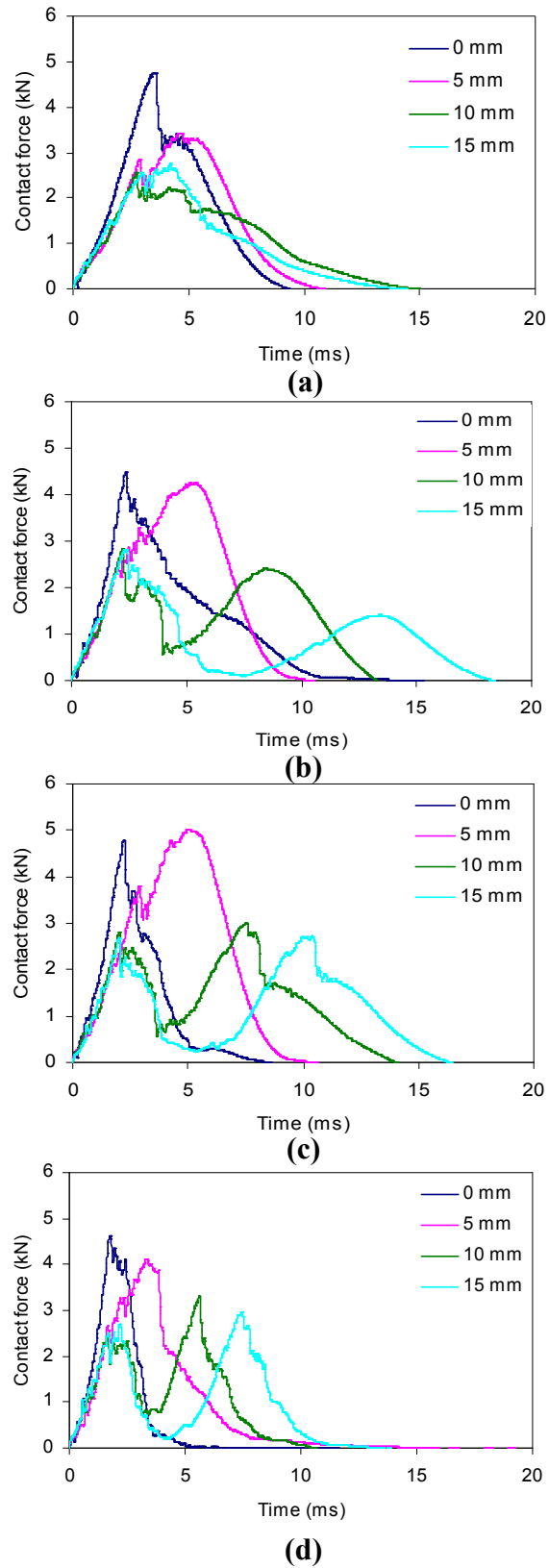
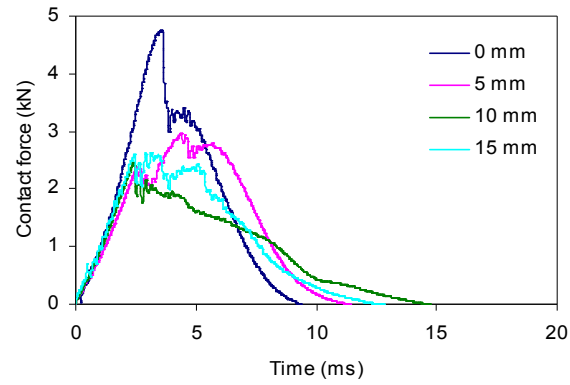
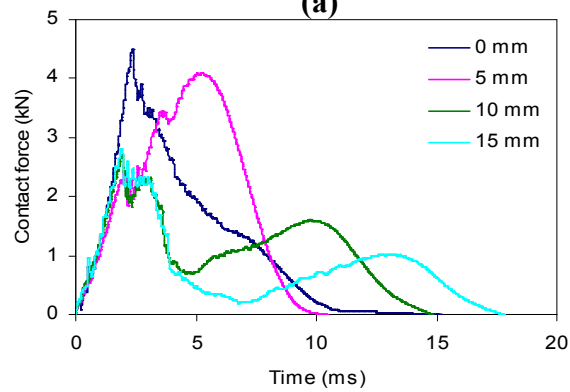


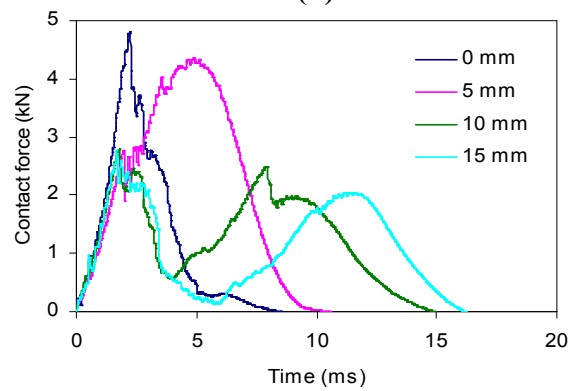
Figure 4.5 Contact force versus time curves of the specimens with PET foam core impacted at (a) 15J, (b) 25J, (c) 30J and (d) 40J



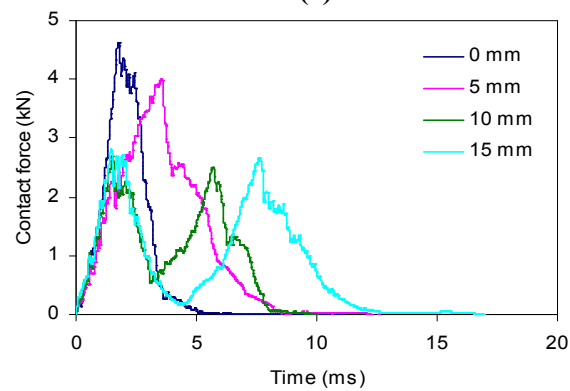
(a)



(b)



(c)



(d)

Figure 4.6 Contact force versus time curves of the specimens with PVC-1 foam core impacted at (a) 15J, (b) 25J, (c) 30J and (d) 40J

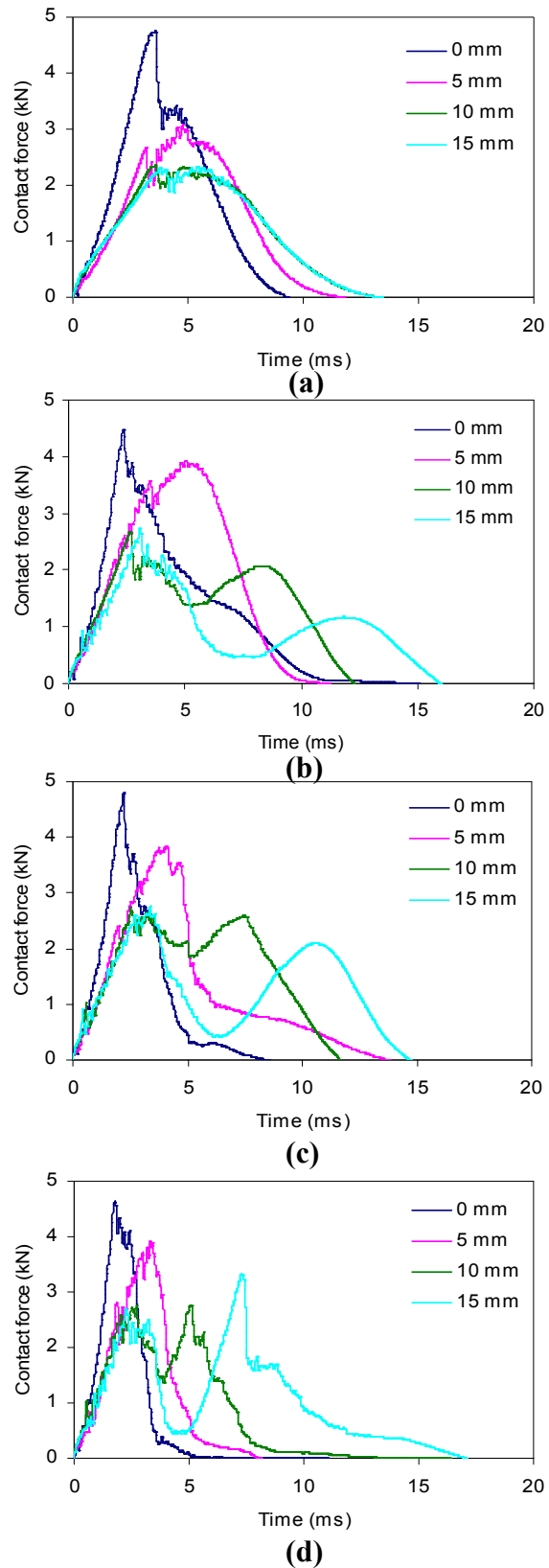


Figure 4.7 Contact force versus time curves of the specimens with PVC-2 foam core impacted at (a) 15J, (b) 25J, (c) 30J and (d) 40J

Contact force-deflection diagrams of specimens with PET foam core impacted at 15J, 25J, 30J and 40J energies for three different core thicknesses and specimens without core materials or with 0 mm core are given in Figure 4.8. From the result of this figure, it is seen that the contact force values decrease by increasing the core thickness in each energy levels. And, maximum deflection values increase by increasing the core thickness in each energy level. The loading portion of the curves for all core thickness is nearly same. However, the unloading portion of the curve is different because of different damage mechanisms. The bending stiffness of the specimen with 0 mm core is higher than all the specimens with cores. The contact force-deflection curve of specimens with PET foam core impacted at 15J (Figure 4.8-a) represents the rebounding case. It is seen that only one peak occurs. This means impactor return from the top face sheet. In Figure 4.8-b, the failure starts in the bottom face sheet and in Figure 4.8-c, impactor damages top and bottom face sheet, respectively and stops in the specimens. This case is named as penetration. And, 30J energy level is the initial of the penetration-perforation transition energy. In the case of perforation illustrated in Figure 4.8-d, it is seen that unloading portions of the curves do not return parallel to loading portions of the curves. This means impactor does not return from the specimen. From Figure 4.8.c-d, second peak value for 10 and 15 mm core thickness is greater than first peak value and also second peak value for 15 mm core thickness is greater than first peak value in Figure 4.10.d. This situation may be explained with the deformation characteristics of the foam core materials. The stiffness of the bottom face sheet during impact event increases by increasing the core thickness that leads to increase the second peak value.

Contact force versus deflection curves of the specimens with PVC-1 and PVC-2 impacted at 15J, 25J, 30J and 40J energies for three different core thicknesses and specimens with 0 mm core are given in Figure 4.9-10, respectively. Contact force-deflection behaviors of those specimens are similar to specimens with PET foam core. But the bending stiffness of the specimen with 0 mm core is nearly same with that of with PVC-1 core. Bending stiffness is the maximum at the specimen with PVC-1, and the minimum at the specimen with PVC-2. This property is compatible with the compressive modulus of the core materials.

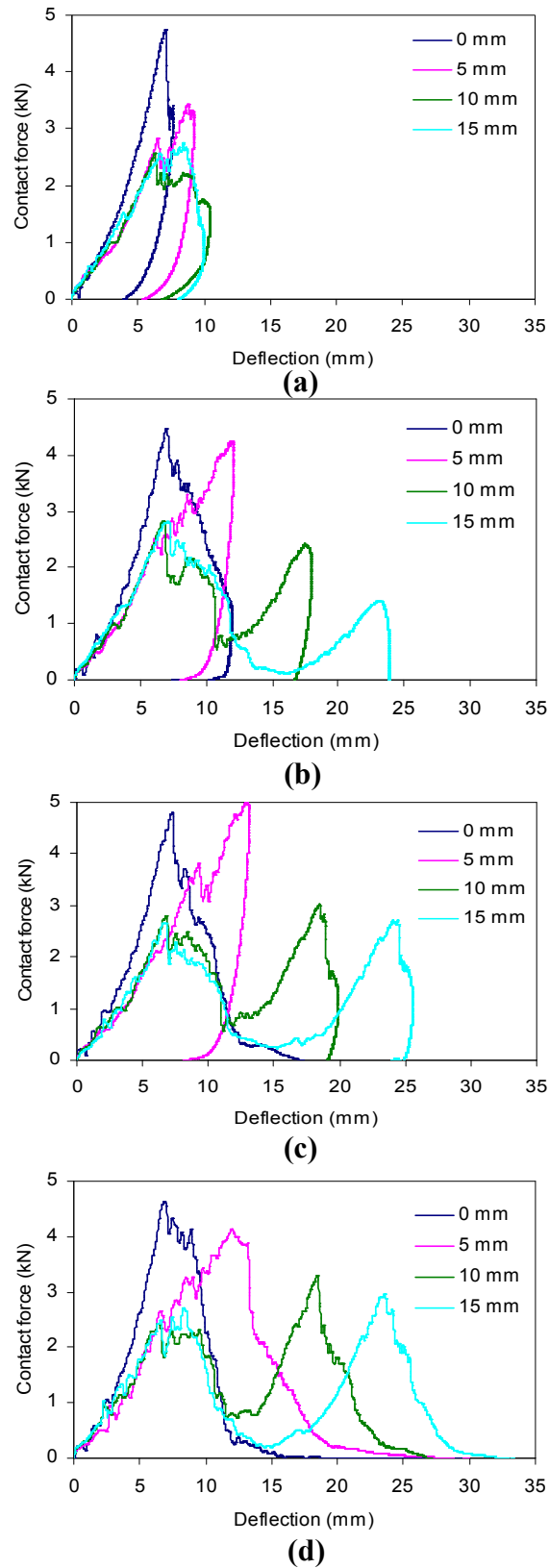
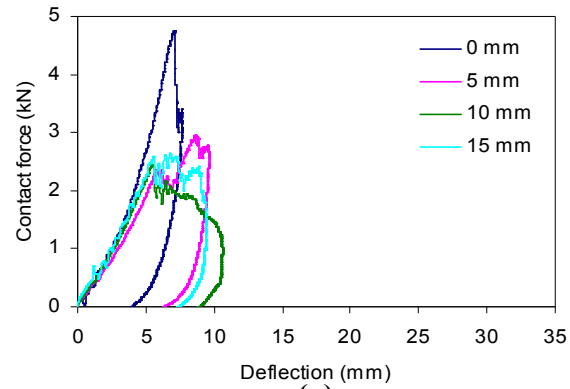
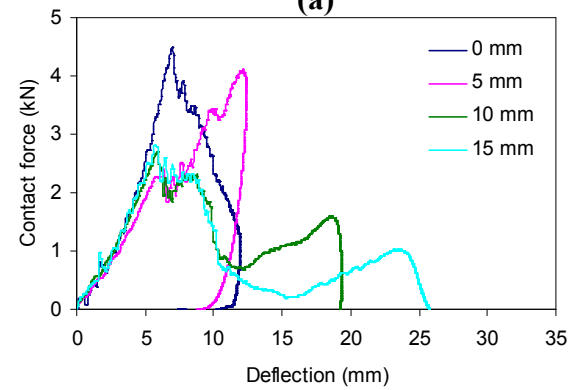


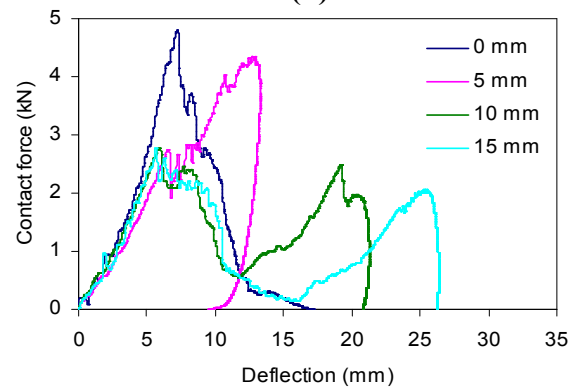
Figure 4.8 Contact force versus deflection curves of the specimens with PET foam core impacted at (a) 15J, (b) 25J, (c) 30J and (d) 40J



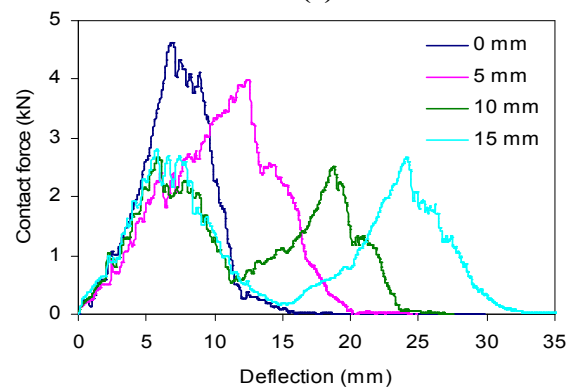
(a)



(b)



(c)



(d)

Figure 4.9 Contact force versus deflection curves of the specimens with PVC-1 foam core impacted at (a) 15J, (b) 25J, (c) 30J and (d) 40J

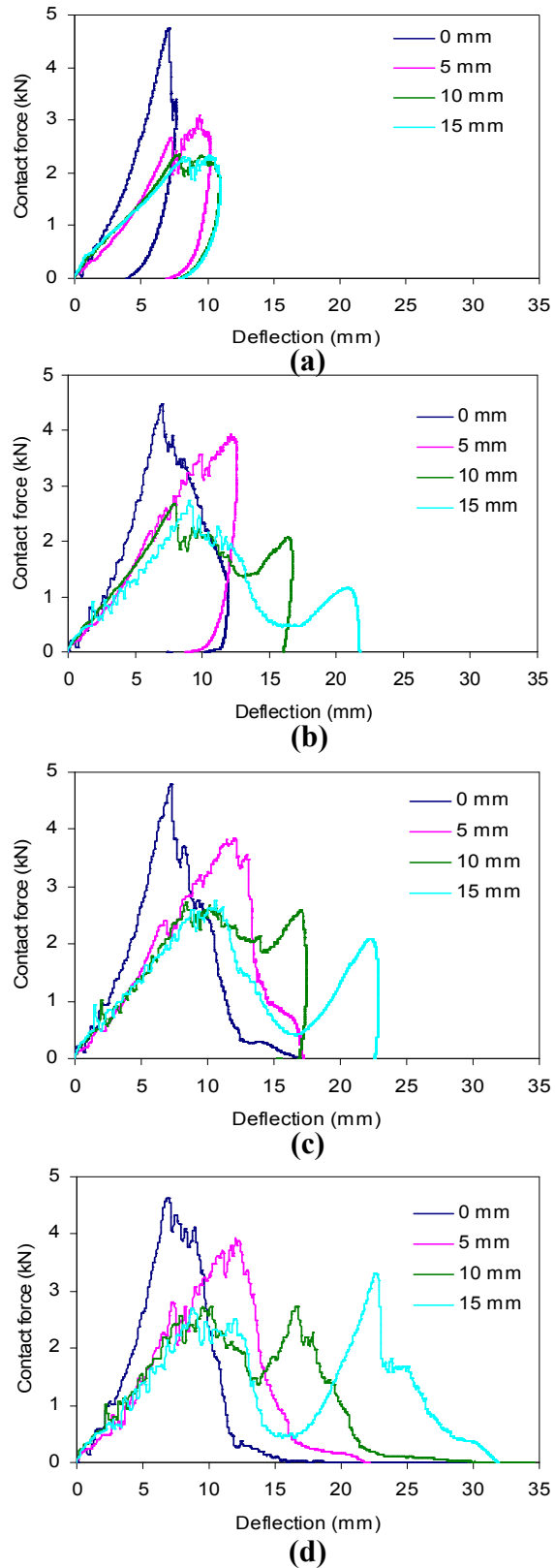


Figure 4.10 Contact force versus deflection curves of the specimens with PVC-2 foam core impacted at (a) 15J, (b) 25J, (c) 30J and (d) 40J

Figure 4.11-13 represent the only peak values of the contact force, contact time and deflection of the specimens according to the impact energy, respectively. Figure 4.11-a shows the maximum contact force-impact energy diagram of specimens with PET foam core for three different core thicknesses and specimens without core materials. The value of maximum contact force decreases by increasing the core thickness except for specimens with PVC-1 and PVC-2 foam cores. Because, the specimens behave more rigid in the small thicknesses. And, specimens having 10 mm and 15 mm core thicknesses show the nearly same characteristic each other. Also, the value of maximum contact force increases rapidly until the peak value of the having 5 mm core thickness and specimens without core materials. After this value, the maximum contact force is nearly same by increasing energy. With increasing the core thickness, variation of contact force value seems the nearly horizontal line in each core material.

Maximum contact force versus impact energy curves of specimens with PVC-1 and PVC-2 foam cores for three different core thicknesses and specimens without core materials are given in Figure 4.11.b-c, respectively. Maximum contact force-impact energy behaviors of those specimens are similar to specimens with PET foam cores. But, in the specimens with PVC-1 and PVC-2 foam cores, the value of maximum contact force in the 15 mm core thickness is greater than 10 mm core thickness.

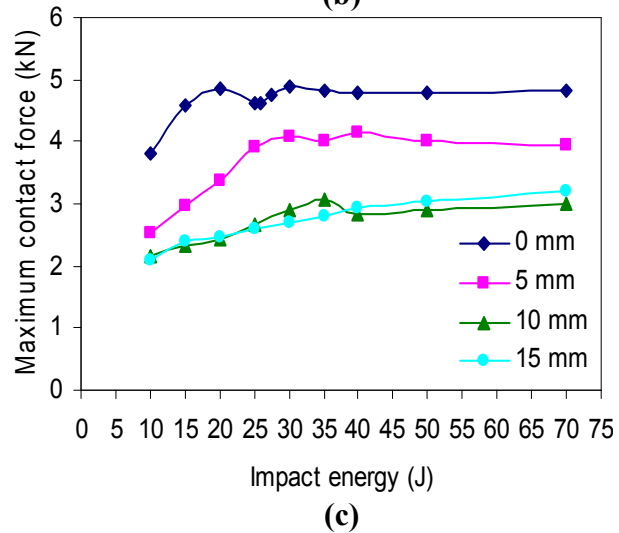
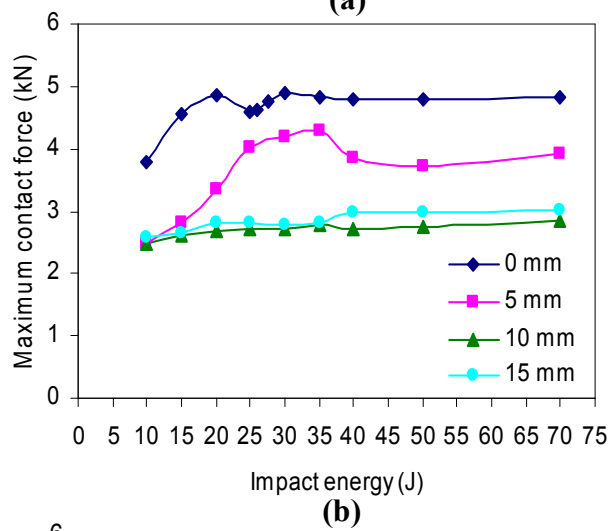
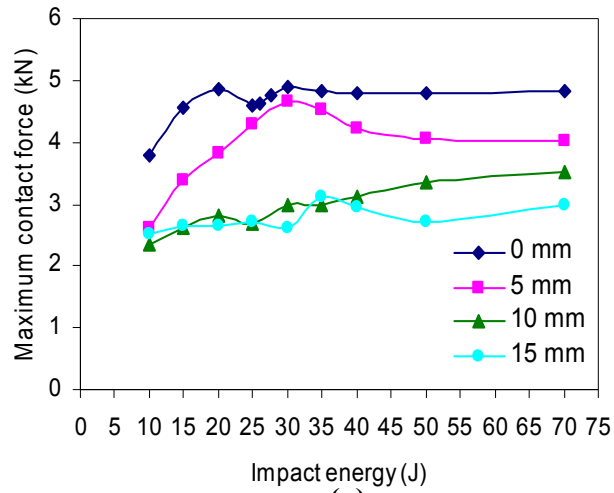


Figure 4.11 Maximum contact force versus impact energy curves of specimens with (a) PET, (b) PVC-1 and (c) PVC-2 foam cores

Contact time-impact energy histories of specimens with PET foam core for three different core thickness and specimens without core materials are given in Figure 4.12-a. specimens, having 5 mm core thickness and without core materials show nearly same characteristic each other. That curves have only one peak value which correspond to perforation threshold. But, the curves of specimens having 10 mm and 15 mm core thicknesses, there are two peaks. First peak and second peak are the perforation threshold of top and bottom face sheet, respectively. After the perforation threshold, contact time decreases and continues nearly linear. And, the contact time value increases by increasing the core thickness in each core material.

Contact time versus impact energy curves of specimens with PVC-1 and PVC-2 foam cores for three different core thicknesses and specimens without core materials are given in Figure 4.12.b-c, respectively. Contact time-impact energy behaviors of those specimens are similar to specimens with PET foam cores. But, the value of contact time of having 5 mm core thickness at the perforation threshold is smaller than specimens without core materials in the specimens with PVC-1 foam cores.

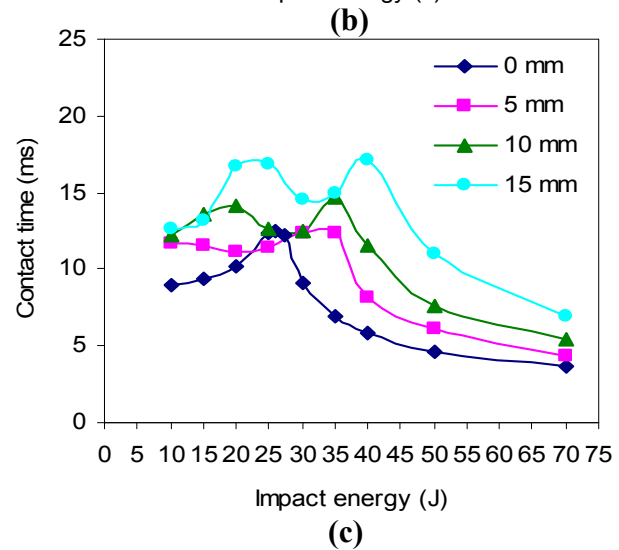
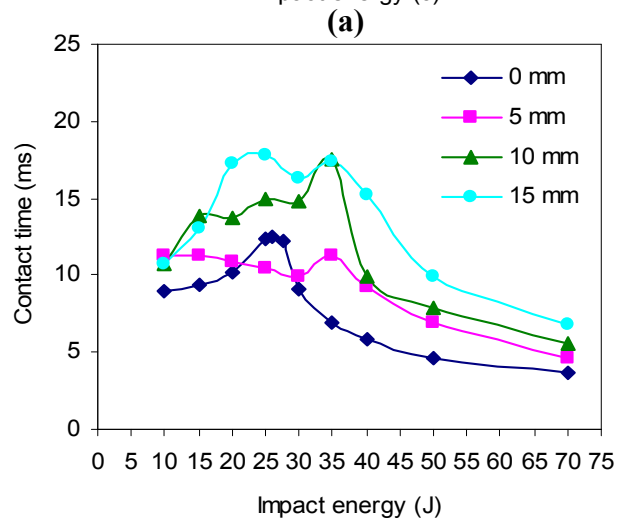
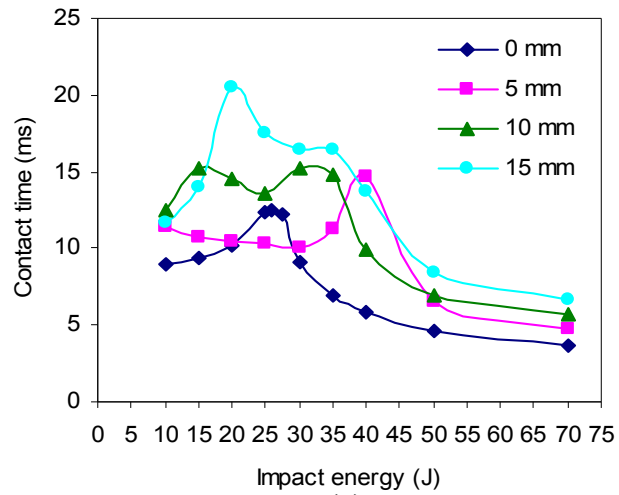
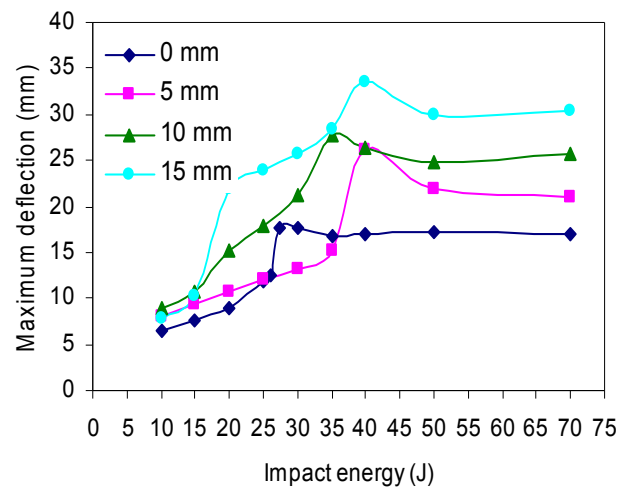


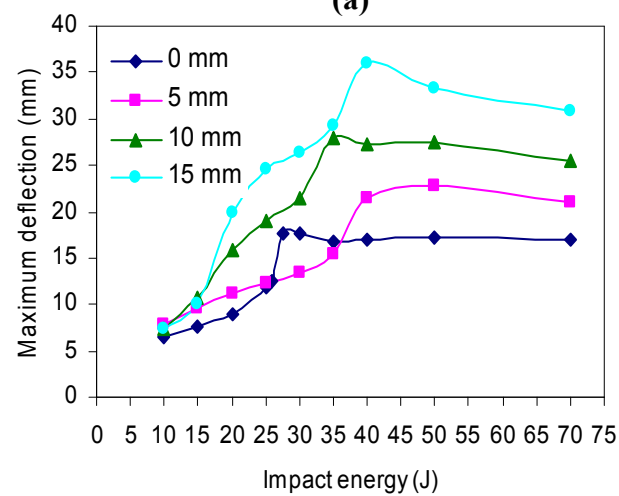
Figure 4.12 Contact time versus impact energy curves of specimens with (a) PET, (b) PVC-1 and (c) PVC-2 foam cores

The maximum deflection-impact energy curves of specimens with PET foam core for three different core thickness and specimens without core materials are given in the Figure 4.13-a. Maximum deflection values increase by increasing the core thickness. The maximum deflection of specimens with PET foam core does not change significantly after 40J energy level. Because, that energy level is the perforation threshold for specimens with PET foam cores.

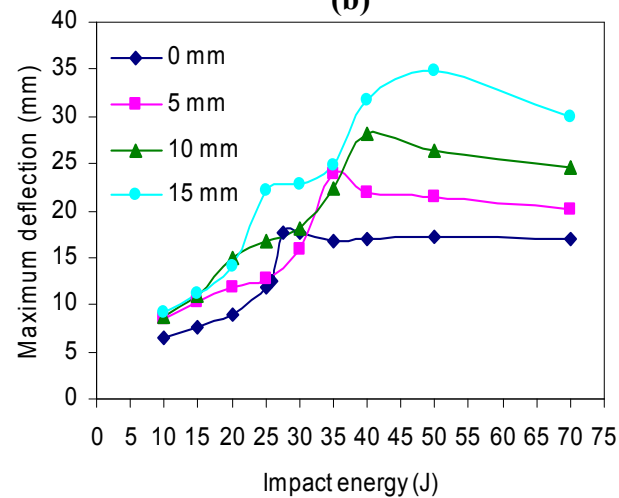
Maximum deflection versus impact energy curves of specimens with PVC-1 and PVC-2 foam cores for three different core thicknesses and specimens without core materials are given in Figure 4.13.b-c, respectively. Maximum deflection-impact energy behaviors of those specimens are similar to specimens with PET foam cores.



(a)



(b)



(c)

Figure 4.13 Maximum deflection versus impact energy curves of specimens with (a) PET, (b) PVC-1 and (c) PVC-2 foam cores

Figure 4.14-16 show the energy profile diagrams of specimens with PET, PVC-1 and PVC-2 foam cores, respectively. It is seen from the figure 4.14, the excessive energy which causes rebound of impactor decreases by increasing the core thickness. In contrast, the absorbed energy increases. The first penetration level is obtained for having 0 mm, 5 mm, 10 mm and 15 mm core thickness specimens in 25J, 35J, 20J and 15J, respectively. Also, penetration portion increases by increasing the core thickness. In the higher core thickness, the penetration case starts 15J and lasts until the perforation case. 25J, 40J, 30J and 35J are the perforation threshold for having 0 mm, 5 mm, 10 mm and 15 mm core thicknesses, respectively. After this impact energy level, the absorbed energy is nearly constant.

Energy profile diagrams of specimens with PVC-1 and PVC-2 foam cores for three different core thickness and specimens without core materials are given in Figure 4.15-16. Behaviors of those specimens are similar to specimens with PET foam cores.

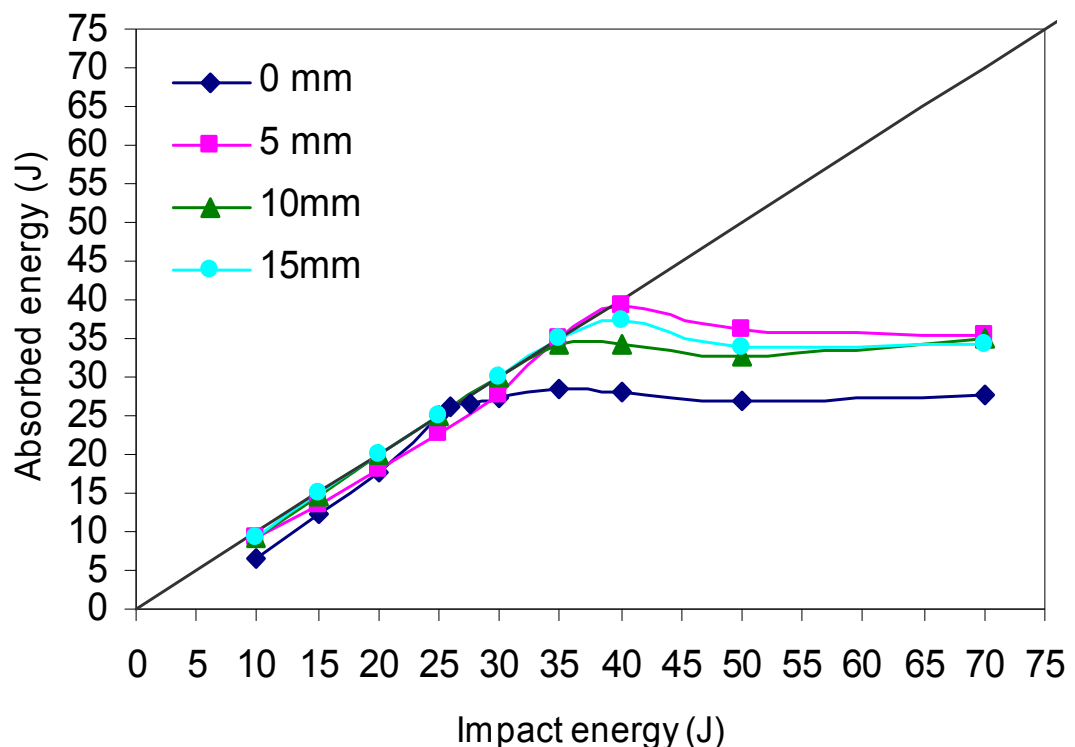


Figure 4.14 The energy profile diagram for specimens with PET foam cores

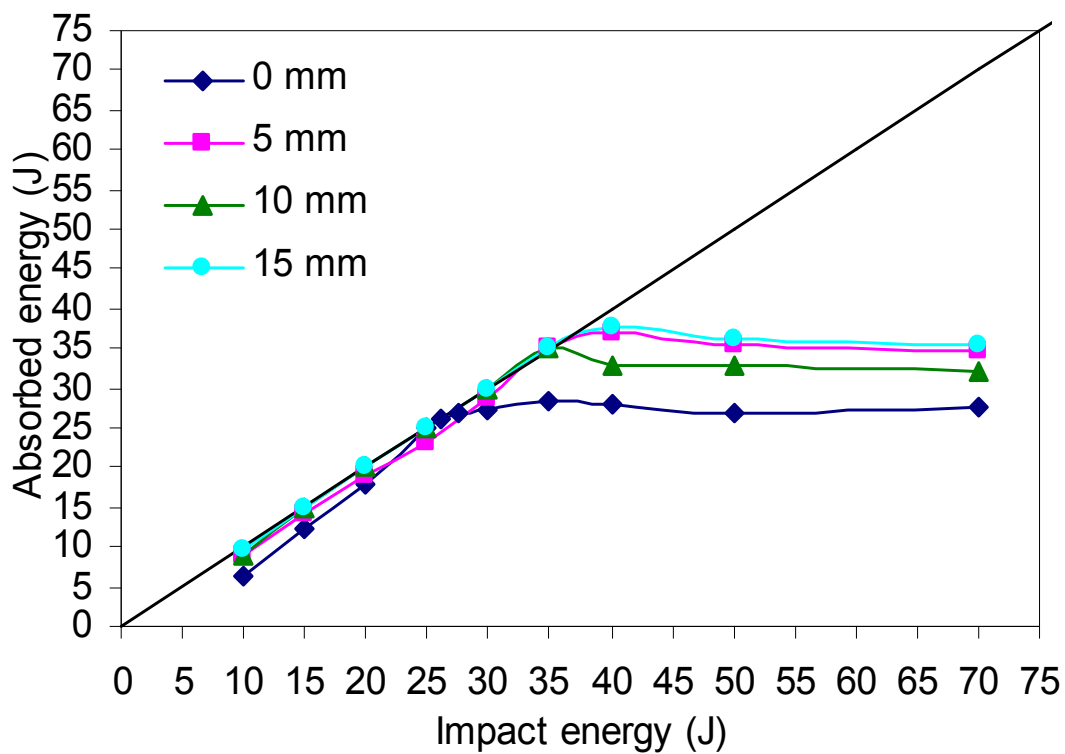


Figure 4.15 The energy profile diagram for specimens with PVC-1 foam cores

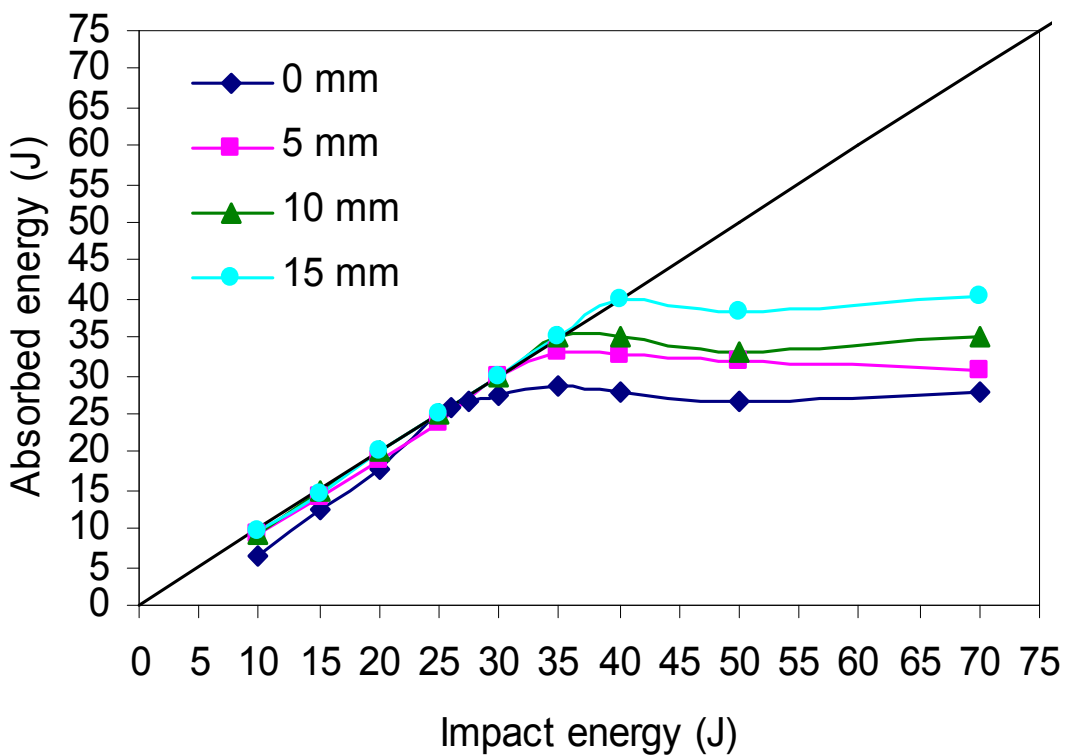
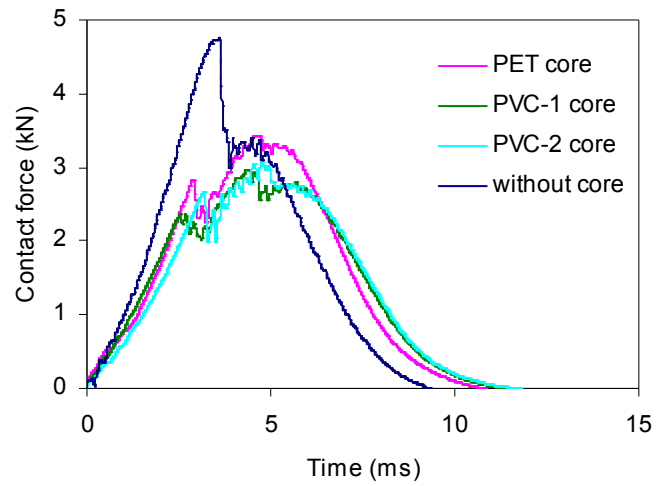


Figure 4.16 The energy profile diagram for specimens with PVC-2 foam cores

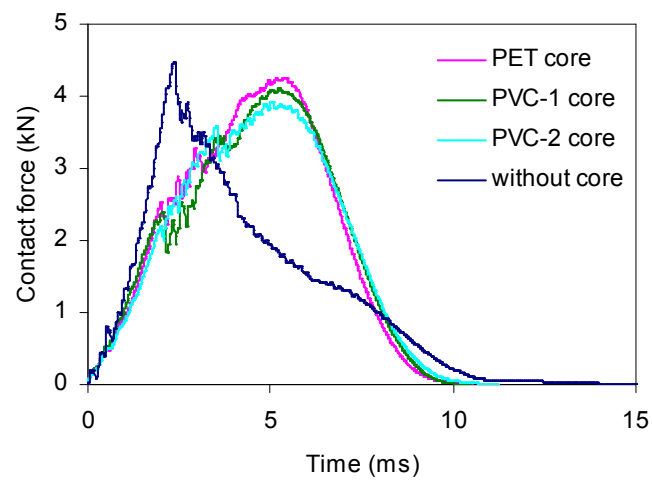
4.1.2 Effect of Core Materials on Impact Behavior of Sandwich Composites

In the previous part, effect of core thicknesses on impact behavior of specimens was investigated with related figures. So in this part, effect of core materials on impact behavior will be discussed. Contact force-time histories of having 5 mm core thickness specimens impacted at 15J, 25J and 40J energies for three different core materials and specimens without core materials are given in Figure 4.17. It is seen from the figure, the core material decreases the maximum contact force in each energy level when compared to specimens without core materials. Because the core materials absorbed the energy and so maximum contact force values decrease. Since specimens with PVC-2 foam core have the lowest mechanical properties especially compressive modulus, the peak value of contact force are the lowest in each energy level.

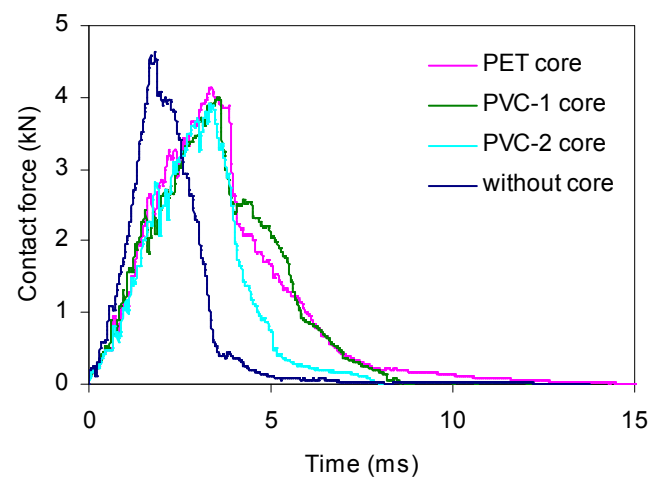
In Figure 4.18-19, the contact force-time diagrams of specimens having 10 mm and 15 mm core thicknesses are given. When the impact energy increases, two peaks occur in the curves (Figure 4.18-19). This situation can be explained with damages in the bottom face sheet. But, in the 15J impact energy level, curves have only one peak and show nearly same characteristic with specimens without core materials.



(a)

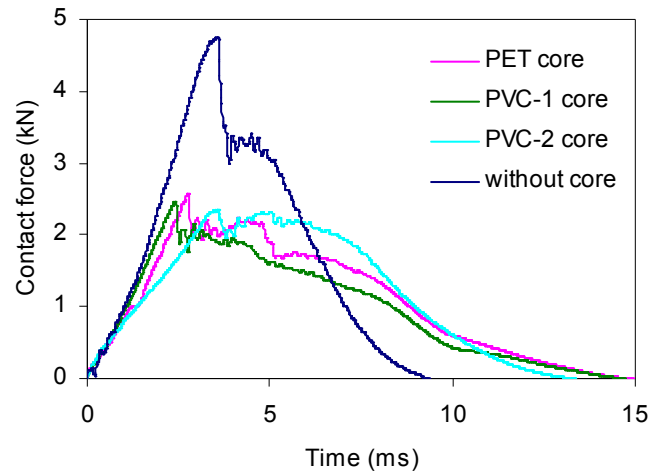


(b)

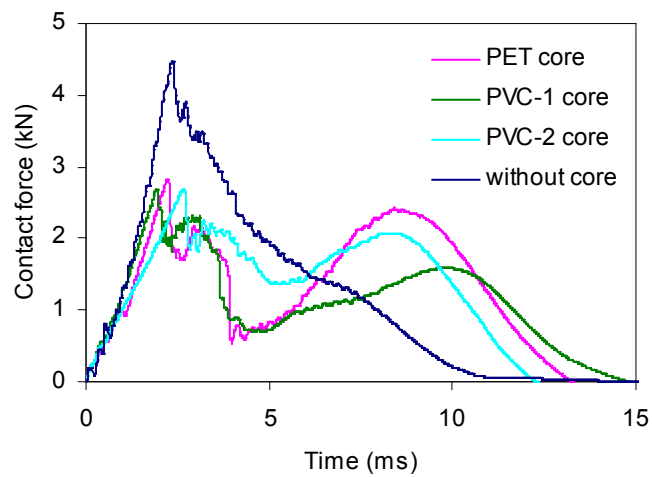


(c)

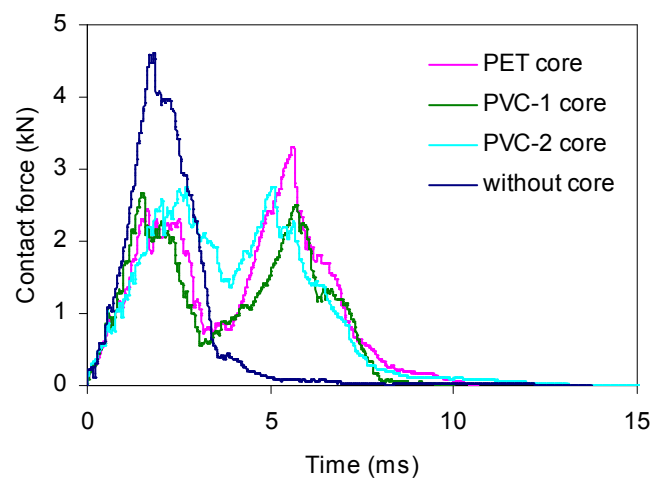
Figure 4.17 Contact force versus time curves of specimens having 5 mm core thickness impacted at (a) 15J, (b) 25J and (c) 40J



(a)

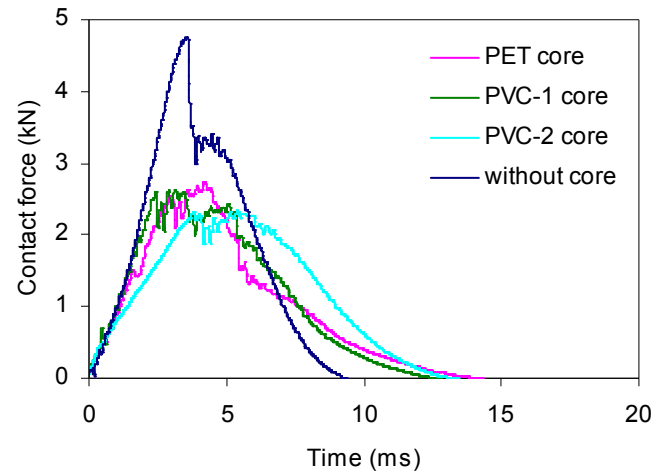


(b)

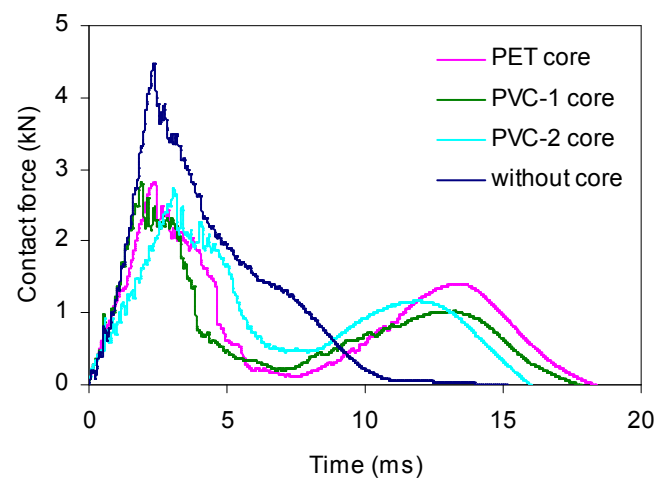


(c)

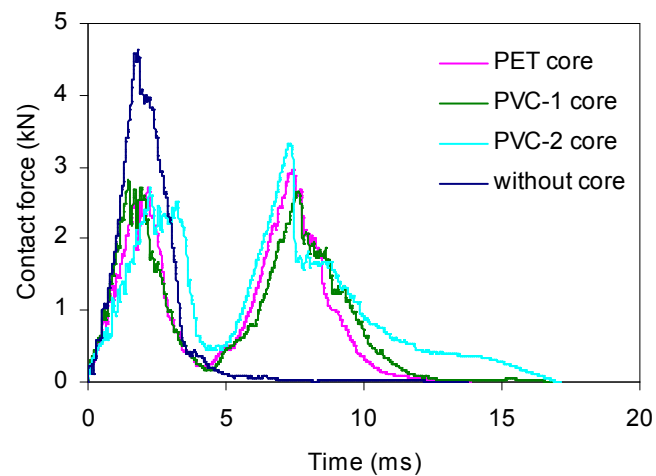
Figure 4.18 Contact force versus time curves of specimens having 10 mm core thickness impacted at (a) 15J, (b) 25J and (c) 40J



(a)



(b)



(c)

Figure 4.19 Contact force versus time curves of specimens having 15 mm core thickness impacted at (a) 15J, (b) 25J and (c) 40J

Contact force-deflection diagrams of specimens having 5 mm core thickness impacted at 15J, 25J and 40J energies for three different core materials and specimens without core materials are given in Figure 4.20. 15J energy level is the rebounding case for all core material (Figure 4.20-a). And the core material decreases the contact force in that energy level when compared to other energy levels. 25J energy level is the initial of the rebounding-penetration transition energy (Figure 4.20-b). Perforation case is illustrated for all core material in Figure 4.20-c. In the 5 mm core thickness specimens, contact force-deflection curves have only one peak. Because the core thickness is small, specimens having 5 mm core thickness show same characteristic with specimens without core materials. Namely, top and bottom face sheet and core material behaves as a whole part. The bending stiffness of the specimen without core materials is higher than the other specimens and bending stiffness is the maximum at the specimen with PVC-1, and minimum at the specimen with PVC foam core. This property is compatible with the compressive modulus of the core materials.

Contact force versus deflection curves of specimens having 10 mm and 15 mm core thicknesses are given in the Figure 4.21-22, respectively. Both core thicknesses show same behavior with specimen having 5 mm core thickness. In those specimens, there are two peaks in the figures. First and second peak represent the damages of top and bottom face sheet, respectively. Also, second peak value of specimens having 10 mm core thickness is smaller than the first peak value while it is greater than in specimens having 15 mm core thickness impacted at 25J and 40J, respectively. Because, at the 25J impact energy level, impactor rebound from the bottom face sheet. But, at the 40J impact energy level, impactor passes the top and bottom face sheet, respectively. And, the deflection of second peak value is maximum in specimen with PVC-1 foam core, and minimum specimen with PVC-2 foam core.

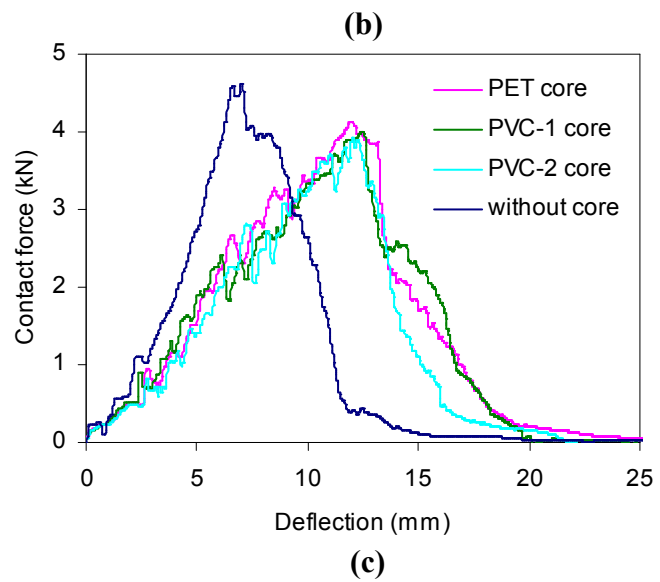
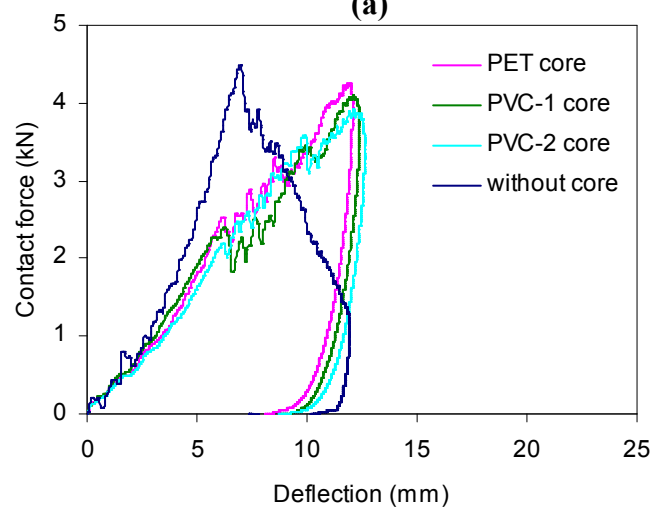
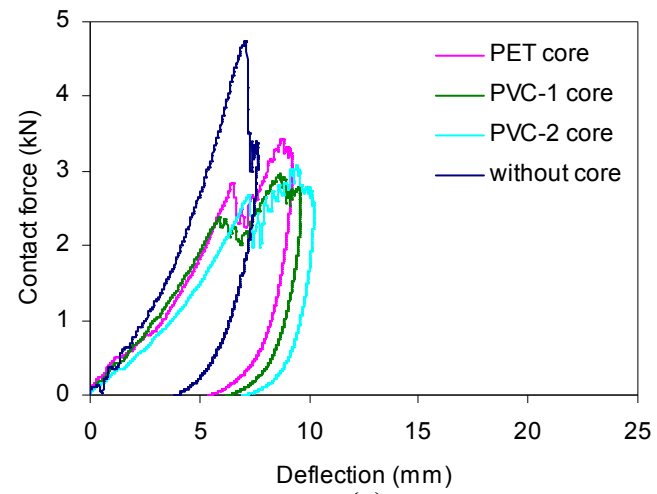
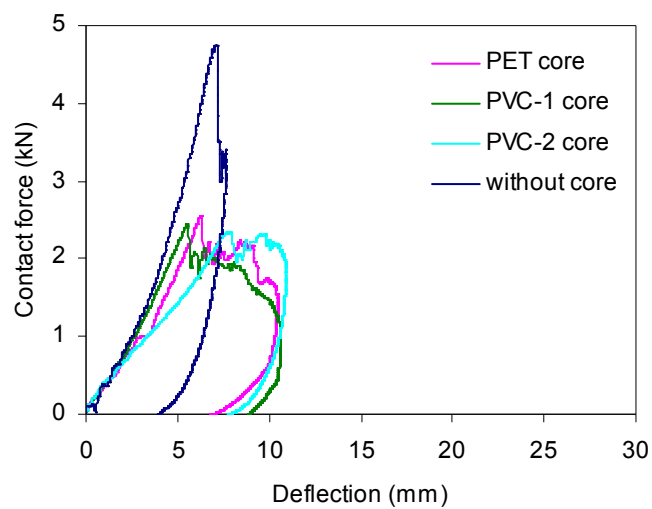
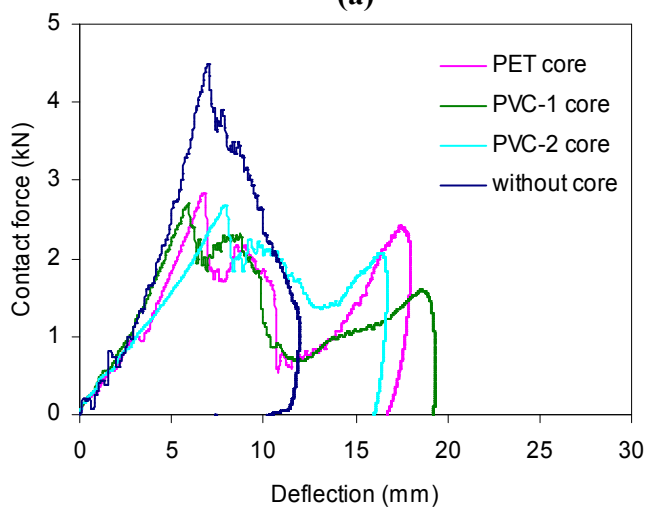


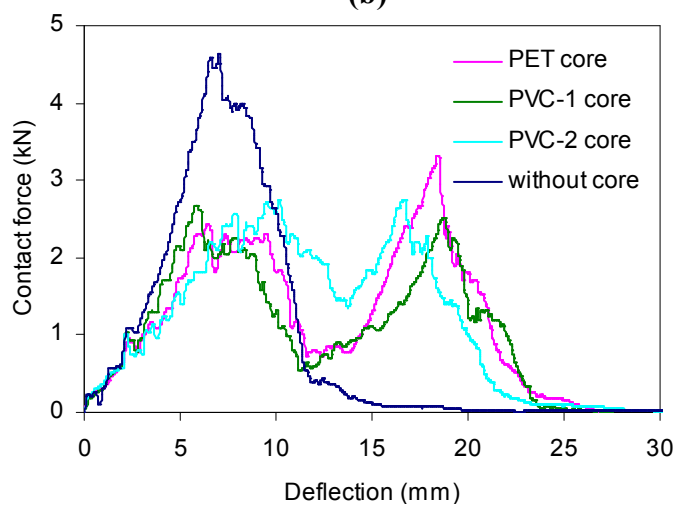
Figure 4.20 Contact force versus deflection curves of specimens having 5 mm core thickness impacted at (a) 15J, (b) 25J and (c) 40J



(a)

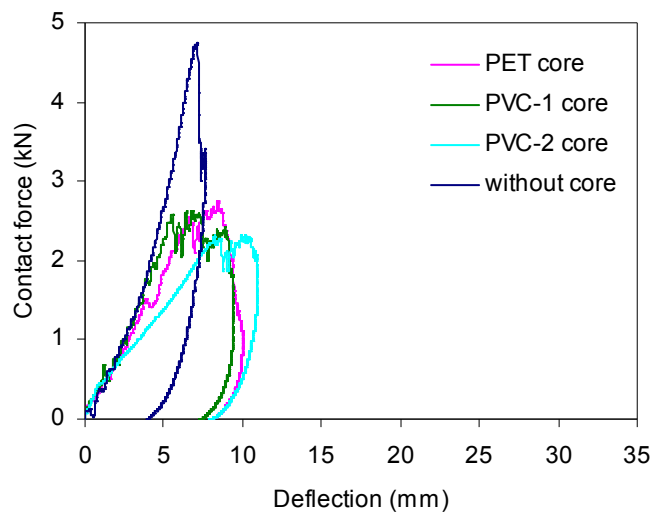


(b)

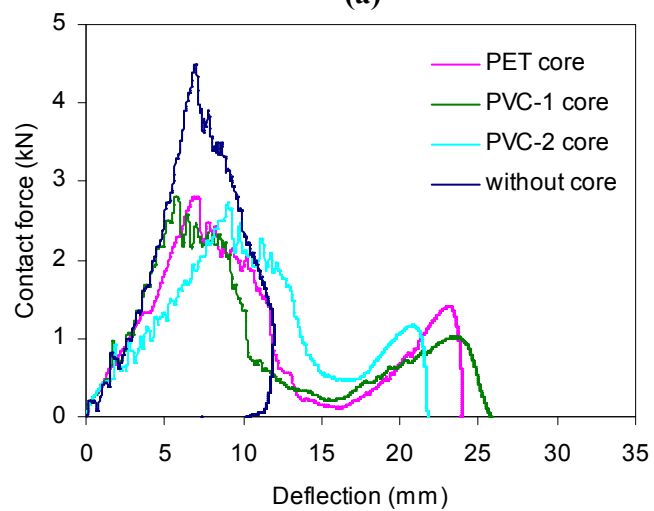


(c)

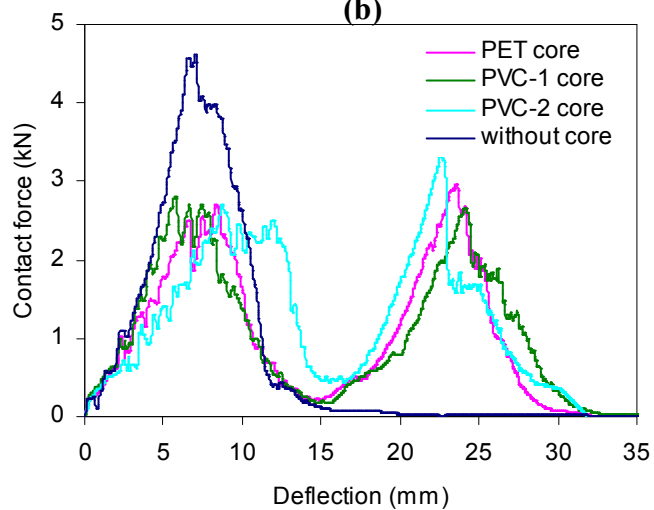
Figure 4.21 Contact force versus deflection curves of specimens having 10 mm core thickness impacted at (a) 15J, (b) 25J and (c) 40J



(a)



(b)

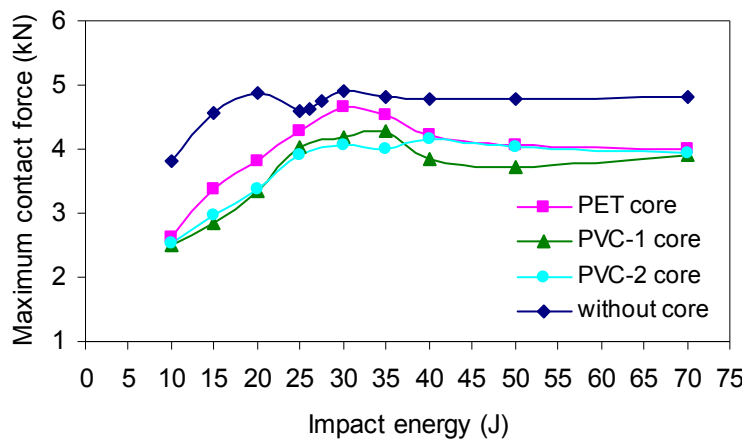


(c)

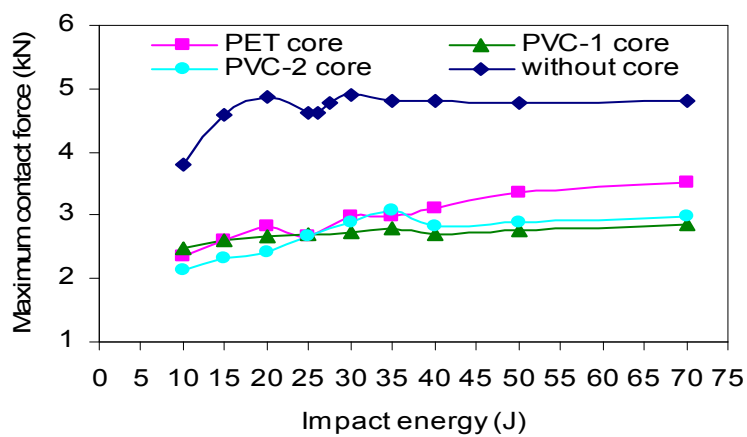
Figure 4.22 Contact force versus deflection curves of specimens having 15 mm core thickness impacted at (a) 15J, (b) 25J and (c) 40J

Maximum contact force-impact energy histories of specimens having 5 mm core thickness for three different core material and specimens without core material are shown in Figure 4.23-a. All core material decreases the maximum contact force value when compared to specimens without core material. Maximum contact force increases linearly until the penetration threshold, after that value increases go on with small increment in each core material. In the higher impact energy, the maximum contact force is nearly same.

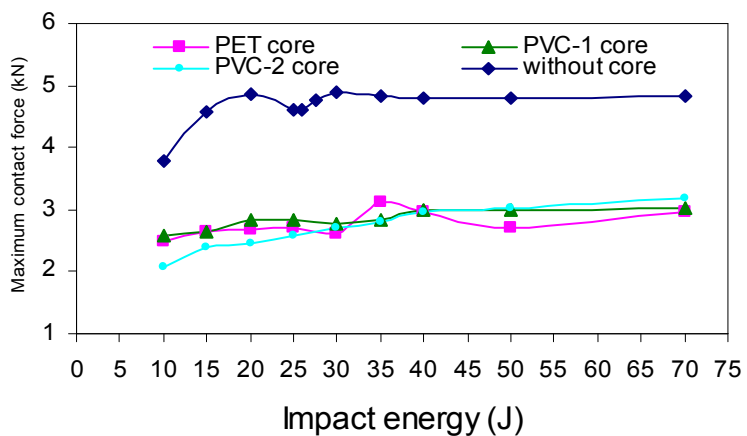
Maximum contact force versus impact energy curves of specimens having 10 mm and 15 mm core thicknesses for three different core material and specimens without core material are given in Figure 4.23.b-c. The effect of core materials on maximum contact force in these specimens is much than the specimens having 5 mm core thickness. Maximum contact force decreases 3 kN in these specimens while it decreases 4 kN in the specimens having 5 mm core thickness. The behaviors of these specimens are nearly same with specimens having 5 mm core thickness. Also, maximum contact force increases with small increments and nearly changes linearly.



(a)



(b)

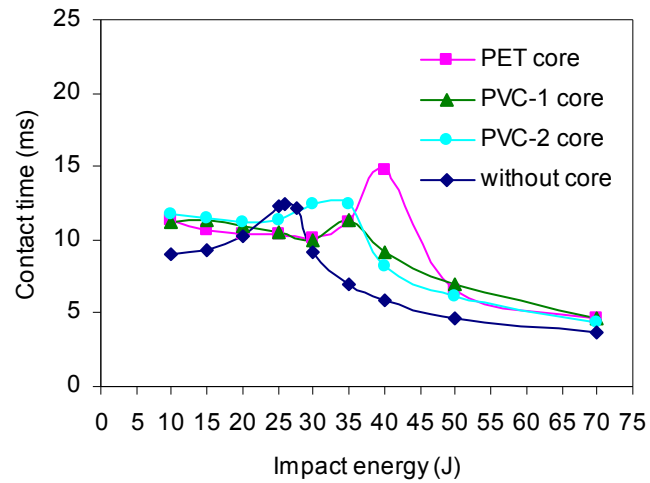


(c)

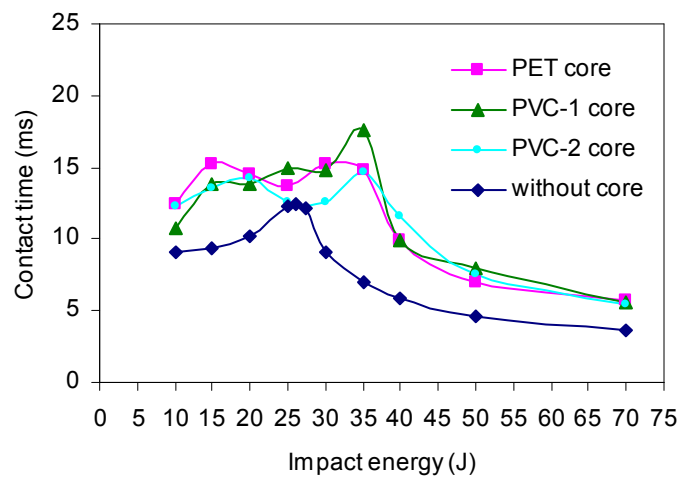
Figure 4.23 Maximum contact force versus impact energy curves of specimens having (a) 5 mm, (b) 10 mm and (c) 15 mm core thicknesses

Contact time-impact energy diagrams of specimens having 5 mm core thickness for three different core material and specimens without core material are given in Figure 4.24-a. The maximum contact time value of specimen with PET foam core is higher than the other core materials. All curves show similar characteristics with the specimen without core materials. The maximum contact time increase with small increments until the peak values in each core then maximum contact time decrease rapidly and increases nearly linearly.

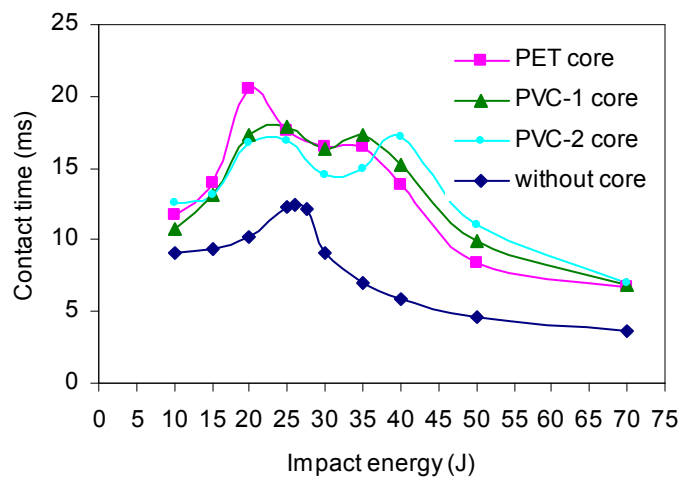
Contact time versus impact energy curves of specimens having 10 mm and 15 mm core thicknesses for three different core material and specimens without core material are shown in Figure 4.24.b-c. The maximum contact time values increase by increasing the core thicknesses in all core materials when compared to specimens without core material.



(a)



(b)



(c)

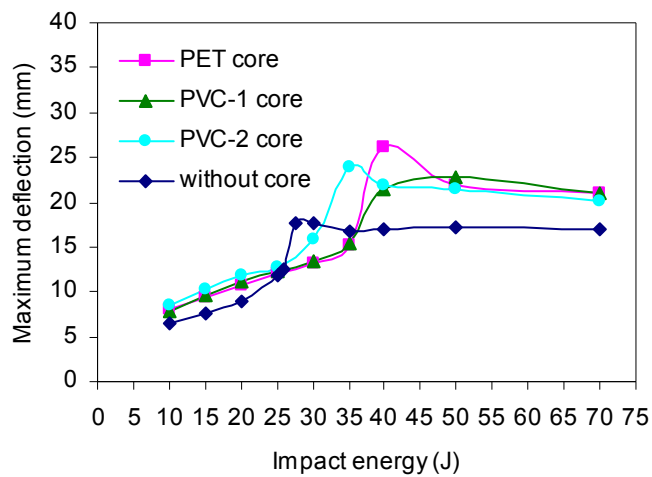
Figure 4.24 Contact time versus impact energy curves of specimens having (a) 5 mm, (b) 10 mm and (c) 15 mm core thicknesses

Maximum deflection-impact energy histories of specimens having 5 mm core thickness for three different core thickness and specimens without core material are shown in Figure 4.25-a. The maximum deflection value occurs in the specimens with PET foam core. The maximum deflection increases with increasing the impact energy level until the penetration threshold. After the penetration threshold energy level, the maximum deflection does not change significantly in all core materials.

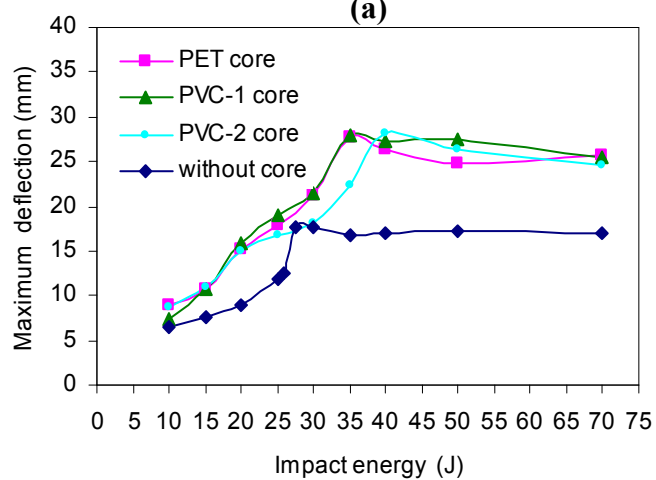
Maximum deflection versus impact energy curves of specimens having 10 mm and 15 mm core thicknesses are given in Figure 4.25.b-c, respectively. Maximum deflection values occur in specimens with PVC-1 foam core and increases by increasing the core thicknesses in all core materials when compared to specimens without core materials.

Figure 4.26-28 represent the energy profile diagrams of specimens having 5 mm, 10 mm and 15 mm core thicknesses for three different core material and specimens without core material. The first penetration level is obtained for specimens with PET and PVC-1 foam cores in 35J, for specimens with PVC-2 foam core and without core material in 30J and 25J, respectively. 40J, 35J, 30J and 25J energy levels are the perforation threshold for specimens with PET, PVC-1, PVC-2 foam core and without core material, respectively. After these energy levels, the absorbed energy is nearly constant with increasing impact energy.

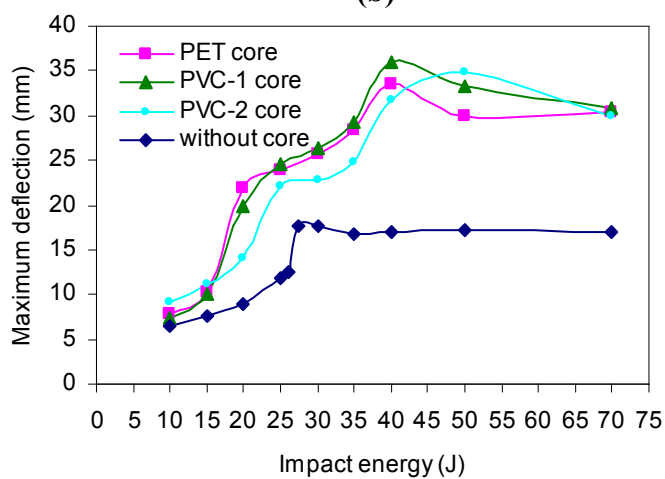
Energy profile diagrams of specimens having 10 mm and 15 mm core thicknesses for three different core material and specimens without core material are given 4.27-28. Behaviors of those specimens are similar to specimens having 5 mm core thickness. But, when the core thickness increases, the penetration portion increases, too. And, it starts 15J and lasts until the perforation case.



(a)



(b)



(c)

Figure 4.25 Maximum deflection versus impact energy curves of specimens having (a) 5 mm, (b) 10 mm and (c) 15 mm core thicknesses

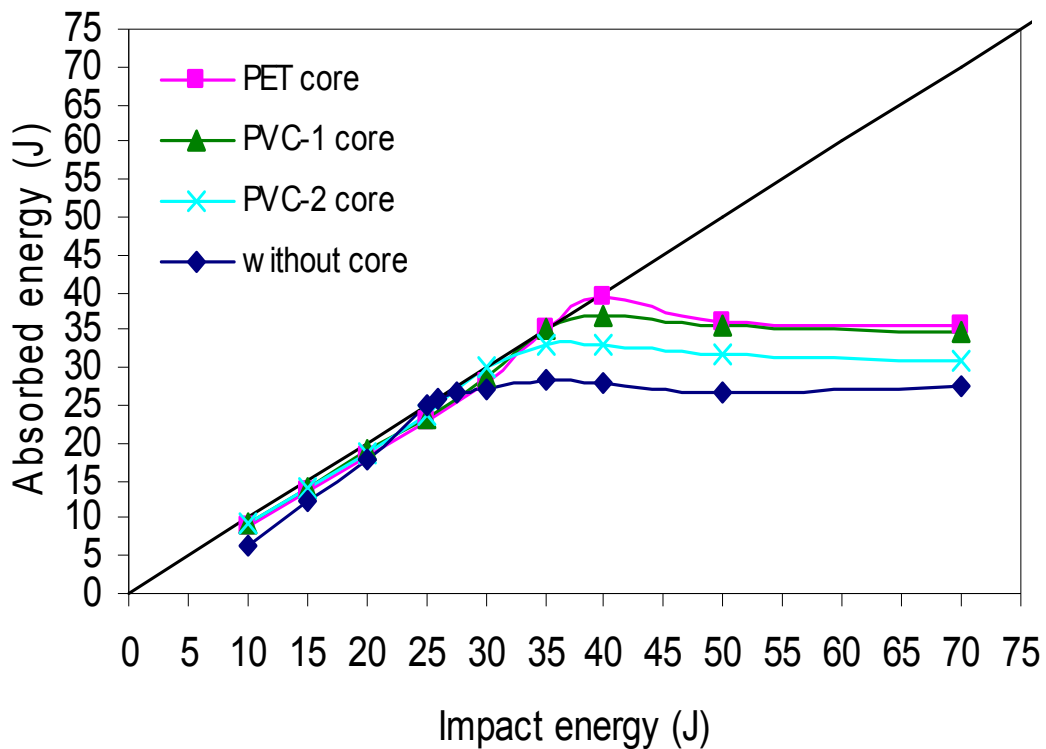


Figure 4.26 The energy profile diagram of specimens having 5 mm core thickness

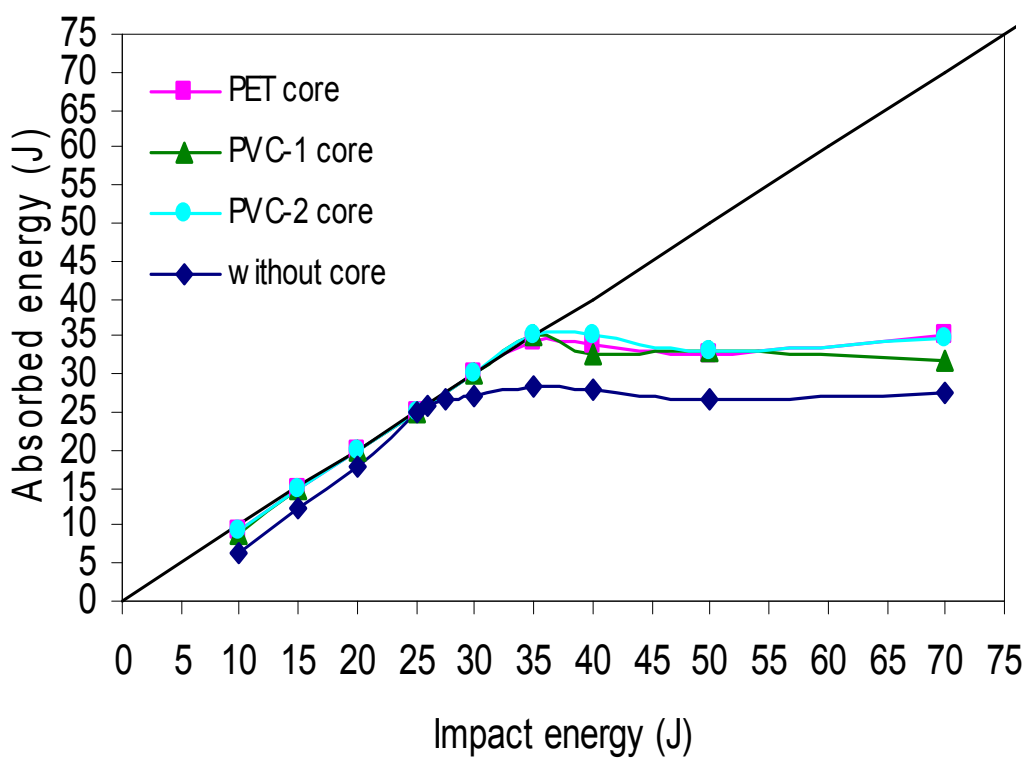


Figure 4.27 The energy profile diagram of specimens having 10 mm core thickness

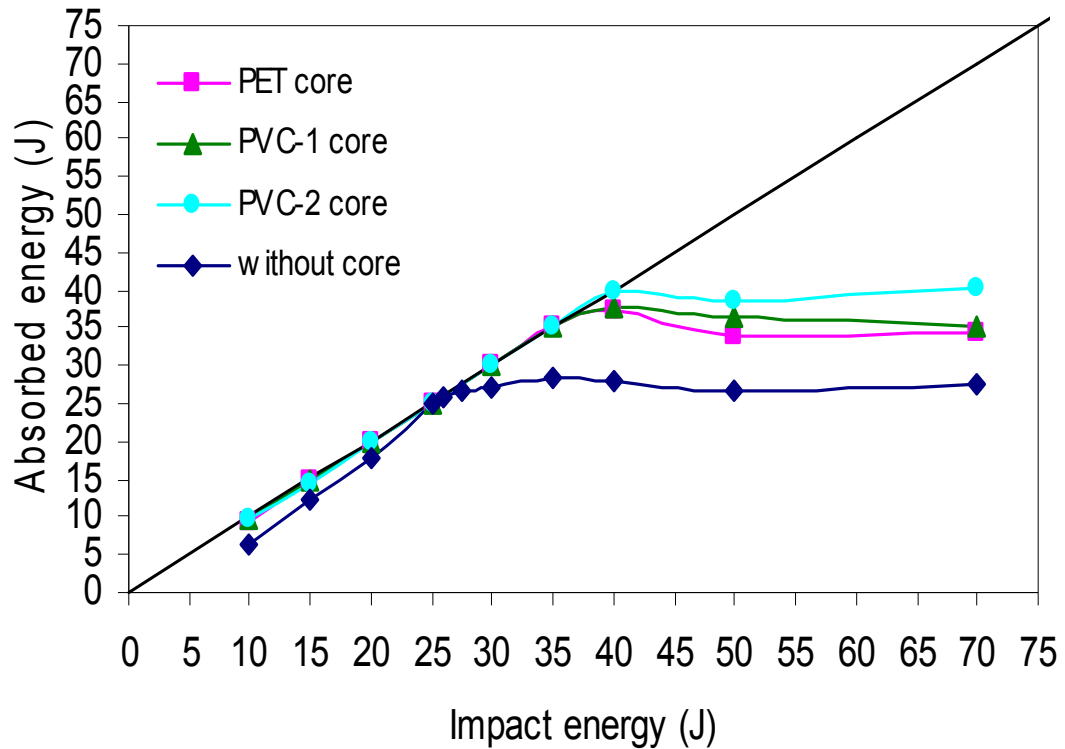


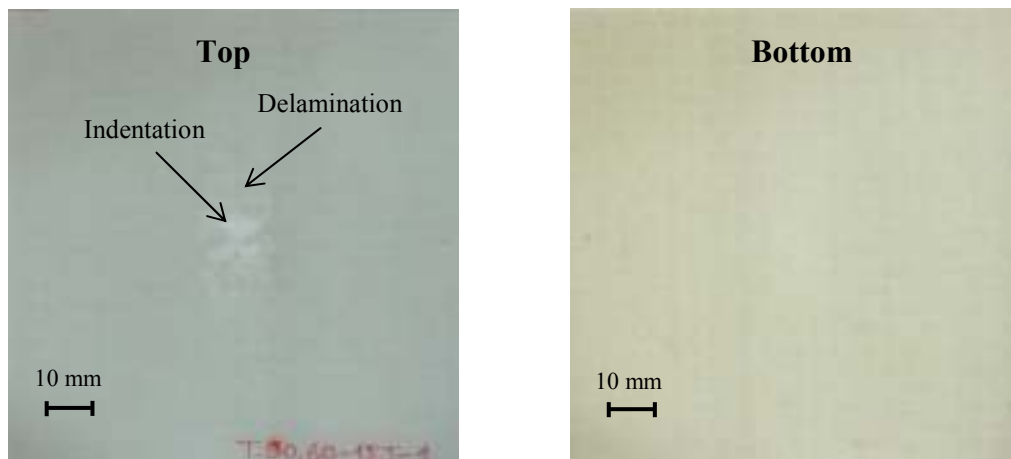
Figure 4.28 The energy profile diagram of specimens having 15 mm core thickness

4.1.3 Damages of Specimens

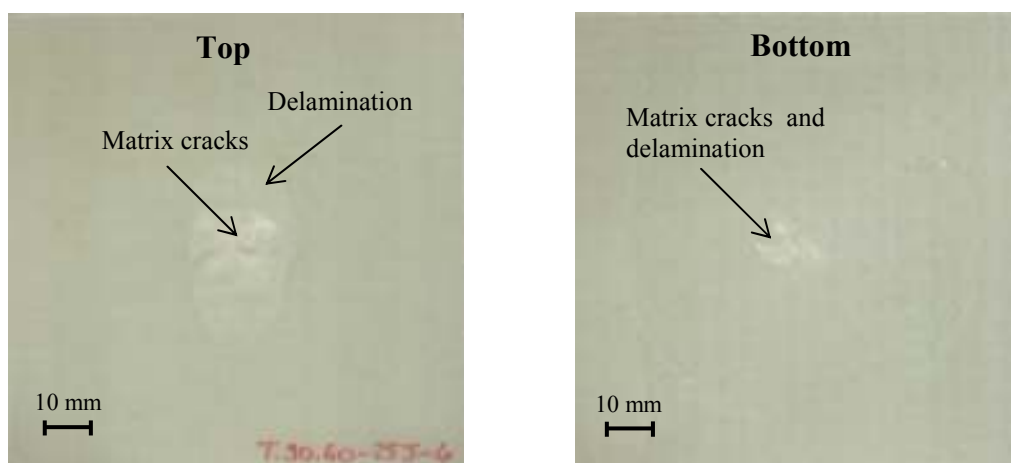
To evaluate the main damage mode of specimens having 5 mm, 10 mm and 15 mm core thicknesses for three different core material and specimens without core material, images of the specimens (at impact energies as 15J, 25J and 40J) are given in Figure 4.29-38. Figure 4.29 shows the impact induced damage of the specimens with PET foam core having 5 mm core thickness according to impact energy. Under the impact energy of 15J, there is no damage seen at bottom face sheet. And, indentation failure, matrix cracks can be seen at the top face sheet and delaminations occur at the bottom interface of top face sheet (Figure 4.29.a). As the impact energy increases to 25J, matrix cracks and delamination in bottom interface were occurred at the top face sheet and matrix cracks were seen at the bottom face sheet (4.29.b). In the photos of the damages specimens under impact energy of 40J, fiber cracks were observed at the bottom face sheet (Figure 4.29.c). Also, delamination areas increase at the top face sheet by increasing the impact energy. When the core thickness increases to 10 mm and 15 mm (Figure 4.30-31) delamination in bottom interface

and fiber cracks were observed at the bottom face sheet under impact energy of 40J. In the other impact energies, the main damage of specimens having 10 mm and 15 mm core thicknesses is same with the specimens having 5 mm core thickness.

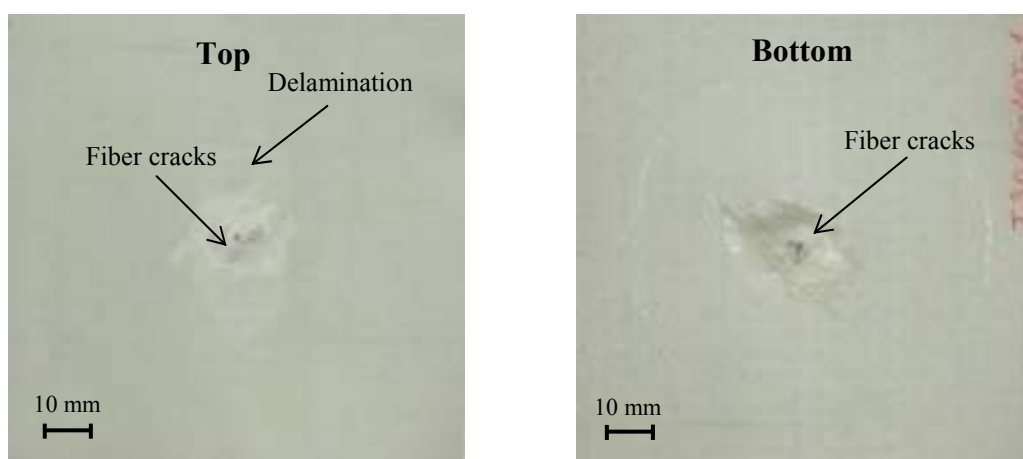
For other core materials and thicknesses, photos of impact induced damage are given in Figure 32-38. Impact induced damage is nearly same with the specimens with PET foam core having 5, 10 and 15 mm core thicknesses. But, there is no damage seen at the bottom face sheet of specimens with PVC-1 foam core having 15 mm core thickness under impact energy of 25J (Figure 34-b), while it is seen the other specimens of same thickness and impact energy.



(a)



(b)



(c)

Figure 4.29 Damages of specimens with PET foam core having 5 mm core thickness impacted at (a) 15J, (b) 25J and (c) 40J

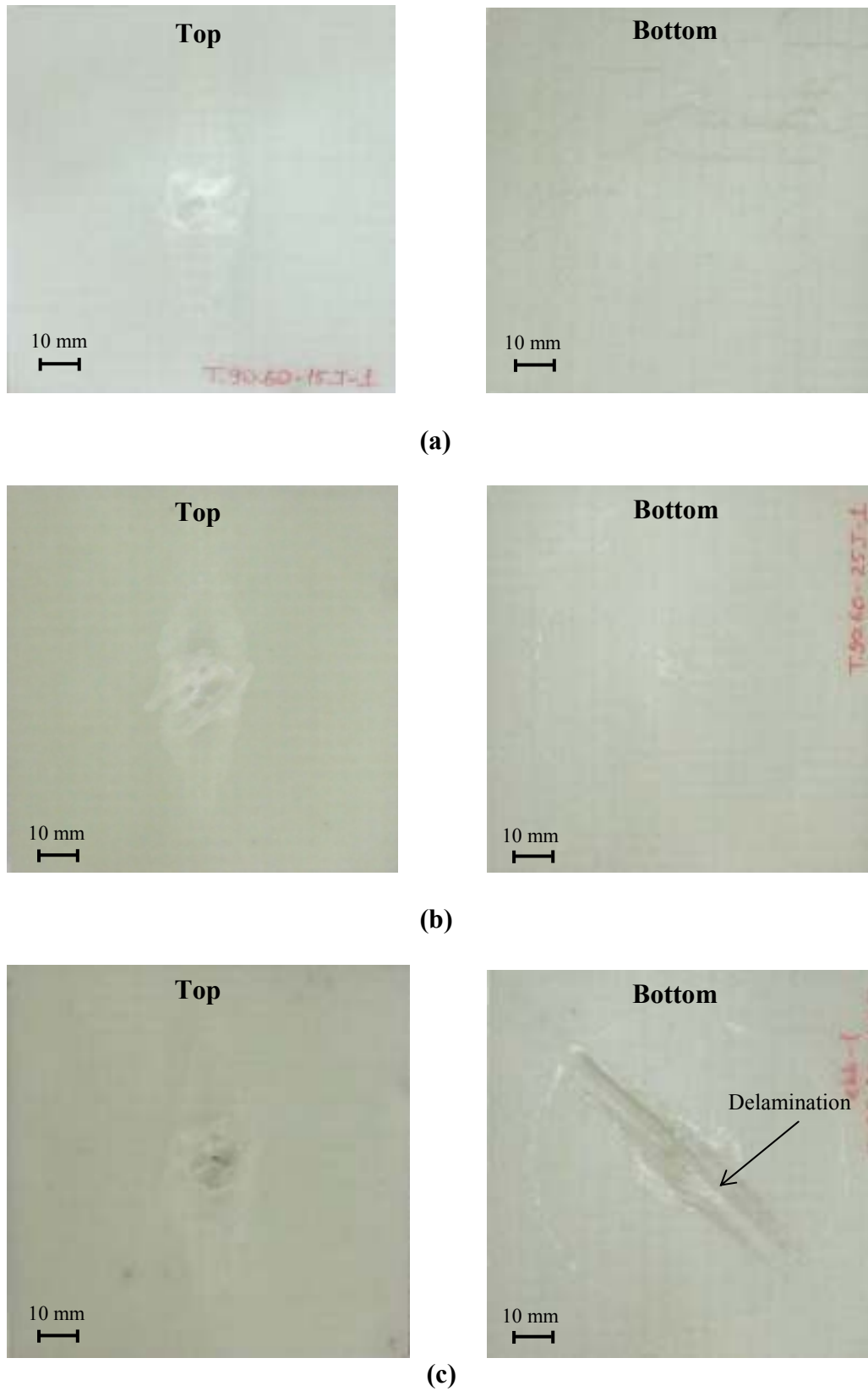


Figure 4.30 Damages of specimens with PET foam core having 10 mm core thickness impacted at (a) 15J, (b) 25J and (c) 40J

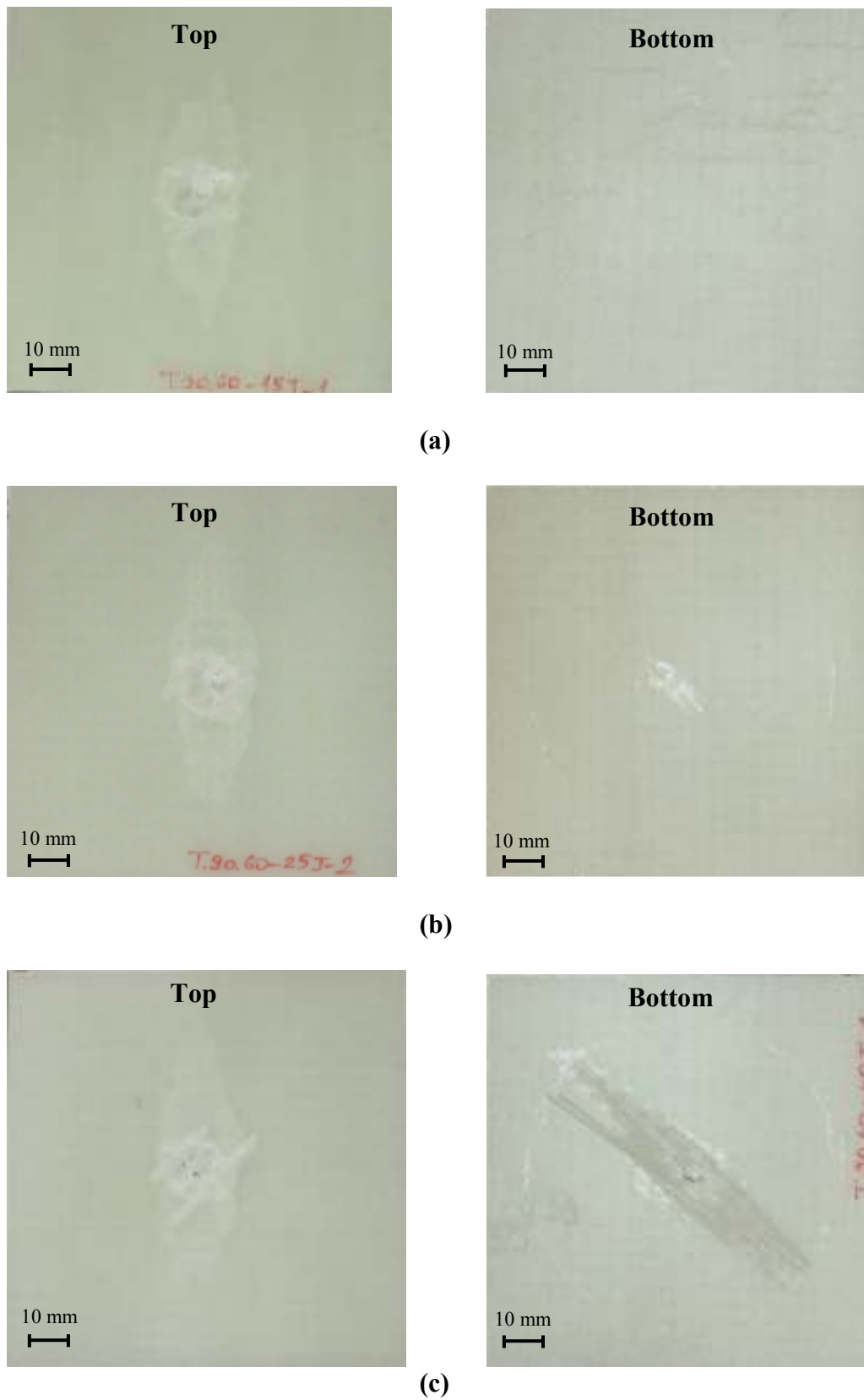


Figure 4.31 Damages of specimens with PET foam core having 15 mm core thickness impacted at (a) 15J, (b) 25J and (c) 40J

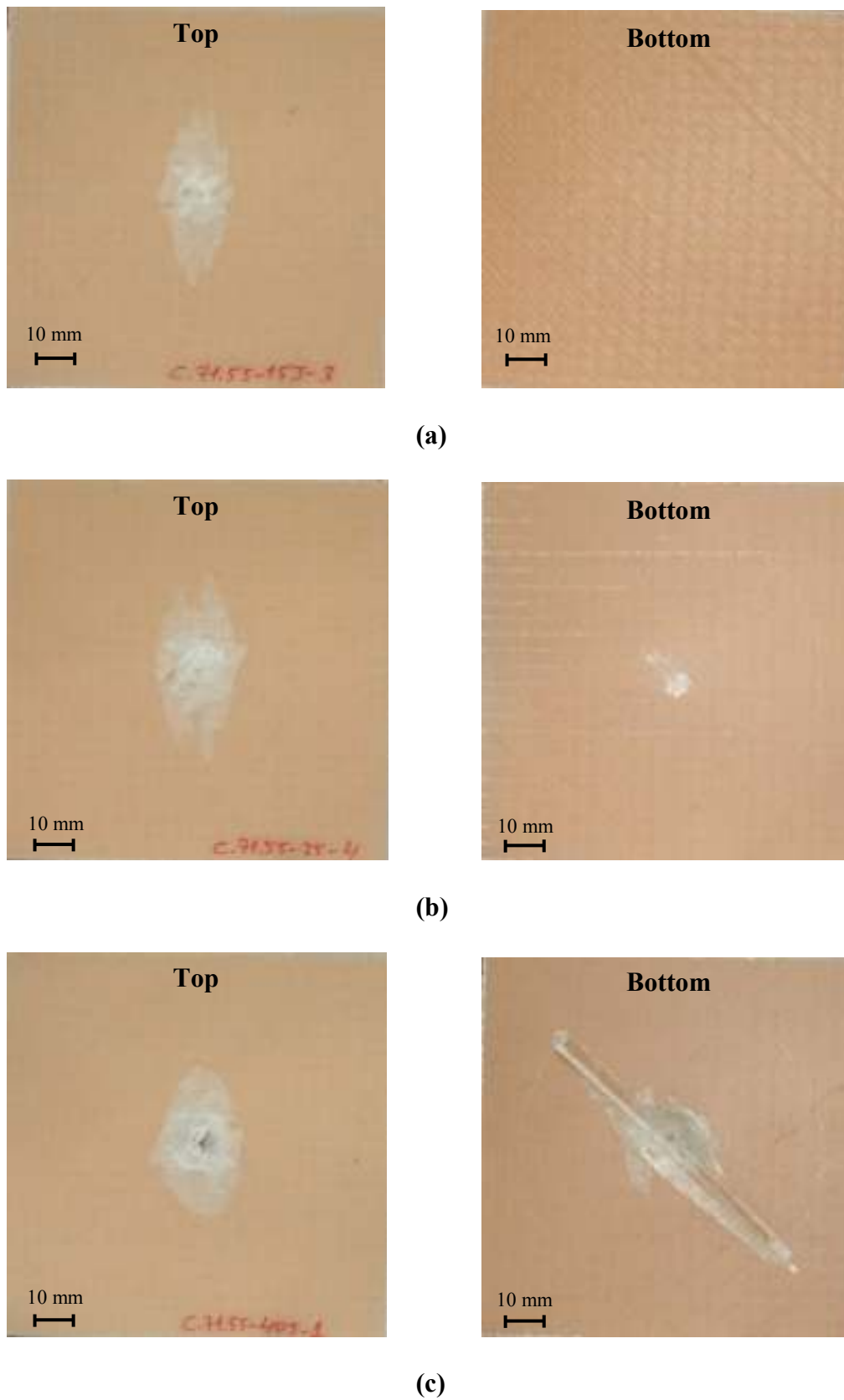


Figure 4.32 Damages of specimens with PVC-1 foam core having 5 mm core thickness impacted at **(a)** 15J, **(b)** 25J and **(c)** 40J

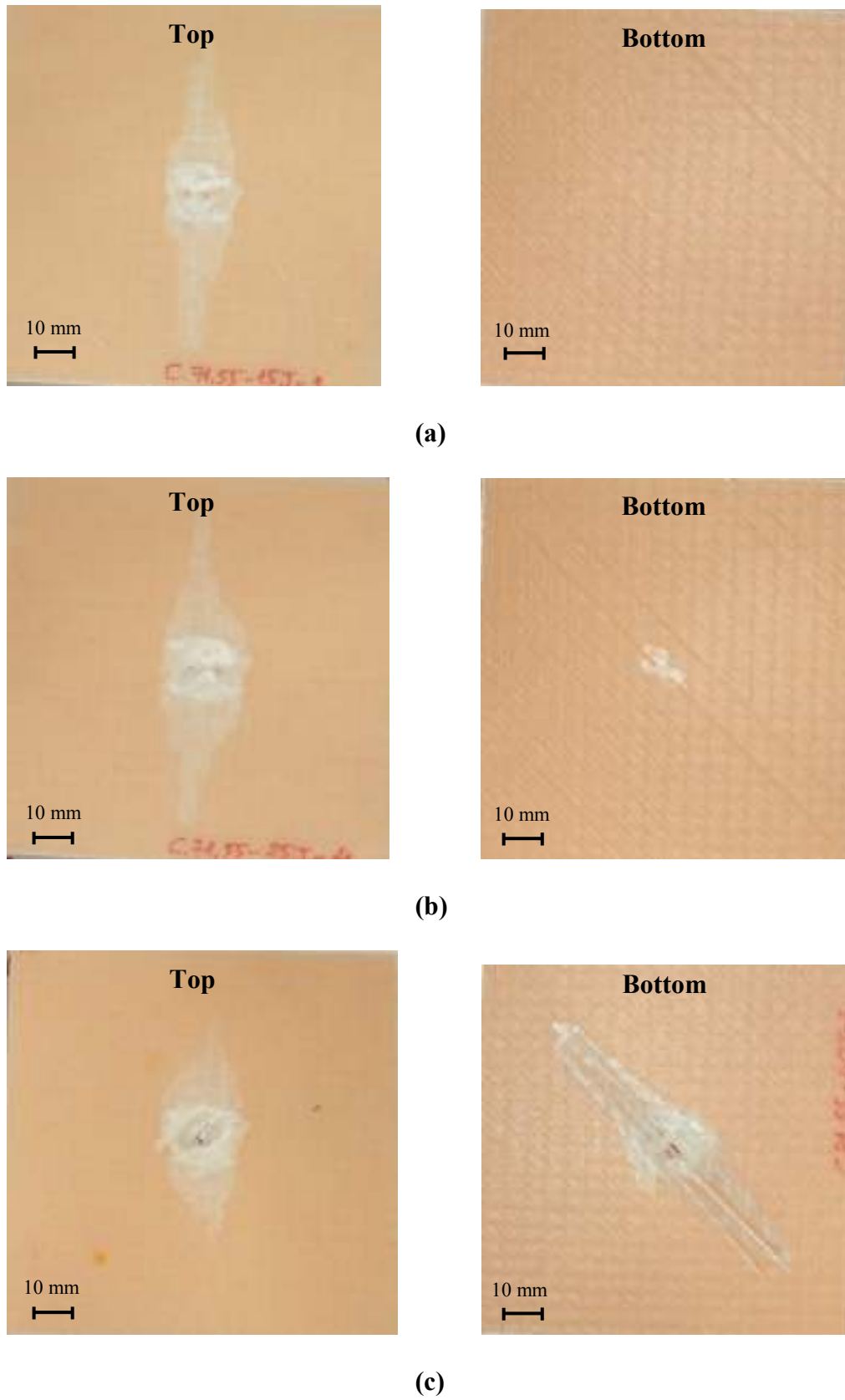


Figure 4.33 Damages of specimens with PVC-1 foam core having 10 mm core thickness impacted at (a) 15J, (b) 25J and (c) 40J

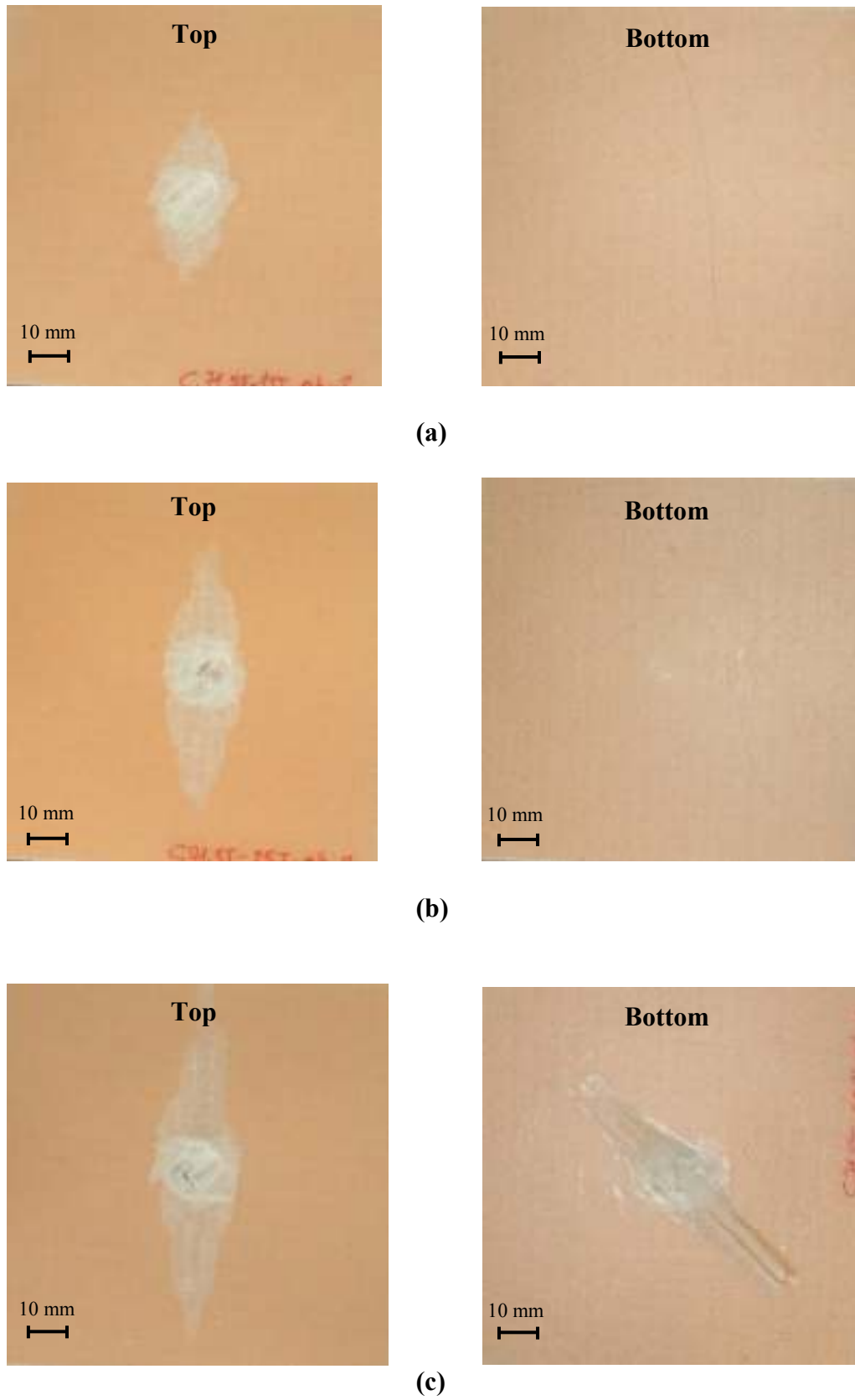


Figure 4.34 Damages of specimens with PVC-1 foam core having 15 mm core thickness impacted at **(a)** 15J, **(b)** 25J and **(c)** 40J

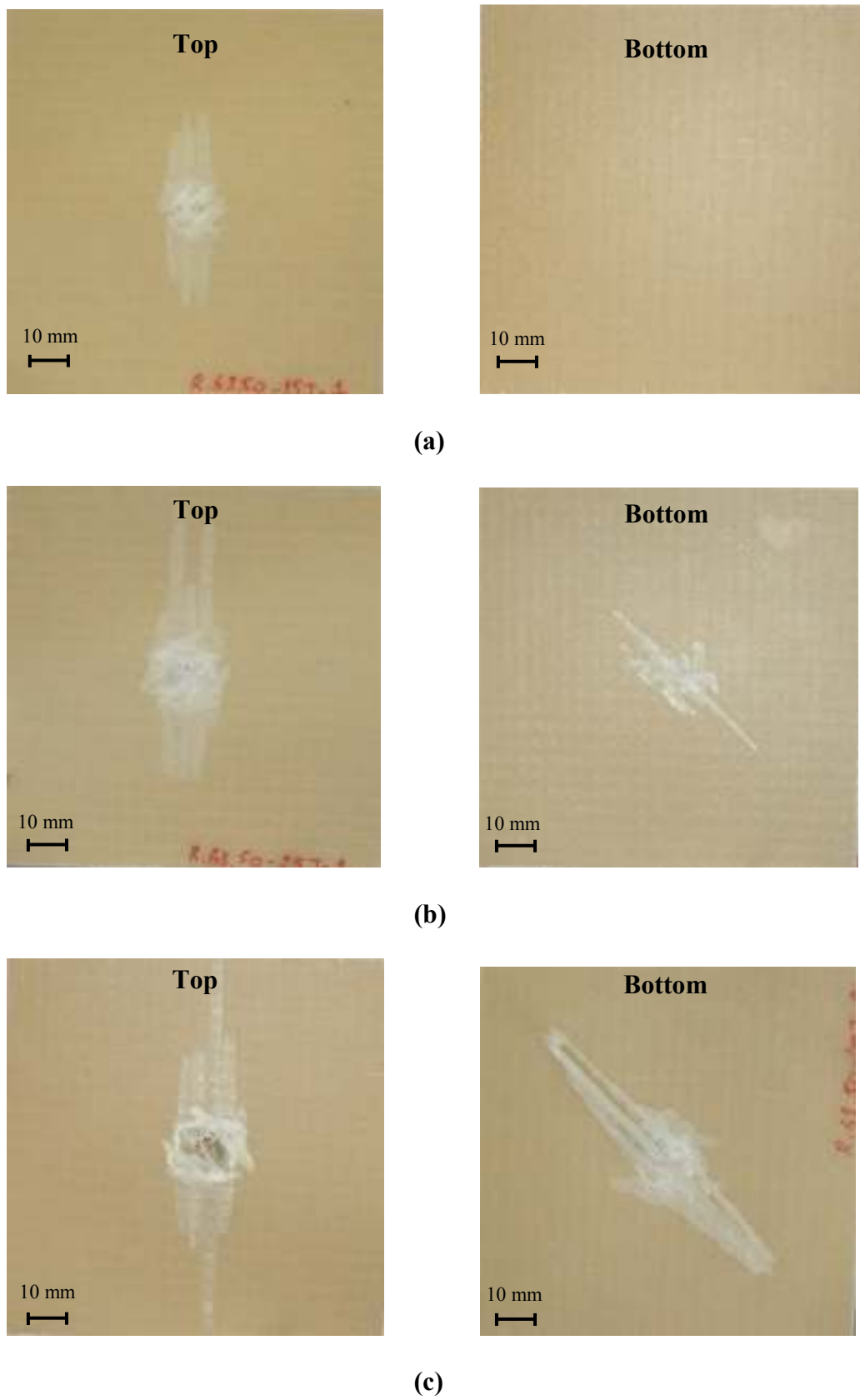


Figure 4.35 Damages of specimens with PVC-2 foam core having 5 mm core thickness impacted at (a) 15J, (b) 25J and (c) 40J

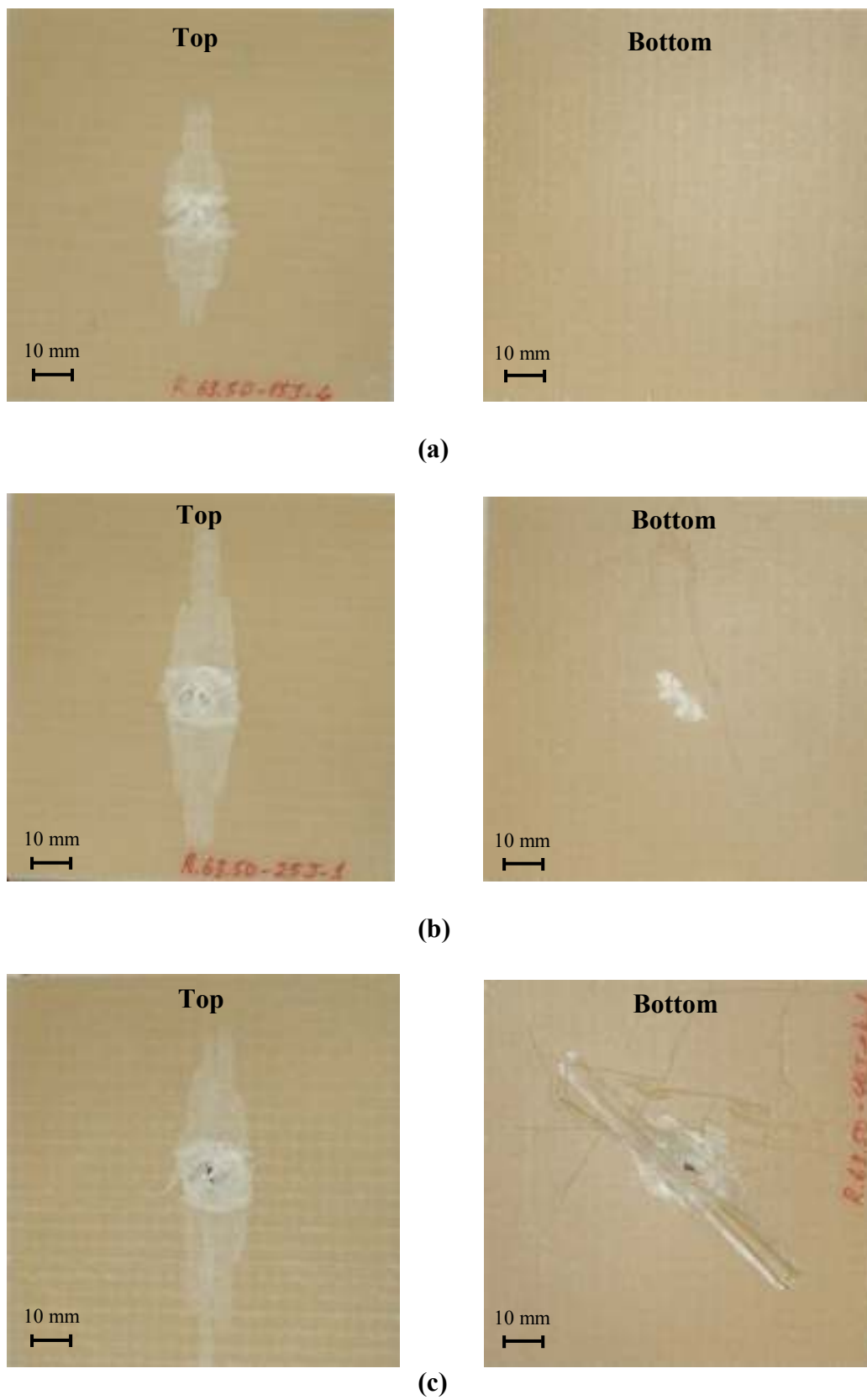


Figure 4.36 Damages of specimens with PVC-2 foam core having 10 mm core thickness impacted at (a) 15J, (b) 25J and (c) 40J

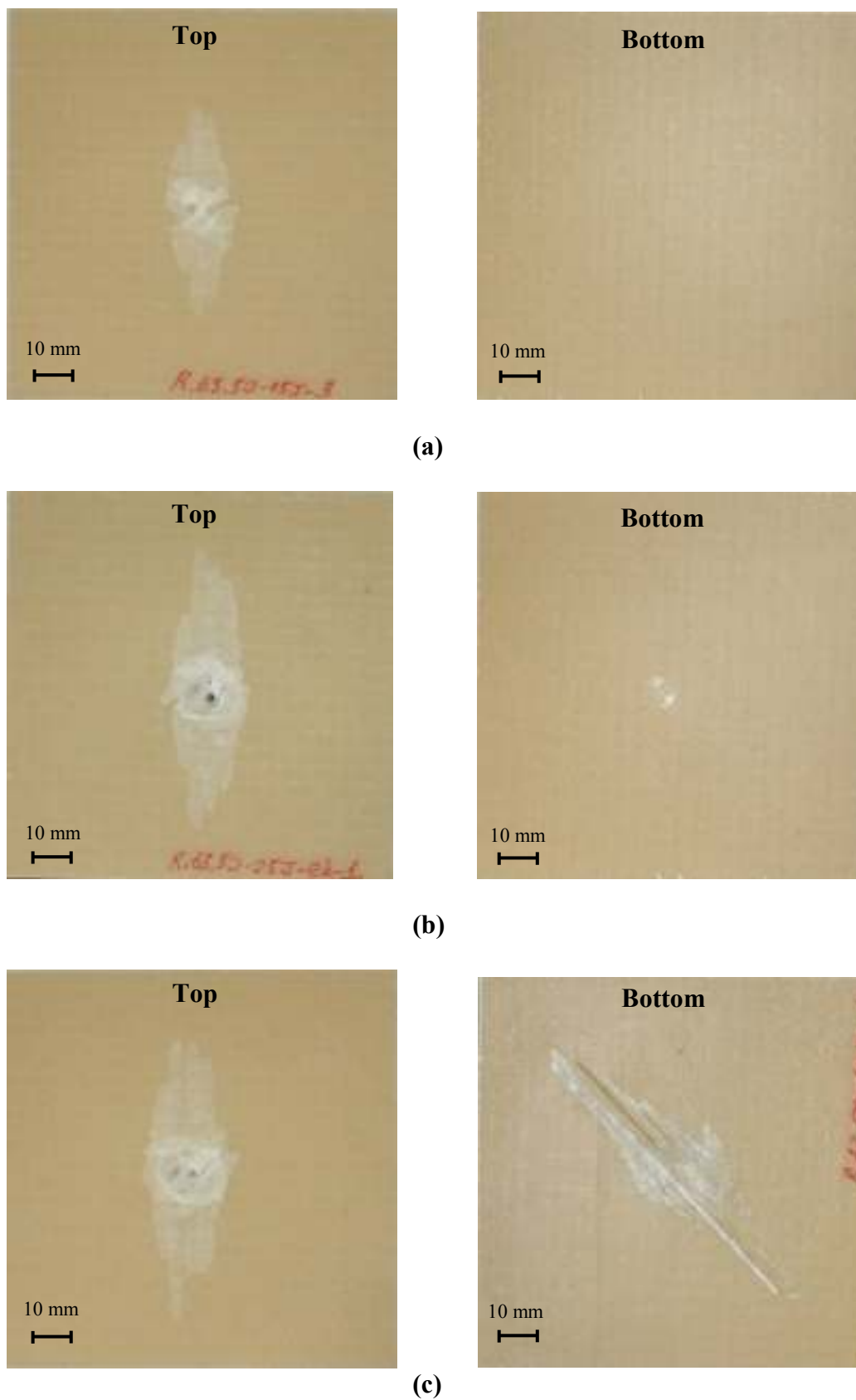
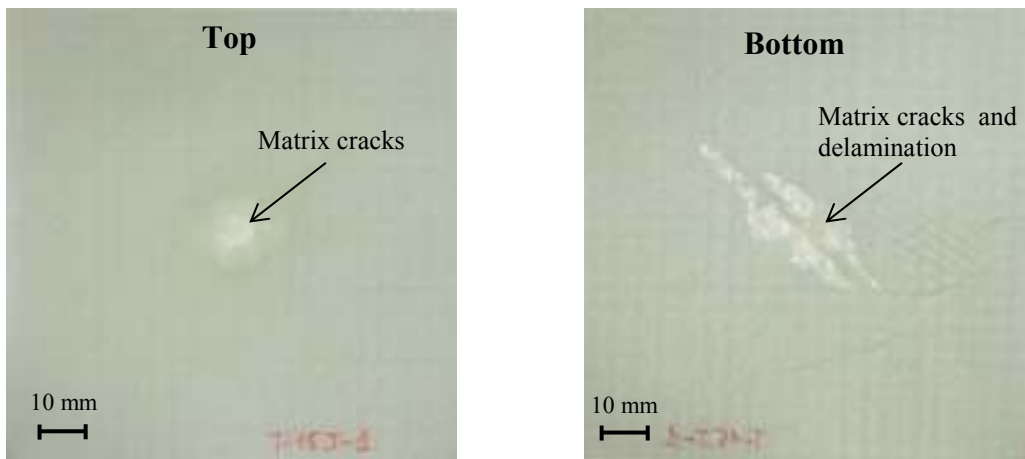
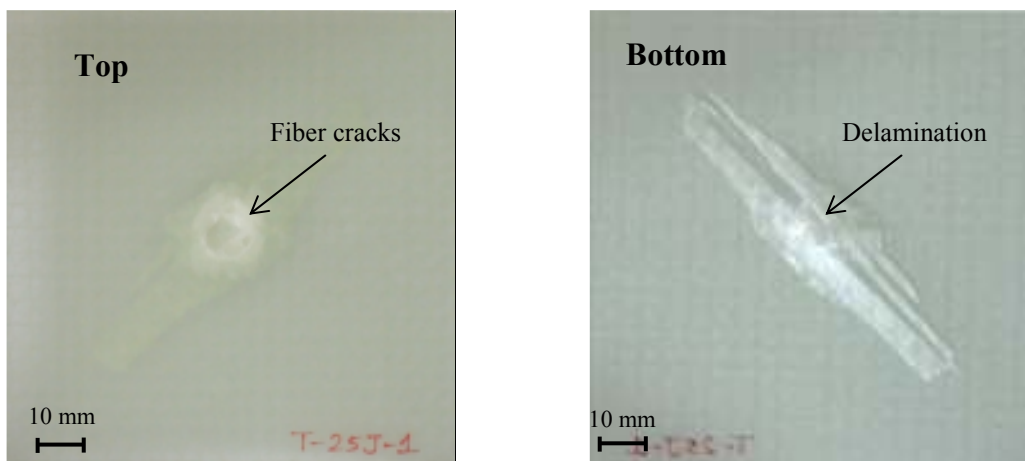


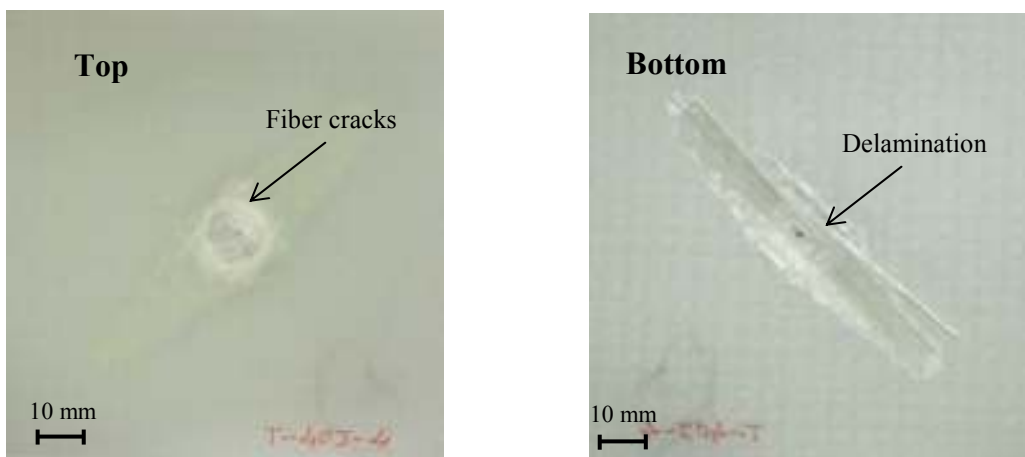
Figure 4.37 Damages of specimens with PVC-2 foam core having 15 mm core thickness impacted at **(a)** 15J, **(b)** 25J and **(c)** 40J



(a)



(b)



(c)

Figure 4.38 Damages of specimens without core material impacted at (a) 15J, (b) 25J and (c) 40J

CHAPTER FIVE

CONCLUSIONS AND RECOMMENDATIONS

In the present study, the effects of PVC and PET foam core materials and their thicknesses on low velocity impact behavior of sandwich composites are investigated, experimentally. Sandwich composites were fabricated by vacuum assisted resin infusion molding method (VARIM) with $[\pm 45/0/90/core/90/0/\mp 45]$ orientations. Impact characteristics like maximum contact force, time, deflection and absorbed energy were obtained and compared for each core material and thickness, and $[\pm 45/0/90]_s$ laminated composite. From the obtained results, the main conclusions are summarized in the following:

- The contact force versus deflection and time curves of having 5 mm core thickness specimens consist of one peak and show nearly same impact characteristics with laminated composite plates. Because, specimens having small core thickness is more stiffness than the thicker core thicknesses and it behaves as a full part.
- As the core thickness increases, specimens show more elastic behavior and so, maximum contact force value decreases while contact time and maximum deflection values increase. Also, in the thicker core thicknesses, the specimens absorbed more energy. Therefore, penetration portion sees in the wide energy ranges.
- The loading portions of the curves are nearly same for all core thickness. But, unloading portions are different because of the different damage mechanism. According to impact energy levels, impactor causes damage in the bottom face sheet or stops in the core material. So, the differences observed in the unloading portion of the curves. The bending stiffness of the specimen without core material is higher than all the specimens with cores. Bending stiffness is the maximum at the specimen with PVC-1, and the minimum at the specimen with

PVC-2 foam cores. This property is compatible with the compressive modulus of the core materials.

- For all type of core materials and their thicknesses, impact damage area increases by increasing the impact energy. Because, as the impact energy is increased, the specimens absorbed more energy that increases the impact damage area. In the small energy levels, the matrix damages and small fiber cracks occur, while these damages were seen clearly in the higher impact energy levels.
- The shear strength and compressive strength value of core materials play a significant role on impact behaviour of specimens especially having small core thickness in the same densities. But, in the thicker core thickness, impact behaviour of specimens are little affected from those values.

In the below, some recommendations for any future work to be performed on sandwich composite structures of the effect of core materials and their thicknesses are listed:

- The impact behaviour of the different core materials such as balsa wood, aluminium honeycomb may be investigated with different core thickness.
- The effect of densities of core material may be tested in different core thickness.
- To obtain the most efficient core thickness, the core thickness may be selected in thicker values.
- The effect of stacking sequence of face sheet materials may be investigated to find optimum value.

REFERENCES

- Abrate, S. (1998). *Impact on composite structures*. Cambridge: Cambridge University Press.
- Abrate, S. (2011). *Impact Engineering of Composite Structures*. Italy: Springer Wien New York.
- Aktas, M. (2007). *Temperature effect on impact behavior of laminated composite plates*. PhD Thesis, Dokuz Eylül University.
- Anderson, T., & Madenci, E. (2000). Experimental investigation of low-velocity impact characteristics of sandwich composites. *Composite Structures*, 50, 239-247.
- Apetre, N.A., Sankar, B.V., & Ambur, D.R. (2006). Low-velocity impact response of sandwich beams with functionally graded core. *International Journal of Solids and Structures*, 43, 2479-2496.
- ASTM Standards and Literature Referances for Composite Materials, (1990). *Standard Test Method for Tensile Properties of Fiber-Resin Composites D 3039–76*, American Society for Testing and Materials. Philadelphia, PA.
- ASTM Standards and Literature Referances for Composite Materials, (1990). *Standard Test Method for Compressive Properties of Unidirection or Cross-Ply Fiber-Resin Composites D 3410–87*, American Society for Testing and Materials. Philadelphia, PA.
- Atas, C., & Sevim, C. (2010). On the impact response of sandwich composites with cores of balsa wood and PVC foam. *Composites Structures*, 93, 40-48.

- Avila, A.F., Carvalho, M.G.R., Dias, E.C., & da Cruz, D.T.L. (2010). Nano-structured sandwich composites response to low-velocity impact. *Composites Structures*, 92, 745-751.
- Besant, T., Davies, G.A.O., & Hitchings D. (2001). Finite element modelling of low velocity impact of composite sandwich panels. *Composites: Part A* 32, 1189-1196.
- Bhuiyan, M.A., Hosur, M.V., & Jeelani, S. (2009). Low-velocity impact response of sandwich composites with nanophased foam core and biaxial ($\pm 45^\circ$) braided face sheets. *Composites: Part B*, 40, 561-571.
- Campbell, F.C. (2010). *Structural Composite Materials*. United States of America: ASM International.
- Cantwell, W.J., Curtis, P.T., & Morton, J. (1986). An assessment of the impact performance of CFRP reinforced with high-strain carbon fibers. *Composites Science & Technology*, 25, 133-148.
- Carlsson, L.A., & Kardomateas, G.A. (2011). *Structural and Failure Mechanics of Sandwich Composites*. New York: Springer.
- Choi, H.Y., & Chang, F.K. (1992). A model for predicting damage in graphite/epoxy laminated composites resulting from low-velocity point impact. *Composite Materials*, 26(14), 2134-2169.
- Davies, G.A.O., Hitchings, D., Besant, T., Clarke, A. & Morgan, C. (2004). Compression after impact strength of composite sandwich panels. *Composites Structures*, 63, 1-9.

- Dear, J.P., Lee, H., & Brown, S.A. (2005). Impact damage processes in composite sheet and sandwich honeycomb materials. *International Journal of Impact Engineering*, 32, 130-154.
- Dorey, G. (1988). Impact damage in composites-development, consequences, and prevention. In *Proc. 6th Int. Conf. on Composite Materials and 2nd European Conf. on Composite Materials*, 3, 1-26.
- Etemadi, E., Khatibi, A.A., & Takaffoli, M. (2009). 3D finite element simulation of sandwich panels with a functionally graded core subjected to low velocity impact. *Composites Structures*, 89, 28-34.
- Freeman, B., Schwingler, E., Mahinfalah, M., & Kellogg, K. (2005). The effect of low-velocity impact on the fatigue life of Sandwich composites. *Composites Structures*, 70, 374-381.
- Gustin, J., Joneson, A., Mahinfalah, M., & Stone, J. (2005). Low velocity impact of combination Kevlar/carbon fiber sandwich panels. *Composite Structures*, 69, 396-406.
- Hazizan, Md. A., & Cantwell, W.J. (2002). The low velocity impact response of foam-based sandwich structures. *Composites: Part B*, 33, 193-204.
- Herup, E.J., & Palazotto, N. (1997). Low-velocity impact damage initiation in graphite/epoxy/nomex honeycomb-sandwich plates. *Composite Science and Technology*, 57, 1581-1598.
- Hosur, M.V., Abdullah, M., & Jeelani, S. (2005). Manufacturing and low-velocity impact characterization of foam filled 3-D integrated core sandwich composites with hybrid face sheets. *Composites Structures*, 69, 167-181.

- Jiang, D., & Shu, D. (2005). Local displacement of core in two-layer sandwich composite structures subjected to low velocity impact. *Composite Structures*, 71, 53-60.
- Joshi, S.P., & Sun, C.T. (1985). Impact induced fracture in a laminated composite. *J.Comp. Mat*, 19, 51-66.
- Kalantari, M., Nami, M.R., & Kadivar, M.H. (2010). Optimization of composite sandwich panel against impact using genetic algorithm. *International Journal of Impact Engineering*, 37, 599-604.
- Li, G., & Muthyala, V.D. (2008). Impact characterization of sandwich structures with an integrated orthogrid stiffened syntactic foam core. *Composites Science and Technology*, 68, 2078-2084.
- Liu, D. (1988). Impact induced delamination-a view of bending stiffness mismatching. *Journal of Composite Materials*, 22, 674-692.
- Mallick, P.K. (2008). *Fiber-reinforced composites* (3rd ed.). New York: CRC Press.
- Mohan, K., Yip, T.H., Idapalapati, S., & Chen, Z. (2011). Impact response of aluminum foam core sandwich structures. *Materials Science and Engineering A*, 529, 94-101.
- Park, J.H., Ha, S.K., Kang, K.W., Kim, C.W., & Kim, H.S. (2008). Impact damage resistance of sandwich structure subjected to low velocity impact. *Journal of Materials Processing Technology*, 201, 425-430.
- Petras, A. (1998). *Design of Sandwich Structures*. PhD Thesis, Cambridge University.

- Salehi-Khojin, A., Mahinfalah, M., Bashirzadeh, R., & Freeman, B. (2007). Temperature effects on Kevlar/hybrid and carbon fiber composite sandwiches under impact loading. *Composites Structures*, 78, 197-206.
- Sawal, N., & Akil, H. Md. (2011). Effect of core thicknesses on impact performance of thermoplastic honeycomb core sandwich structure under low-velocity impact loading. *Key Engineering Materials*, (471-472), 461-465.
- Schubel, P.M., Luo, J., & Daniel, I.M. (2005). Low velocity impact behavior of composite sandwich panels. *Composites: Part A*, 36, 1389-1396.
- Typical properties for AIREX®*. (n.d). Retrieved May 5, 2012 from <http://www.metyx.com/Turkish/Composites/>
- Vaidya, U.K., Hosur, M.V., Earl, D., & Jeelani, S. (2000). Impact response of integrated hollow core sandwich composite panels. *Composites: Part A*, 31, 761-772.
- Wu, H.Y., & Springer, G.S. (1988). Measurements of matrix cracking and delamination caused by impact on composite plates. *Comp. Materials*, 22, 518-532.
- Xiong, J., Vaziri, A., Ma, L., Papadopoulos, J., & Wu, L. (2012). Compression and impact testing of two-layer composite pyramidal-core sandwich panels. *Composites Structures*, 94, 793-801.

APPENDICES

In this section, average values and standard deviations of test results are given for each experimental parameter in Table A.1-10. Also, average values and standard deviations of mechanical properties of laminated composite plate are given in Table A.11.

Table A.1 Values of test results of specimens with PET foam core having 5 mm core thickness

	Maximum contact time (ms)	Maximum deflection (mm)	Maximum contact force (N)	Absorbed energy (J)	Impact energy (J)
Average	11.42	8.12	2590	9.07	10
Std. dev.	0.39	0.08	122	0.25	
Average	10.81	10.52	3306	13.56	15
Std. dev.	0.31	0.29	205	0.40	
Average	10.42	10.80	3825	18.16	20
Std. dev.	0.35	0.17	177	0.38	
Average	10.20	12.05	4403	22.54	25
Std. dev.	0.42	0.40	267	0.52	
Average	10.25	13.05	4682	27.98	30
Std. dev.	0.03	0.21	141	0.30	
Average	11.23	15.49	4141	35	35
Std. dev.	0.23	0.41	93	0.13	
Average	15.32	26.11	4192	39.05	40
Std. dev.	0.29	0.59	88	0.47	
Average	6.52	21.94	4032	35.19	50
Std. dev.	0.31	0.76	127	0.27	
Average	4.66	20.45	4084	35.64	70
Std. dev.	0.24	0.66	130	0.46	

Table A.2 Values of test results of specimens with PET foam core having 10 mm core thickness

	Maximum contact time (ms)	Maximum deflection (mm)	Maximum contact force of top face sheet (N)	Maximum contact force of bottom face sheet (N)	Absorbed energy (J)	Impact energy (J)
Average	12.42	8.97	2361	-	9.22	10
Std. dev.	0.59	1.05	35	-	0.43	
Average	15.68	10.86	2637	-	14.84	15
Std. dev.	0.75	0.96	194	-	0.50	
Average	14.70	15.44	2764	1109	20	20
Std. dev.	0.43	0.95	124	86	0.10	
Average	13.62	17.95	2588	2380	25	25
Std. dev.	0.45	0.62	179	154	0.28	
Average	14.87	21.06	3059	3165	30	30
Std. dev.	1.28	1.23	253	134	0.25	
Average	14.52	26.18	2910	3003	35	35
Std. dev.	0.48	0.49	176	230	0.46	
Average	9.94	26.52	2519	3121	35.04	40
Std. dev.	0.47	0.35	231	176	0.45	
Average	7.13	24.98	2668	3162	32.42	50
Std. dev.	0.41	0.60	129	96	0.48	
Average	5.31	24.72	2648	3669	35.77	70
Std. dev.	0.47	0.68	237	196	0.47	

Table A.3 Values of test results of specimens with PET foam core having 15 mm core thickness

	Maximum contact time (ms)	Maximum deflection (mm)	Maximum contact force of top face sheet (N)	Maximum contact force of bottom face sheet (N)	Absorbed energy (J)	Impact energy (J)
Average	11.74	7.83	2502	-	9.23	10
Std. dev.	0.44	0.12	183	-	0.41	
Average	14.39	10.19	2655	-	15	15
Std. dev.	0.67	0.24	158	-	0.47	
Average	20.51	21.84	2613	308	20	20
Std. dev.	0.43	0.55	156	74	0.17	
Average	17.56	23.88	2706	1404	25	25
Std. dev.	0.55	0.34	162	195	0.07	
Average	16.51	25.60	2534	2625	30	30
Std. dev.	0.63	0.52	103	54	0.24	
Average	16.59	30.07	3113	2545	35	35
Std. dev.	0.47	0.56	184	207	0.28	
Average	13.88	33.16	3033	2793	37.36	40
Std. dev.	0.80	0.87	215	169	0.43	
Average	8.50	30.44	2498	2770	34.52	50
Std. dev.	0.53	0.72	83	159	0.71	
Average	6.64	30.30	2770	2966	34.03	70
Std. dev.	0.24	0.50	148	248	0.49	

Table A.4 Values of test results of specimens with PVC-1 foam core having 5 mm core thickness

	Maximum contact time (ms)	Maximum deflection (mm)	Maximum contact force (N)	Absorbed energy (J)	Impact energy (J)
Average	11.24	7.92	2484	9.13	10
Std. dev.	0.14	0.11	89	0.18	
Average	11.32	9.71	2831	14.07	15
Std. dev.	0.26	0.11	125	0.28	
Average	10.87	11.13	3335	19.08	20
Std. dev.	0.09	0.19	170	0.19	
Average	10.49	12.27	4018	23.23	25
Std. dev.	0.26	0.12	173	0.22	
Average	9.95	13.34	4183	28.62	30
Std. dev.	0.35	0.12	157	0.39	
Average	11.28	15.41	4275	35	35
Std. dev.	0.75	0.53	200	0.43	
Average	9.94	20.59	3902	37.59	40
Std. dev.	0.34	0.38	146	0.45	
Average	6.59	21.42	3723	35.58	50
Std. dev.	0.56	0.14	51	0.14	
Average	4.66	20.45	3906	34.79	70
Std. dev.	0.37	0.43	127	0.49	

Table A.5 Values of test results of specimens with PVC-1 foam core having 10 mm core thickness

	Maximum contact time (ms)	Maximum deflection (mm)	Maximum contact force of top face sheet (N)	Maximum contact force of bottom face sheet (N)	Absorbed energy (J)	Impact energy (J)
Average	10.92	7.41	2414	-	9.09	10
Std. dev.	0.31	0.14	114	-	0.26	
Average	14.29	10.07	2612	-	15	15
Std. dev.	0.41	0.43	96	-	0.39	
Average	13.76	16.12	2672	756	20	20
Std. dev.	0.49	0.65	205	172	0.11	
Average	15.01	19.10	2701	1581	25	25
Std. dev.	0.49	0.58	198	67	0.07	
Average	14.84	21.54	2718	2430	30	30
Std. dev.	0.47	0.92	159	127	0.22	
Average	16.20	26.64	2786	2525	35	35
Std. dev.	0.28	0.33	58	136	0.08	
Average	9.95	27.00	2712	2210	32.40	40
Std. dev.	0.29	0.29	174	251	0.30	
Average	7.92	26.22	2755	2704	33.48	50
Std. dev.	0.75	0.32	136	153	0.55	
Average	5.53	25.48	2850	2702	31.45	70
Std. dev.	0.05	0.27	76	182	0.40	

Table A.6 Values of test results of specimens with PVC-1 foam core having 15 mm core thickness

	Maximum contact time (ms)	Maximum deflection (mm)	Maximum contact force of top face sheet (N)	Maximum contact force of bottom face sheet (N)	Absorbed energy (J)	Impact energy (J)
Average	10.76	7.33	2515	-	9.56	10
Std. dev.	0.31	0.15	143	-	0.25	
Average	13.09	9.78	2638	-	15	15
Std. dev.	0.66	0.61	95	-	0.49	
Average	17.07	21.18	2824	479	20	20
Std. dev.	0.50	0.54	200	97	0.17	
Average	17.84	24.94	2829	1021	25	25
Std. dev.	0.64	0.54	221	174	0.13	
Average	16.32	26.46	2769	2211	30	30
Std. dev.	0.30	0.54	229	134	0.12	
Average	17.35	29.05	2831	2625	35	35
Std. dev.	0.27	0.55	205	99	0.13	
Average	15.27	35.18	2999	2629	37.27	40
Std. dev.	0.40	0.44	123	176	0.38	
Average	9.95	32.73	2997	2509	36.01	50
Std. dev.	0.36	0.46	96	204	0.64	
Average	6.83	30.42	2607	3024	35.82	70
Std. dev.	0.23	0.33	155	170	0.44	

Table A.7 Values of test results of specimens with PVC-2 foam core having 5 mm core thickness

	Maximum contact time (ms)	Maximum deflection (mm)	Maximum contact force (N)	Absorbed energy (J)	Impact energy (J)
Average	11.68	8.51	2478	9.21	10
Std. dev.	0.28	0.08	124	0.35	
Average	11.48	10.19	2978	13.93	15
Std. dev.	0.40	0.21	171	0.18	
Average	11.19	11.78	3370	18.79	20
Std. dev.	0.23	0.26	132	0.28	
Average	11.39	12.73	3898	23.89	25
Std. dev.	0.93	0.21	114	0.62	
Average	12.00	14.86	4077	30	30
Std. dev.	0.61	0.56	220	0.42	
Average	11.76	23.47	3999	33.28	35
Std. dev.	0.65	0.45	51	0.69	
Average	8.14	21.78	4144	33.04	40
Std. dev.	0.24	0.38	150	0.50	
Average	6.12	20.96	4022	31.63	50
Std. dev.	0.49	0.32	155	0.37	
Average	4.39	20.59	3938	30.94	70
Std. dev.	0.28	0.46	84	0.62	

Table A.8 Values of test results of specimens with PVC-2 foam core having 10 mm core thickness

	Maximum contact time (ms)	Maximum deflection (mm)	Maximum contact force of top face sheet (N)	Maximum contact force of bottom face sheet (N)	Absorbed energy (J)	Impact energy (J)
Average	12.27	8.63	2147	-	9.39	10
Std. dev.	0.30	0.11	111	-	0.09	
Average	13.53	10.97	2326	-	14.78	15
Std. dev.	0.36	0.14	84	-	0.17	
Average	14.38	14.56	2414	1421	20	20
Std. dev.	0.50	0.62	41	87	0.15	
Average	12.60	16.74	2668	1989	25	25
Std. dev.	0.21	0.27	212	139	0.10	
Average	12.50	17.71	2899	2561	30	30
Std. dev.	0.63	0.53	155	270	0.32	
Average	14.28	21.12	2579	3073	35	35
Std. dev.	0.61	0.68	151	187	0.15	
Average	11.04	27.70	2413	2836	34.26	40
Std. dev.	0.29	0.69	145	90	0.80	
Average	7.61	26.43	2650	2897	33.83	50
Std. dev.	0.23	0.72	133	37	0.46	
Average	5.44	24.51	2984	3174	33.91	70
Std. dev.	0.19	0.68	247	178	0.45	

Table A.9 Values of test results of specimens with PVC-2 foam core having 15 mm core thickness

	Maximum contact time (ms)	Maximum deflection (mm)	Maximum contact force of top face sheet (N)	Maximum contact force of bottom face sheet (N)	Absorbed energy (J)	Impact energy (J)
Average	12.61	9.11	2085	-	9.56	10
Std. dev.	0.35	0.15	95	-	0.12	
Average	13.17	11.07	2381	-	14.61	15
Std. dev.	0.25	0.20	147	-	0.23	
Average	16.89	14.04	2447	-	20	20
Std. dev.	0.50	0.36	116	-	0.28	
Average	16.86	22.07	2596	557	25	25
Std. dev.	0.88	0.63	87	122	0.07	
Average	14.59	22.69	2693	2282	30	30
Std. dev.	0.24	0.31	126	238	0.15	
Average	14.94	24.89	2596	2795	35	35
Std. dev.	0.57	0.62	156	54	0.05	
Average	17.32	31.16	2539	2946	40	40
Std. dev.	0.41	0.48	166	228	0.40	
Average	11.06	32.14	2820	3040	38.42	50
Std. dev.	1.44	0.58	181	141	0.48	
Average	6.92	29.76	2804	3193	41.04	70
Std. dev.	0.31	0.66	178	139	0.58	

Table A.10 Values of test results of specimens manufactured without core material

	Maximum contact time (ms)	Maximum deflection (mm)	Maximum contact force (N)	Absorbed energy (J)	Impact energy (J)
Average	9.03	6.45	3798	6.49	10
Std. dev.	0.09	0.02	67	0.22	
Average	9.32	7.66	4569	12.33	15
Std. dev.	0.26	0.11	244	0.50	
Average	10.17	9.02	4868	17.87	20
Std. dev.	0.46	0.36	145	0.64	
Average	12.35	11.74	4603	25	25
Std. dev.	0.57	0.41	299	0.51	
Average	9.09	17.15	4892	27.44	30
Std. dev.	0.57	0.61	117	0.57	
Average	6.94	16.83	4820	28.25	35
Std. dev.	0.44	0.42	148	0.64	
Average	6.05	16.84	4795	27.80	40
Std. dev.	0.47	0.65	320	0.49	
Average	4.64	17.95	4783	26.18	50
Std. dev.	0.40	0.60	258	0.61	
Average	3.64	16.88	4815	27.50	70
Std. dev.	0.21	0.78	369	0.66	

Table A.11 Values of mechanical properties of specimens manufactured without core material

	Average Value (MPa)	Standard Deviation
$\bar{X}_{tension}$	653.81	25.20
$\bar{X}_{compression}$	301.81	56.54
$\bar{Y}_{tension}$	62.35	3.00
$\bar{Y}_{compression}$	100,82	0.95